

Sedimentology of the Battfjellet Formation, Liljevalchfjellet, Svalbard

Master of Science Thesis
Basin and Reservoir Studies

By
Torbjørn Trygve Aamelfot
September 2019



**Department of Earth Science
University of Bergen¹**



**Department of Arctic Geology
The University Centre in Svalbard²**

Abstract

A regressive megasequence of Eocene age consisting of the offshore Frysjaodden Formation, the shallow-marine Battfjellet Formation, and the continental Aspelintoppen Formation (together constituting the “GBA-unit”) represents the last of three depositional cycles filling in the Central Basin on Spitsbergen, Svalbard. This foreland basin developed in front the West Spitsbergen Fold and Thrust Belt (WSFTB) during the breakup between Svalbard and Greenland. The Battfjellet Formation has been subject to extensive research, especially on the shelf edge deltas and clinothems in the western and central parts of the basin. This study however, investigates the facies distribution and sandbody geometry of the lesser-documented Battfjellet Formation shelf deltas in the eastern part of the basin, in an area of approximately 5km² at Liljevalchfjellet, Svalbard.

Analysis of facies and facies associations revealed a wide range of depositional environments from offshore to continental. The internal structure of these regressive successions suggests a highly wave-dominated deltaic setting. However, due to a significant presence of carbonaceous detritus, distributary fluvial channels incising shallow marine deposits and previous studies documenting a complex delta lobe stacking pattern, a fluvio-wave interaction delta is suggested for the Battfjellet Formation. A combination of high subsidence and sedimentation rate lead to rapid progradation of the delta lobes into a wave-agitated basin, while transgressive reworking of interdistributary bay/lagoons took place simultaneously between the delta lobes.

A total of six stacked parasequences with an overall regressive low angle ascending shoreline trajectory was identified by combining work from Olsen (2012) with this study. Paleocurrent measurements points to a southeastward-directed outbuilding of the system, different to the generally interpreted eastwards outbuilding for the GBA-Unit. Thus, a shift towards a more southward directed progradation likely took place in the later stages of basin infill. To better view the sandbody geometries and facies distributions, a 3D conceptual reservoir model focusing on the Battfjellet Formation is presented.

Acknowledgements

This thesis is part of a master's degree in Basin and Reservoir Studies (BRS) at the Department of Earth Science at the University of Bergen.

First and foremost, I would like to thank my main supervisor William Helland-Hansen for his excellent guidance during fieldwork, for outlining and correcting the thesis, and for teaching me several courses at UiB.

I would also like to thank my co-supervisor Angel Arantegui for corrections and suggestions during the writing process. An extra special thank you to Angel for voluntarily being a field assistant and sacrificing your knees on the steep barren cliffs of Liljevalchfjellet. I will always remember our days of logging in four seasons of weather, tenting under the midnight sun and feasting at the cantina in Svea. Your contribution was truly invaluable.

Thank you to my brother Aasmund Olav Løvestad for help during the 3D modelling process.

Thanks to The University Centre in Svalbard (UNIS) for providing the necessary equipment and safety training, making the fieldwork possible, and to the people at Svea for their assistance during our stay there.

Last but not least, thank you to my fellow students at UiB for five amazing years of friendship and academic discussion, and my soon to be wife Xuexue for her continuous love and support.

Torbjørn Trygve Aamelfot

11.09.2019

Table of Content:

Abstract	2
1. Introduction	1
1.1 Purpose of study.....	1
1.2 Study area.....	1
1.3 Previous work.....	2
2. Geological Framework	4
2.1 Introduction to the Svalbard Archipelago	4
2.2 Pre-Cenozoic Stratigraphy and evolution.....	6
2.2.1 The Proterozoic and Paleozoic Eras.....	6
2.2.2 The Mesozoic Era.....	6
2.3 Cenozoic Stratigraphy and evolution	7
2.3.1 Introduction.....	7
2.3.2 Formation of the West Spitsbergen Fold and Thrust Belt and Central Basin.....	8
2.3.3 The Central Basin fill.....	11
2.4 Time Constraints.....	15
3. Methodology:	17
3.1 Data acquisition.....	17
3.2 Digitalization.....	17
3.3 Rose Diagrams	17
4. Lithofacies and Facies Associations	18
4.1 Lithofacies:	18
4.2 Facies associations	19
4.2.1 Facies association 1 (FA1): Offshore deposits (Figures 4.1 and 4.2)	21
4.2.2 Facies association 2: Prograding wave-dominated delta deposits (figures 4.3-4.7).....	24
<i>Facies association 2-A (FA2-A): Offshore transition zone deposits (Figure 4.4)</i>	26
<i>Facies association 2-B (FA2-B): Lower shoreface deposits (Figure 4.5)</i>	29
<i>Facies association 2-C (FA2-C): Upper shoreface and Foreshore deposits (Figure 4.6)</i>	32
<i>Interpretation of FA2 (Prograding wave-dominated delta deposits)</i>	34
4.2.3 Facies association 3 (FA3): Distributary fluvial channel deposits (Figure 4.8 and Figure 4.9) .	36
4.2.4 Facies association 4 (FA4): Continental deposits (Aspelintoppen formation) (Figure 4.10)....	40
5. Paleocurrent Data	43
5.1 Introduction.....	43
5.2 Paleocurrent of FA1 (Offshore deposits) and FA2 (Prograding wave-dominated delta)	43
5.3 Paleocurrent of FA3 (Distributary fluvial channel deposits)	45
6. Sandbody Geometry	46

6.1 Introduction.....	46
6.2 Methods of correlation	46
6.3 Correlation principles	47
6.4 Parasequence stacking pattern	48
6.5 Correlation panels	50
6.5.1 Transect A.....	51
7.5.2 Transect B.....	57
7.5.3 Transect C:.....	59
7. Digital 3D Reservoir Model.....	61
7.1 Introduction.....	61
7.2 3D Modelling	61
8.3 Volumetrics	66
7.4 Reservoir Modelling Errors:.....	66
8. Discussion.....	67
8.1 Introduction.....	67
9.2 Depositional environment.....	67
8.3 Sequence stratigraphy.....	69
8.3.1 Introduction.....	69
8.3.2 Shoreline trajectory.....	69
8.3.3 Cause of transgressions.....	70
8.5 Delta type	70
8.5.1 Modern Analogue.....	72
8.5.2 Delta size	73
9. Summary and Conclusions	74
Suggestions for further work.....	75
10. References.....	76
Appendix 1: Logs.....	85
Appendix 2: Paleocurrent Data	102

1. Introduction

1. Introduction

1.1 Purpose of study

The exceptionally well-exposed Eocene Battfjellet Formation, in the Central Tertiary Basin, has been extensively investigated in Nathorst Land and Nordenskiöld Land (Kellogg, 1975; Steel, 1977; Dalland, 1979; Helland-Hansen, 1985, 1990, 1992; Plink-Bjørklund et al., 2001; Mellere et al., 2002; Deibert et al., 2003; Plink-Bjørklund and Steel, 2004; Crabaugh and Steel, 2004; Johannesen and Steel, 2005; Løseth et al., 2006; Petter and Steel, 2006; Clark and Steel, 2006; Uroza and Steel, 2008; Olsen, 2008; Stene, 2009; Skarpeid; 2010; Gjelberg, 2010; Helland-Hansen, 2010; Osen, 2012; Grundvåg et al., 2014b; Skjærpe, 2017). Though the stratigraphic framework is well established, most of the studies have been focusing on the clinothems and basin floor fans in the western and central parts of the Central Basin. Still, there are localities that are poorly studied and understood. Liljevalchfjellet (west of Svea) is one such area (Figure 1.1). The purpose of this study is to establish an understanding of facies distribution and sandbody geometry of the Battfjellet Formation in the study area, through detailed sedimentological studies, facies analysis and sequence stratigraphy. The results will be used to reconstruct the paleoenvironment and paleogeography. A 3D digital reservoir model of the study area is also presented.

1.2 Study area

The topography of central Spitsbergen is characterized by cliffy mountains separated by river valleys and fjords. The mountains commonly contain remnants of an uplifted and warped Paleogene peneplane at 400-500m (Harland et al., 1997). The Battfjellet Formation, which is the focus of this thesis, commonly forms cliffs in contrast to the underlying softer and gentler sloped shales of the offshore Frysjaodden Formation. The steep cliffs, combined with the sparse vegetation on Svalbard allows for some excellent outcrops.

The outcrops studied in this thesis are located in the range of 600-850 m above sea level at the southeast side of Liljevalchfjellet, Nordenskjold Land, Svalbard (Figure 1.1). The outcrops consists of the Eocene sedimentary rocks of the Gilsonryggen member of the Frysjaodden Fm, the Battfjellet Fm, and the Aspelintoppen Fm, which will be further referred to as the GBA-Unit (Helland-Hansen and Grundvåg, in prep). The area was chosen due to the excellently exposed outcrops along the mountain ridges of Liljevalchfjellet, and the lack of studies done on the Battfjellet Fm within that area. The outcrops show a great abundance of sedimentary structures, and have a significant lateral extent that provides a great opportunity for both detailed facies descriptions and reservoir scale correlation.

1. Introduction

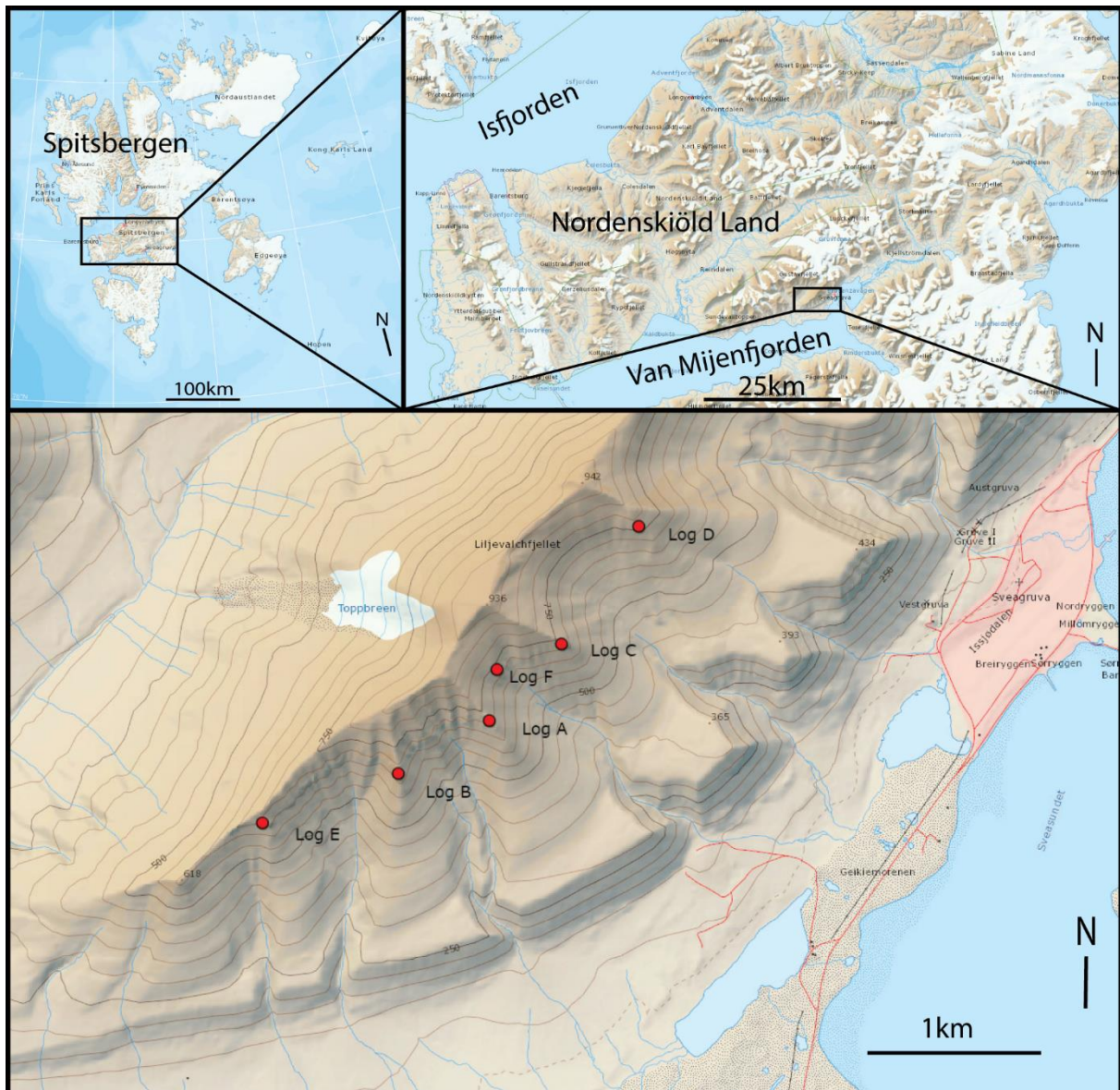


Figure 1.1: Map showing the location of the study area, north of Van Mijenfjorden, in the central parts of Spitsbergen, Svalbard. Red circles show logged sections (Modified from Norsk Polarinstitutt).

1.3 Previous work

Due to the Battfjellet Formation's significant cliff-forming nature relative to the underlying shales of the Frysjaodden Formation and the overlying heterolithic sandstones and siltstones of the Aspelintoppen Formation, it is generally easily recognizable in field. Therefore, it has therefore been regarded as a stratigraphic unit since the first studies were done on the Van Mijenfjorden Group in the early 20th century (Nathorst, 1910; Ljutkevich, 1937; Orvin, 1940). Interest for the Battfjellet Formation was limited for several decades due to a greater interest in more economically important units on Svalbard. Regional studies of structures and stratigraphy in the Central Spitsbergen incorporated the Battfjellet Formation in the 1970's (Major and Nagy, 1972; Kellogg, 1975; Steel, 1977; Dalland, 1979),

1. Introduction

and in the 1980's, studies conducted by Helland-Hansen (1985) and Steel et al (1985), established a paleogeographical and paleoenvironmental understanding of the Battfjellet Formation. During the last decades, the clinoforms and associated basin floor fans have been subject to extensive sedimentological studies by Ronald J. Steel and his coworkers (e.g. Steel, 1977; Plink- Björklund and Steel, 2004; Crabaugh and Steel, 2004; Johannesen and Steel, 2005; Petter and Steel, 2006; Clark and Steel, 2006; Uroza and Steel, 2008). These studies were conducted with a focus on the depositional architecture of the shelf edge deltas creating the clinoforms, and the processes responsible for transporting sediments to the basin floor fans.

The excellent outcrops of the Battfjellet Formation provides a seismic scale view of its depositional architecture, which in the last decades has received great interest to the oil and gas industry. This initiated several studies with focus on sequence stratigraphy, development of the shoreline trajectory and sandbody geometries (Helland-Hansen et al., 1994; Plink- Björklund et al., 2001; Mellere et al., 2002; Deibert et al., 2003; Plink- Björklund and Steel, 2004; Crabaugh and Steel, 2004; Johannesen and Steel, 2005; Løseth et al., 2006; Petter and Steel, 2006; Clark and Steel, 2006; Uroza and Steel, 2008; Olsen, 2008; Stene, 2009; Skarpeid, 2010; Helland-Hansen, 2010; Gjelberg, 2010; Osen, 2012; Grundvåg et al., 2014a, b).

No detailed studies of the Battfjellet Formation has been done previously in the study area, but a study in the Urdkolldalen area, west of Liljevalchfjellet, was conducted by Osen (2012). The results of Osen's study will be used for the interpretation of sandbody geometry, reconstruction of paleogeography and creation of a 3D reservoir model in this thesis.

2. Geological Framework

2. Geological Framework

2.1 Introduction to the Svalbard Archipelago

The Svalbard archipelago is located between the Barents Sea and the Arctic Ocean, and stretches from 74-81°N and 10-35°E. Due to its well-exposed, diverse and extensive post-Caledonian stratigraphic record, the archipelago has been subject to extensive geological surveys for decades (Steel and Worsley, 1984). From the Devonian to the Paleogene, Svalbard moved northward from being close to the equator, to its current position. The change in environments during the movement is well reflected in the sedimentary rocks of the area.

Coal bearing successions of lower Paleogene age have been successfully mined in several locations on Spitsbergen. The island has also been subject to hydrocarbon exploration, only yielding minor non-commercial shows. However, with Svalbard being an uplifted part of the Barents Sea Shelf (Figure 2.1), it serves as a unique onshore analogue to the shelf's subsurface rocks. The Barents Sea Shelf, with its first oil and gas discoveries dating back to the 1980's, is still considered a highly lucrative area for hydrocarbon exploration.



Figure 2.1: Bathymetric and satellite map of Svalbard, the Barents Sea Shelf and the surrounding areas (Google maps).

Geologically, Svalbard is divided into several provinces (Figure 2.2). The oldest rocks are located along the west-coast of Spitsbergen and in the northeastern areas of the archipelago, consisting of metamorphic rocks from Precambrian to early Silurian age. This is where the shelf uplift was most extensive, with the western part also being further uplifted through the West Spitsbergen fold-and-

2. Geological Framework

thrustbelt (Steel et al., 1985; Friend et al., 1997; Dallmann, 1999). The northern parts of Svalbard consist of Devonian grabens, the central and eastern parts of Late Paleozoic and Mesozoic platform sediments, and the central and southern parts (Nordenskiöld Land and Nathorst Land) of The Central Basin (also known as the Central Tertiary Basin) (Steel et al., 1985; Friend et al., 1997; Dallmann, 1999).

The Central Basin is a foreland basin that developed as a response to the Paleogene West Spitsbergen Fold and Thrust belt (WSFTB) (Helland-Hansen, 2010), and might have later evolved into a piggyback basin (Blythe and Kleinspehn, 1998). It has an asymmetrical geometry with an axis close to the western part, and a width of about 60km. The Battfjellet Formation, which is the focus of this thesis, is one of seven Paleocene-Eocene (possibly Oligocene) formations included in the Van Mijenfjorden Group, which fills this basin (Harland, 1969).

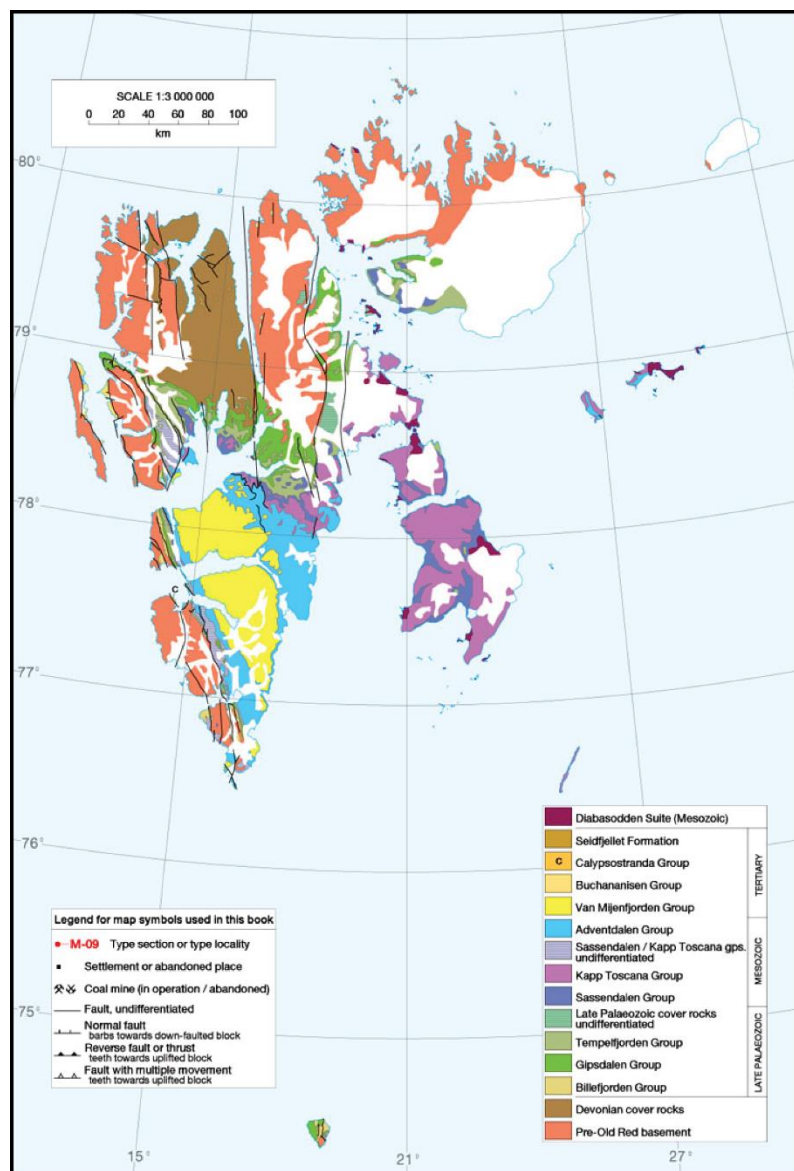


Figure 2.2: Geological map of the Svalbard Archipelago by Dallmann (1999).

2. Geological Framework

2.2 Pre-Cenozoic Stratigraphy and evolution

2.2.1 The Proterozoic and Paleozoic Eras

Referred to as “Hecla Hoek”, the Precambrian to early Silurian basement rocks on Svalbard consists of igneous, sedimentary and metasedimentary rocks with a thickness of up to 20km. Due to folding, thrusting and faulting by several orogenic events, such as the Grenvillian Orogeny (late-Mesoproterozoic) and the Caledonian Orogeny (Ordovician to Silurian), they show a highly complex arrangement (Dallmann, 1999; Worsley, 2008). Rocks younger than Devonian age, on the other hand, have been deformed relatively little (Gee et al., 1952).

The late Silurian to early Devonian sedimentation consist of the post-orogenic several kilometer thick “Old Red” sandstone facies, localized to a major graben on northern Spitsbergen (Worsley, 2008). Early to mid-Devonian marks a shift from red to grey sedimentation, reflecting the change in latitude from a dry southern environment to a more humid equatorial tropical region (Figure 2.3) (Worsley and Aga, 1986). In the late Devonian, Spitsbergen then went through a last compressional tectonic event called the Svalbardian Movements (the final phase of the Caledonian Orogeny) (Worsley, 2008).

Following the Svalbardian Movements, widespread intratectonic rifting occurred. Then, until the mid-Permian, the development of an immense post-rift carbonate platform accompanied by several large-scale basins followed. These basins were subject to episodes of extensive evaporitic deposition (Worsley, 2008; Steel and Worsley, 1984). In the mid-Permian, there was a decrease in tectonic activity, and the deposition of these warm water carbonates and evaporites was replaced by cool-water carbonates and clastics (Worsley, 2008).

2.2.2 The Mesozoic Era

Transition into the Mesozoic Era is marked by an unconformity with early Triassic non-siliceous shales on top of late Permian silica rich shales (Worsley, 2008). As the movement of the Eurasian plate continued northwards through the Triassic and Early Jurassic, deposition on Svalbard consisted mostly of delta-related coastal and shallow shelf sediments (Dallmann, 1999; Riis et al., 2008). Further transgression in the mid to late Jurassic led to the development of anoxic deep-water conditions, and deposition of organic rich shales (Worsley, 2009). Immediately overlying these organic rich shales are early Cretaceous fluvial deposits (Gjelberg and Steel, 1995). Another transgression into shallow marine deltaic deposition then followed, before Spitsbergen was uplifted and subjected to erosion during the Late Cretaceous (Steel and Worsley, 1984). As a result, no upper Cretaceous rocks are found on Spitsbergen, and the Cenozoic rocks are deposited directly on top of the lower-Cretaceous rocks (Harland, 1969; Steel and Worsley, 1984).

2. Geological Framework

Late Jurassic to Early Cretaceous dolerite sills and basaltic lavas are sign of the break-up between Greenland and Europe, which marks the opening of the Arctic and North Atlantic Oceans (Dallmann, 1999, Senger et al, 2014).

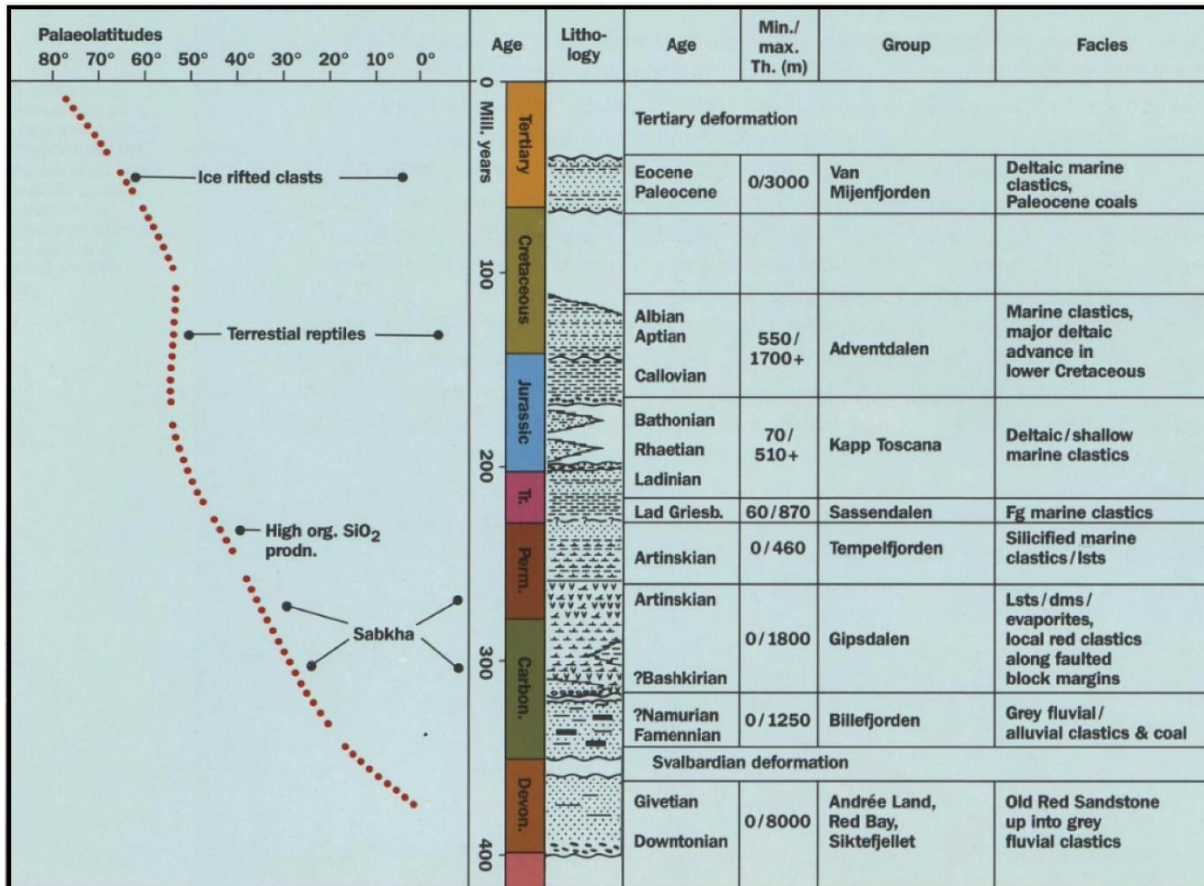


Figure 2.3: The Devonian to Cenozoic (previously Tertiary) stratigraphic column of Svalbard (Worsley and Aga, 1986). The stratigraphy reflects large-scale climatic changes as this part of the European plate moved from the southern hemisphere to its current high-arctic position. This rock record also reflects the varying change in global sea level, and regional changes in tectonic regime.

2.3 Cenozoic Stratigraphy and evolution

2.3.1 Introduction

The most pronounced Cenozoic tectonic event on Svalbard is the creation of the West Spitsbergen Orogeny, also referred to as the West Spitsbergen Fold and Thrust Belt (WSFTB). It was created as a result of dextral transpression between East-Greenland and Spitsbergen during the opening of the Arctic and North- Atlantic seaways (Helland-Hansen 2010). Along the east side of this 300km long NNW-SSE trending fold and thrust belt, flexure and tectonic loading created the 60 x 200 km Central Basin, classified as a foreland basin (Helland-Hansen, 1990). The Paleocene- Eocene (possibly

2. Geological Framework

Oligocene), sedimentary filling of this basin took place through three distinct depositional cycles consisting mostly of continental and marine clastics. This Chapter will go through the development of the WSFTB and Central Basin pair (Chapter 2.3.2), and present the sedimentary deposition within the Central Basin (Chapter 2.3.3).

2.3.2 Formation of the West Spitsbergen Fold and Thrust Belt and Central Basin

The initial opening of the Norwegian-Greenland Sea took place in the Late Cretaceous to Early Cenozoic (Braathen et al., 1999). Then, in Eocene to Early Oligocene, as the spreading ridge migrated northwards, Svalbard and Greenland were separated along the transform Hornsund fault zone. This sheared margin between the Eurasian Plate and Greenland Plate experienced a dextral movement of about 750km (Gaina et al., 2009), which resulted in a phase of dextral transpression in the Svalbard region, and the formation of the WSFTB (Figure 2.4) (Harland, 1969; Braathen et al., 1999; Dallmann and Elvevold, 2015). Bergh et al (1997) and Braathen et al (1999) divided the WSFTB into the following five structural zones:

1. The first structural zone was created through complex basement deformation of the western hinterland, which included both normal faulting and thrusting during the Late Cretaceous to Early Paleocene phase of the orogeny. The uplift of the Barents Shelf and the Svalbard region lead this early contraction to have a north-south orientation, oblique to the axis of the WSFTB (Roest and Strivastava, 1989; Braathen et al., 1999). This compression and crustal shortening lead to the growth of a low taper critical to supercritical wedge of basement rocks in the central parts of the orogeny (Braathen et al, 1999).
2. Uplift and shortening of the crust continued during the Early to Middle Paleocene creating new thrusts and rotating pre-existing thrusts in the basement rocks. The central areas of the orogeny experienced piggyback thrusting as well due to thrust progradation, while the Central Basin experienced layer parallel shortening and thrusting along decollements (Braathen et al., 1999).
3. Contraction continued, leading to basin inversion and further thrust uplifting. The previously mentioned low taper critical to supercritical wedge of basement rocks continued to form in the central parts of the orogeny, and the Central Basin experienced further shortening and decollement thrusting (Braathen et al., 1999).

2. Geological Framework

4. At the fourth stage, there was a temporary change in the direction of the crustal shortening to a northeast-southwest orientation, and a stabilization of the supercritical wedge. This led to an out-of-sequence reverse reactivation of previously established faults in the central and foreland regions creating large monoclines. Hinterland lineaments experienced dextral movement starting the creation of the Forlandsundet Graben (regional transpressive setting) (Braathen et al., 1999).
5. The last stage, of Late Eocene to Oligocene age, witnessed a structural regime change to an east-northeast, west-southwest extension, and collapse of the West Spitsbergen Orogeny (Braathen et al., 1999).

Loading from thrust sheets in the WSFTB led to regional flexural subsidence and the formation of the Central Basin (Figure 2.5), a broad north-northwest to south-southeast trending syncline (Steel et al., 1985; Müller and Spielhagen, 1990; Braathen et al., 1999). Helland-Hansen (1990), pointed to these reasons for the interpretation of the Central Basin to be a foreland basin:

- The basin's location adjacent to the orogeny.
- Syndepositional tilting of the basin floor towards the flanking orogen.
- The incorporation of the orogenic wedge into the deformation.

This interpretation is widely accepted (Steel et al., 1985; Helland-Hansen, 1990; Müller and Spielhagen, 1990; Bruhn and Steel, 2003), with Blythe and Kleinspehn (1998) also suggesting that the Central Basin might later have evolved into a piggyback basin. There is however not a general consensus whether or not the entire Paleogene basin fill has been deposited in a foreland basin setting. An extensional, possibly transtensional early to Mid Paleocene phase which in Late Paleocene to Early Oligocene had changed to a transpressional regime for the basin development was suggested by Steel et al., (1981), Steel et al., (1985) and Müller and Spielhagen, (1990). Bruhn and Steel (2003) on the other hand suggests a foreland basin setting for the entire basin fill due to a compressional regime dating all the way back to the Late Cretaceous to Early Paleocene. This interpretation is, according to Bruhn and Steel (2003), more up to date and in line with regional seafloor spreading models, recent tectonic studies and studies of the basin fill.

2. Geological Framework

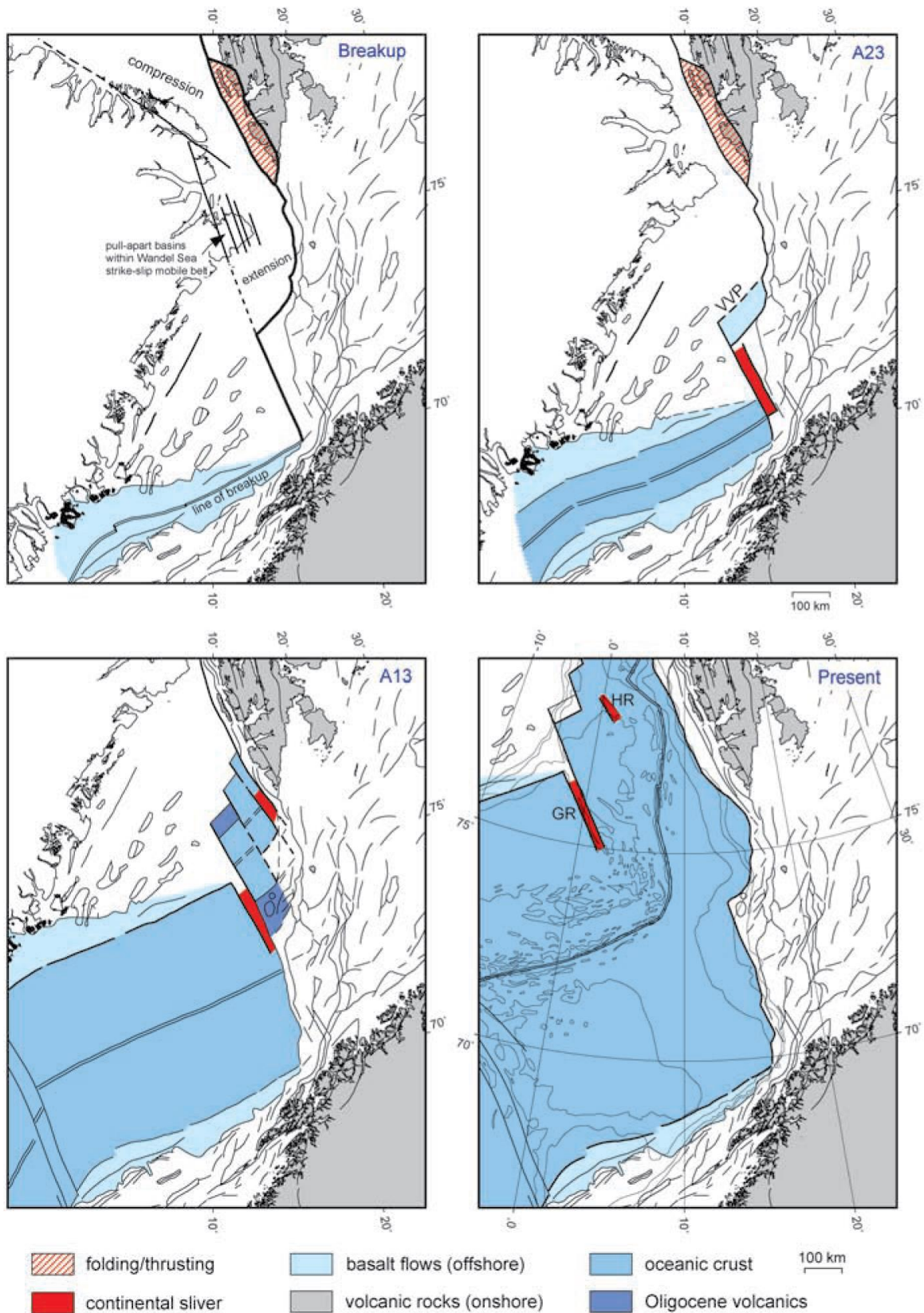


Figure 2.4: Depiction of the Cenozoic opening of the Norwegian-Greenland Sea (Faleide et al, 2008). GR: Greenland Ridge, HR: Hovgård Ridge, VVP: Vestbakken Volcanic Basin.

2. Geological Framework

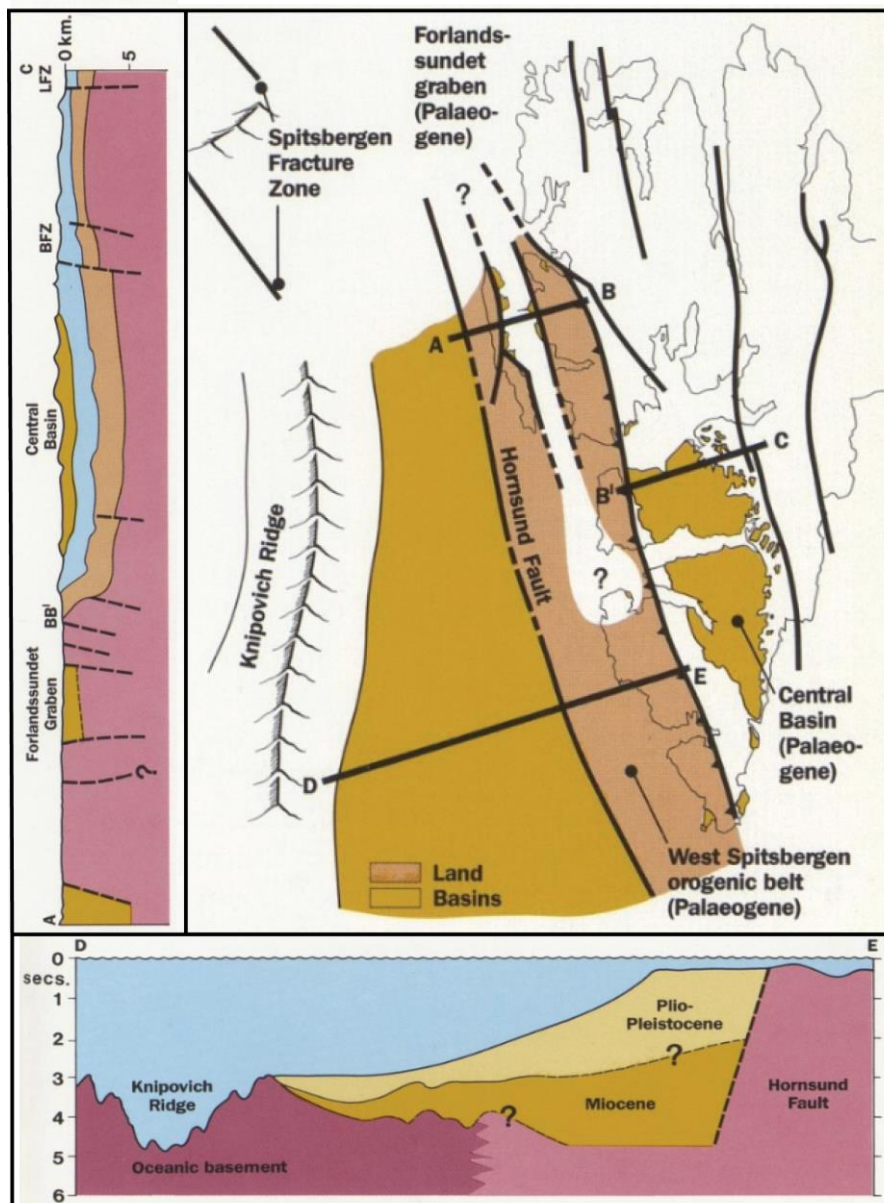


Figure 2.5: Paleogene tectonic framework and major sedimentary basins (modified from Worsley and Aga, 1986). Comparative cross-sections show onland Paleogene and offshore Neogene successions.

2.3.3 The Central Basin fill

The basin fill of the Central Basin (Figure 2.5 and Figure 2.6) reflects the shape of the asymmetric basin with thickness of 1,5km in the North-East and 2,5km in the South-west (Steel and Worsley, 1984). Vitrinite reflectance study by Manum and Thronsdon (1978) estimated an average denudation of around 1000m of overburden in addition to the >1500 m preserved succession. The basin fill of the Central Basin has been divided by Steel et al (1981), into the following three main depositional cycles:

2. Geological Framework

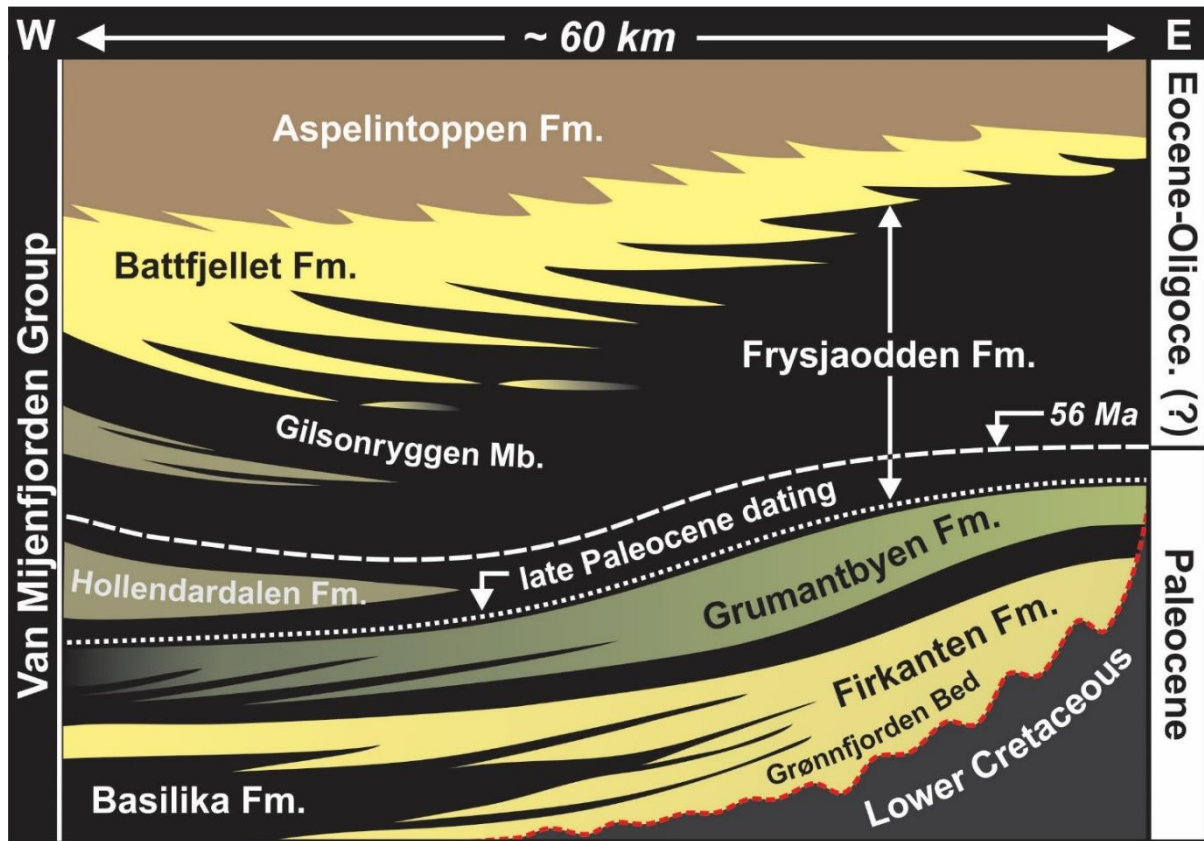


Figure 2.6: Stratigraphy of the Central Basin, modified from Grundvåg et al (2014a).

The transgressive first depositional cycle (Firkanten and Basilika formations)

Firkanten Formation:

During the first depositional cycle of the Van Mijenfjorden Group, the source area was located to the east, west and north of the Central Basin (Helland-Hansen 2010). The first deposits of the Central Basin is composed of the Firkanten Formation situated on top of the Early Cretaceous Carolinefjellet Formation, creating an unconformity (Harland et al., 1997). This unconformity is easily recognizable as it consists of the braided riverbed lag conglomerates of the Grøn fjorden Bed, on top of the Late Cretaceous Carolinefjellet Fm shelf deposits, and represents a significant hiatus of approximately 32My. The Firkanten Formation is about 80 m thick to the east, and thickens to about 200 m in the west (Bruhn and Steel, 2003).

On top of the Grøn fjorden Bed is the fluvial dominated, coal rich delta-plain deposits of the Todalen Member (Bruhn and Steel, 2003). This package interfingers with the overlying shallow marine wave-dominated sandstones of the Endalen Member (Harland et al., 1997; Steel et al., 1985), and the continental Endalen Member further interfingers with its overlying outer shelf mudstones of the Kalthoffberget Member and Basilika Formation. This overall transgressive succession has several

2. Geological Framework

smaller regressive trends within it, most notably the transition from the continental Todalen Member into the shallow marine Endalen Member.

Basilika Formation:

Capping the transgressive megasequence of the first depositional cycle is the Late Paleocene Basilika Formation (Nagy et al., 2001). This succession has been interpreted to be prodelta deposits, and is dominated by black shales. However, in the northeast and towards the top of the formation there is a coarsening and interfingering into siltstones and sandstones. The formation thickens from 20 m in the northeast part of the basin, to up to 300 m in the south and southwest (Steel et al., 1981). Scattered throughout the formation are ice-rafted pebbles, evidence of the arctic location of the Svalbard Archipelago in the Paleogene (Dalland, 1977).

The regressive second depositional cycle (Grumantbyen and Hollendardalen formations)

Grumantbyen Formation:

Overlying and interfingering with the Basilika Formation is the greenish highly bioturbated sandstones of the Grumantbyen Formation. Steel et al., (1981) and Bruhn and Steel (2003) interpreted the formation to be of a “shallow marine offshore bar complex” consisting of five major sandstone sheets with six smaller scale sequences. They further interpreted the two lowest sandstone sheets to be the more proximal equivalents of the Basilika Fm. The thickness of the Grumantbyen Fm is about 450 m in the east to northeast parts of the basin, and thins to about 200 m in the west to south west (Dallmann, 1999). Throughout the formation, there is a shallowing upwards trend, witnessing an overall regressive setting (Bruhn and Steel, 2003).

Hollendardalen Formation

Intercalate with the lower shales of the Fryjaodden Formation, is the tidal-dominated delta sandstones of the Hollendardalen Formation (Steel et al., 1985). This formation consists of several wedges with a total collective thickness of up to 150 m that thins towards the east and eventually pinches out into the Fryjaodden Fm (Dalland, 1979). This succession is the first recorded evidence of the sediment input being derived from the WSFTB (Dallmann, 1999).

As the Grumantbyen Fm and the Hollendardalen Fm is separated by a significant flooding surface, one can separate the second depositional cycle into two regressive units (Bruhn and Steel, 2003).

2. Geological Framework

The regressive third depositional cycle (The Frysjaodden, Battfjellet and Aspelintoppen formations)

The Frysjaodden Formation:

The drowning of the Grumantbyen Formation led to deposition of the prodelta shales and interbedded turbidite beds of the Frysjaodden Formation. This formation varies in thickness from around 200 m in the north, and close to 400 m in the south part of the basin (Steel et al., 1981). Overthrusting during the Late Paleocene to Early Eocene resulted in a westerly-derived sediment input, different from the underlying easterly-derived sediments (excluding the westerly derived Hollendardalen Formation) (Dallmann, 1999; Helland-Hansen, 1990). The source of the shales and interbedded turbidites are believed to be from deltas that correspond to the overlying Battfjellet Formation (Grundvåg et al., 2014a; Harland et al., 1997; Steel et al., 1985).

The Battfjellet Formation:

The Battfjellet Formation, which is the focus of this thesis, consists of deltaic wave-influenced deposits. Transition from the underlying Gilsonryggen Member of the Frysjaodden Formation into Battfjellet Fm takes place by a gradual coarsening upwards from offshore shales to more proximal siltstones and sandstones. Transition into the overlying Aspelintoppen Formation is more abrupt going from thick shallow marine sandstones to continental heterolithic. Both Gilsonryggen Member and Aspelintoppen Fm interfingers with Battfjellet Fm, and together the three formations represent the third and last depositional cycle of the Central Basin (the GBA-unit). During the early to mid-Paleogene, this depositional cycle developed in front of the West Spitsbergen Orogeny, which led to a regressive eastward migrating depocenter (Helland-Hansen, 1990; Helland-Hansen, 2010).

The Battfjellet Fm has 1-10 superimposed parasequences, each 10-30 m thick (Figure 2.4). These parasequences generally coarsen, thicken and shallow upwards. Additionally there are 100-300 m thick wedge-shaped sandstone clinothems in the lower part of Battfjellet formation in western localities, below the tabular parasequences. These are basinward extensions of the parasequences, that might, or might not extend into basin floor fans, laterally accreting towards the east. Features of these clinothems are high sediment supply, strong fluvial impact, mass gravity slope sediment transport and background wave action (Deibert et al., 2003; Crabaugh & Steel, 2004; Plink-Bjørklund & Steel, 2004). Space for shelf deltas was generated during repeated transgressions, on top of the lower steeping parts of the clinothems. Deltas would prograde in shallow water all the way to the front, eventually becoming shelf-edge deltas. Lower gradient slopes lead to less gravity flows to the east (distal part of the basin), leaving thinner sedimentary packages and absence of clinothems. The eastern part also demonstrates fewer parasequences (some places only one). Typically, the shelf- deltas have tabular

2. Geological Framework

geometries in both the east and the west, and show evidence of stronger wave influence than that of the shelf-edge deltas and clinothems (Helland-Hansen, 1985, 1990). The deltas building out on the shallow flooded shelf after transgression, on the other hand, had a flat bathymetric relief. Here, the energy of the water column played the biggest role, leaving sand-shale sediments in flat tabular facies belts.

The Aspelintoppen Formation:

Overlying the Battfjellet Formation is the Eocene to possible Oligocene continental Aspelintoppen Formation (Plink-Björklund, 2005; Steel et al., 1985). This formation represents the last sedimentary infill of the Central Basin, and is comprised of fluvial channel, floodplain and interdistributary lake and bay deposits. Its alternating layers of siltstones, shales, coals and channel sandstones reach a thickness of over 1000 m, and comprises the mountaintops of the study area. The boundary between the Aspelintoppen Fm and the underlying Battfjellet Fm is easily distinguished in field by a rooted horizon and the first occurrence of coal beds or fine-grained shales above the cliff forming sandstones of the Battfjellet Fm. Internally, the succession has extensive soft sediment deformation and is littered with plant remains. This has given leeway for abundant fossil collection and paleoflora studies, that suggests a depositional environment similar to the present temperate Canadian arctic environment (Manum, 1962; Clifton, 2012).

2.4 Time Constraints

Time constraints on structuring of the WSFTB and the accompanying Central Basin deposition is limited to only a few datings. One gives a Late Paleocene age, based on dinoflagellate species in the lowermost part of the Frysjaodden Fm (cf. Manum and Thronsen, 1986). Other studies using radiometric dating of bentonites in combination with astrochronology estimated a ca.56 Ma at the level of the Paleocene-Eocene thermal maximum (PETM), close to the base of the GBA-unit (Charles et al., 2011; Harding et al., 2011). Age of the Aspelintoppen Fm has also been suggested to be of early Eocene, based upon comparison of other Arctic floras (Manum & Thronsen, 1986; Kvaček, 1994; Golovneva, 2000; Clifton, 2012). Furthermore, it is mostly assumed that the GBA-Unit is of predominantly Eocene, and possibly Oligocene age, due to its large thickness and the previously mentioned post late Paleocene age.

2. Geological Framework

A Foraminifera study by Nagy et al., (2001), and a fission track dating study of apatite grains by Blythe and Kleinspehn (1998), was done to determine the age of other formations within the Van Mijenfjorden Group. They established a late Paleocene age for the Basilika formation, a Selandian age of the Kalthoffberget Member, and Danian age for the Endalen and Todalen members of the Firkanten Formation.

3. Methodology

3. Methodology:

3.1 Data acquisition

Three weeks of sedimentological fieldwork was done on Liljevalchfjellet, Svalbard. The area is approximately 5 x 1.5 km, stretching from northeast to southwest, west of Svea and north of Van Mijenfjorden (Figure 1.1). Six logs were collected, along with paleocurrent measurements and photos. While logging, thickness measurements were taken using a meter stick. GPS based meters above sea level estimates taken at top and bottom of each logged section showed a total offset of up to 20m when using this method. Tracing the lateral extent of sandstone bodies proved difficult in some areas due to a combination of steep mountain cliffs and abundant scree cover.

Deposits were divided into fourteen different lithofacies, based upon their rock properties and then grouped into four facies associations based upon their genetic relation and environmental significance (see Chapter 4).

3.2 Digitalization

The logs were scanned and redrawn using Adobe Illustrator CC 2015 software. The logs in the appendix are shown in a 1:50 scale while the logs in the facies association descriptions are shown in a 1:20 scale (excluding the log presenting FA4, which is shown in 1:50 scale). Adobe Illustrator CC 2015 software was also used when making figures, and transferring referenced figures from other scientific papers.

3.3 Rose Diagrams

For visualization of the paleocurrent measurements, several rose diagrams were made. First, the measurements were separated by area, facies association and type of depositional structure (see Appendix 2). They were then transferred to Excel, and sorted by their orientations into 32 batches, each representing 11.25° of a 360° orientation. The data were then used to create rose diagrams using the rose diagram creator on geographyfieldwork.com

4. Lithofacies and Facies Associations

4. Lithofacies and Facies Associations

4.1 Lithofacies:

Based upon the studied outcrops, the sedimentary deposits have been subdivided into lithofacies based upon the following properties: grain-size, grain-size trend, sedimentary structures, texture, bioturbation, bed shape, bed thickness and boundary type. The lithofacies are presented in Table 4.1 below:

Table 4.1: Lithofacies with dominant grain sizes, main depositional features and depositional interpretation. HCS = hummocky cross stratification, PPL= planar parallel lamination.

Lithofacies	Lithology	Description	Interpretation
F1	Shale/ Mudstone	Dark grey to black (can appear purple) shales and mudstones with weakly undulating lamination and abundant bioturbation.	Fallout from suspension in a tranquil environment.
F2	Siltstone and very fine sandstone	Thin lense shaped silt and sandstone beds of up to 2 cm thickness and 5 cm width, and tabular sandstone beds of a few millimeters to 10 cm. Thicker beds have erosive bases with sole marks and rare siderite concretions.	Turbiditic deposits, induced by veining stage storm bottom flows.
F3	Very fine sandstone	10 cm to 1 m sandstone beds with mainly hummocky cross stratification (HCS). Capping the beds are a few centimeters of wave ripples and occasional combined flow ripples. Abundant soft sediment deformation exists throughout.	Storm deposits (tempestites).
F4	Very fine - fine sandstone	Amalgamated sandstone beds with alternating layers of PPL and wave ripples. The PPL beds are generally thicker (10-20cm) than the rippled layers (5-10cm). Occasional siltstone drapes with abundant carbonaceous detritus and vertical burrows.	Veining combined unidirectional and oscillatory flow deposits.
F5	Fine - medium sandstone	Truncating trough cross-stratified sandstones of 7-20 cm thickness. Wave-rippled horizons of 5-10 cm thickness exists between some of the smaller troughs.	Deposits from locally eroding, possibly breaking waves
F6	Fine – medium sandstone	Tabular cross-stratificatied sandstone beds ranging in thickness from 10-40 cm.	Combined longshore currents and waves deposits
F7	Fine – medium sandstone	0.5-1.5 m thick lichen covered and heavily fractured sandstones capped with low angle PPL. Abundant roots in the top 5-10 cm.	Breaking wave's swash and backwash deposits.
F8	Conglomerate (pebbles - cobbles)	1-5cm thick mudclast rich siderite-cemented layer with a highly erosive base, immediately overlain by conglomerate of varying thickness (5cm-40cm). The conglomerate has abundant carbonaceous detritus, is clast supported, polymikt, with sub-rounded to sub-angular clasts and has a coarse to very coarse-grained sandy matrix. Laterally the grainsizes vary dramatically from pebbles to 10 cm cobbles	High competence fluvial channel floor deposits
F9	Conglomerate – medium sandstone	Tabular cross-stratified sandstones with a thickness of 15 cm – 1 m. Conglomerate extends upwards from the lower parts of the foresets.	2D dunes migrating on a fluvial channel floor.

4. Lithofacies and Facies Associations

F10	Medium – coarse sandstone	Trough cross-stratified sandstones with a thickness of 14-40 cm containing scattered pebbles and coal chips throughout. The dominant structure changes to current ripples in the top	3D dunes migrating on a fluvial channel floor.
F11	Medium sandstone	Current rippled sandstones with a fining upwards trend, capped by a 5-10 cm rooted horizon.	Deposits from low flow velocities in the inner turn of a fluvial meander.
F12	Siltstone and fine sandstone	1-2 m thick, heterolithic deposits with 2-10 cm fine sandstones separated by thin 0.1–2 cm layers of siltstones. Sandstone beds have abundant current ripples, while the siltstones consist of finely laminated PPL. Abundant roots, leaves and bioturbation exist throughout.	Floodplain, overbank deposits.
F13	Coal	2-5 cm thick layers of coal	Plant material deposited in dense forests.
F14	Siltstone and fine sandstone	30 cm to 1 m of heterolithic deposits with 1-10 cm wave-rippled and some combined-flow-rippled fine sandstones, separated by thin 0.1-1 cm siltstones. Abundant roots, leaves and bioturbation exist throughout.	Interdistributary lake deposits.

4.2 Facies associations

Stacking patterns of the 14 lithofacies gathered from the six outcrops are not random. Based upon genetic relation and environmental significance, the facies have been grouped together into four facies associations that define a particular depositional environment. These facies associations are summarized in Table 4.2 below, and will be more thoroughly presented in the following sub chapters.

Table 4.2: Facies associations

Facies associations	Facies	Depositional environment	Formation	Thickness	Figure
FA1	F1, F2	Prodelta/ offshore	Frysjaodden	> 200 m	4.1 4.2
FA2		Prograding wave-dominated delta	Battfjellet	12 - 60 m	4.6
- FA2-A	F1, F2, F3	- Offshore transition zone		10 – 55 m	4.3
- FA2-B	F2, F4, F5	- Lower shoreface		1 – 14 m	4.4
- FA2-C	F5, F6, F7	- Upper shoreface and foreshore		1 – 6 m	4.5
FA3	F8, F9, F10, F11	Distributary fluvial channel	Aspelintoppen	9 - 14 m	4.8 4.9
FA4	F 12, F13, F14	Deltaplain (floodplain and interdistributary lake deposits)	Aspelintoppen	> 200 m	4.10

4. Lithofacies and Facies Associations

Not all of the four facies associations are present in each logged section (Table 4.3). Worth noting is that though Log D, Log E and Log F do not contain FA1 (Prodelta/Offshore deposits), FA1 exists below the logged section in these areas (observed in field). These deposits were not included in these logged sections due to them being completely covered by scree. Table 4.3 below presents the facies associations present at each logged location:

Table 4.3: Presence of the different facies associations at each logged section.

Locality	FA1	FA2	FA3	FA4
Log A	X	X	X	X
Log B	X	X	X	X
Log C	X	X	X	X
Log D		X		X
Log E		X	X	X
Log F		X	?	X

All interpreted facies associations of Battfjellet Fm contains soft sediment deformation structures and abundant carbonaceous detritus in the form of coal chips or plant fragments. This indicates an environment with a high rate of deposition and a large amount of the sediments being terrestrially supplied.

Importantly, abundant scree cover is present in FA1 (Prodelta/Offshore deposits), FA2-A (Offshore transition zone deposits) and FA2-B (Lower shoreface deposits). In these areas, logs and interpretations are based on incomplete outcrops with low lateral continuity. This makes facies transitions difficult to interpret. For example, no areas of only amalgamated beds of HCS were located, even though they might be present. Transition from FA2-A (Offshore transition zone deposits) to FA2-B (Lower shoreface deposits) is therefore (in this thesis) set at the transition where there is a change from HCS into PPL and wave ripples being the dominant sedimentary structure.

4. Lithofacies and Facies Associations

4.2.1 Facies association 1 (FA1): Offshore deposits (Figures 4.1 and 4.2)

This facies association consists of the soft and extensively weathered deposits of the over 200 m thick Gilsonryggen Member of the Frysjaodden Formation. Therefore, most of FA1 are covered by black shale scree, making it hard to determine exact facies transition into the overlying FA2-A (Offshore transition zone deposits). The base of the logs starts at the lowest outcrop found. This means that FA1 as described in this thesis only represents the uppermost parts of the Gilsonryggen member.

Description:

FA1 consists of heterolithic with mudstones, siltstones and very fine sandstones (Figure 4.1). The dark grey to black (can appear purple) shales and mudstones (F1) demonstrates weakly undulating lamination. Bioturbation is abundant in these beds, but it is hard to tell what type of burrows are present due to the weathering. Sands (F2) are present as thin lenses of up to two cm thickness and five cm width in the lower part, while tabular beds become more abundant upwards throughout the FA1. These sands range in thickness from a few millimeters up to 10 cm, having ripples (some current and some wave ripples), tiny coal fragments (< 0.5 cm), and abundant bioturbation at tops and bases. The thicker beds have erosive bases sometimes with sole marks, rare siderite rich concretions (Figure 4.1 B), rare water escape structures (Figure 4.1 C) and slight fining upwards. Towards the top of the facies association, the sands become thicker, more abundant and more amalgamated, before transitioning into FA2-A (Offshore transition zone deposits).

Figure 4.1 below presents a detailed log of FA1 with accompanying photos of depositional structures commonly found in the facies association, while Figure 4.2 presents a section of FA1 from Log A and overview photos of how the outcrops and scree covered slopes of the facies association.

4. Lithofacies and Facies Associations

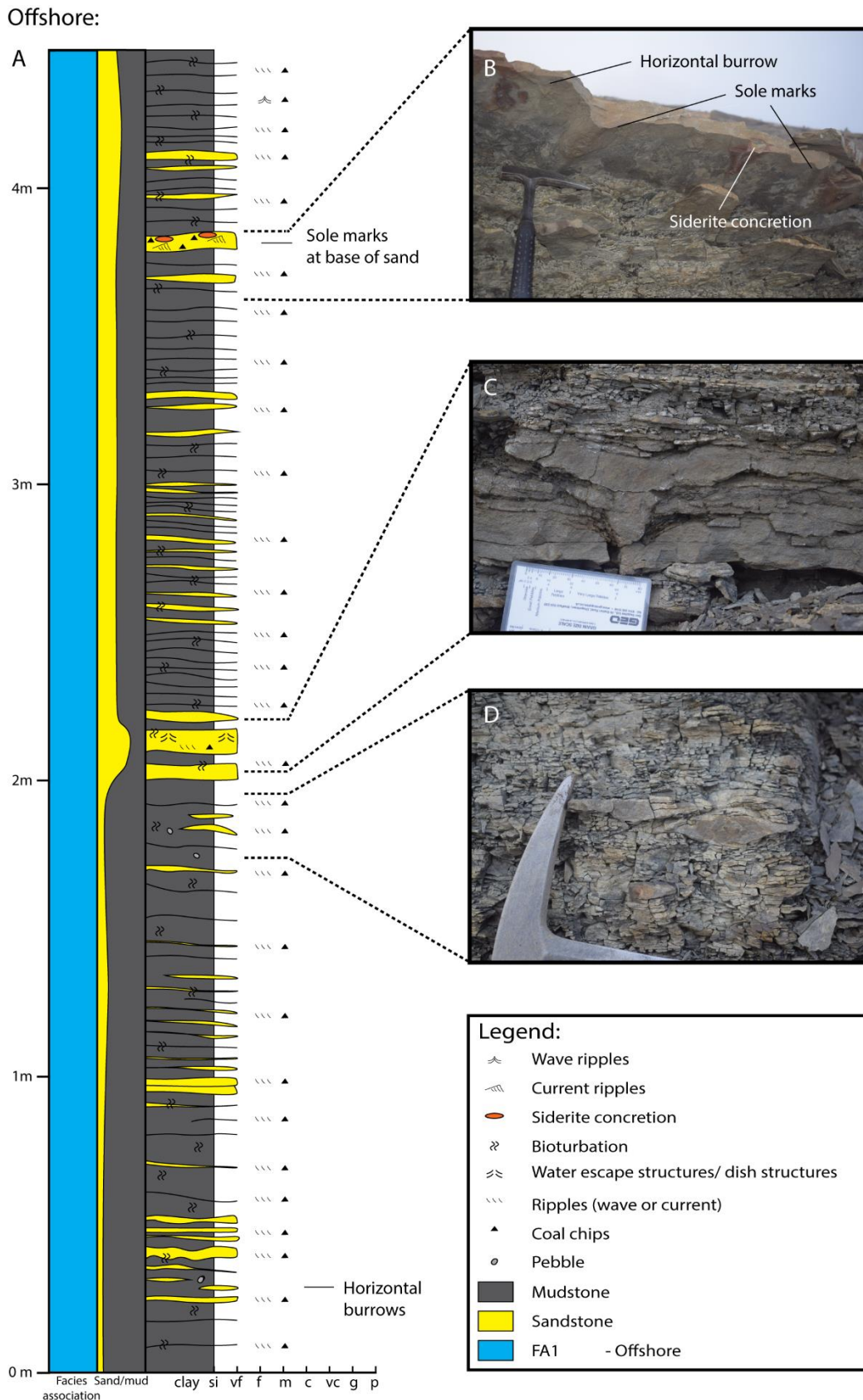


Figure 4.1: (A) Detailed log of FA1: Offshore deposits (excerpt from Log C). (B-D) Photographs showing typical features of FA1. (B) Horizontal burrows, siderite concretion and sole marks. (C) Water escape structure in thicker sand layer. (D) Sand lenses in mudstone.

4. Lithofacies and Facies Associations

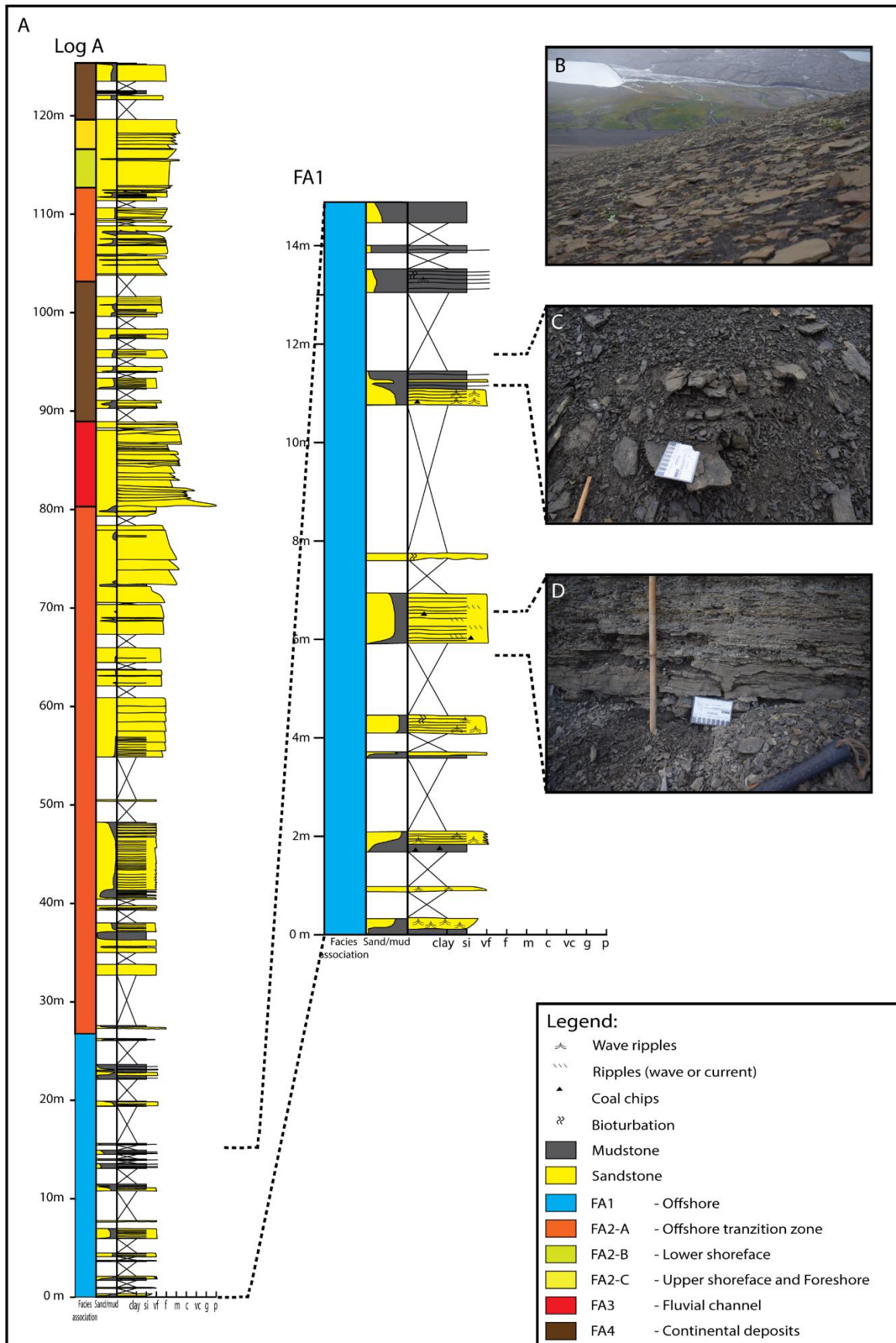


Figure 4.2: (A) Section of FA1: Offshore deposits, from Log A. (B) Overview photo of the scree slopes of FA1. (C) Typical thin outcrop of offshore deposits. (D) Outcrop with offshore heterolithic sandstones and siltstones.

4. Lithofacies and Facies Associations

Interpretation:

Due to dominance of fine grained material and lack of evidence for waves or tidal influence, the mudstones are interpreted to be deposited by fallout from suspension. This must have been in longer periods of tranquil water, below the storm-weather wave base, leading to the interpretation of an offshore depositional environment for FA1. The very fine sandstone layers are interpreted to be beds deposited in the distal parts of rare and dramatic storm events. During the veining stage of these storms, water piled up against the shoreline, flows back in far stretching density currents along the sea floor. This can create thin turbidity currents in the outer reaches below the storm-weather wave base, depositing thin lenses and tabular beds of sand like in Facies A (Hamblin and Walker, 1979). The rippled sands present in FA1 are interpreted to be the C part of the Bouma sequence. Further supporting this interpretation are the few water escape structures found in the thicker beds of sand. This is commonly in turbidites due to rapid deposition (Moretti et al., 2001). In addition, sole marks at base of some of the thicker sands show the erosive nature of the turbidity currents.

The general coarsening and thickening upwards trend, overlain by FA2-A (Offshore transition zone deposits) suggests a shallowing upwards trend throughout the section. In addition, the horizontal burrows (some of which was simple, gently curved *Planolites*) found at tops and bases of the sands suggests a *Cruziana* ichnofacies, which is common for shallow marine and offshore environments (Seilacher, 2007).

4.2.2 Facies association 2 (FA2): Prograding wave-dominated delta deposits (figures 4.3-4.7)

FA2 have been subdivided into FA2-A (Offshore transition zone deposits), FA2-B (Lower shoreface deposits) and FA2-C (Upper shoreface and Foreshore deposits) which are stacked on top of each other in a shallowing upwards and coarsening upwards fashion (Figure 4.3). In its lower part, FA2 transitions gradually from FA1 (offshore deposits), while at the top, it is sharply capped by FA 3 (Distributary fluvial channel deposits) or FA4 (Continental deposits). The thicknesses of FA2 in the logged sections ranges from 12-60 m, and a high amount of carbonaceous detritus is present throughout. This chapter presents thorough descriptions and interpretations of FA2-A, FA2-B and FA2-C, followed by the interpretation of the total succession of FA2.

A log interval of FA2 from Log A, and overview photos of some of the deposits are presented in Figure 4.3 below:

4. Lithofacies and Facies Associations

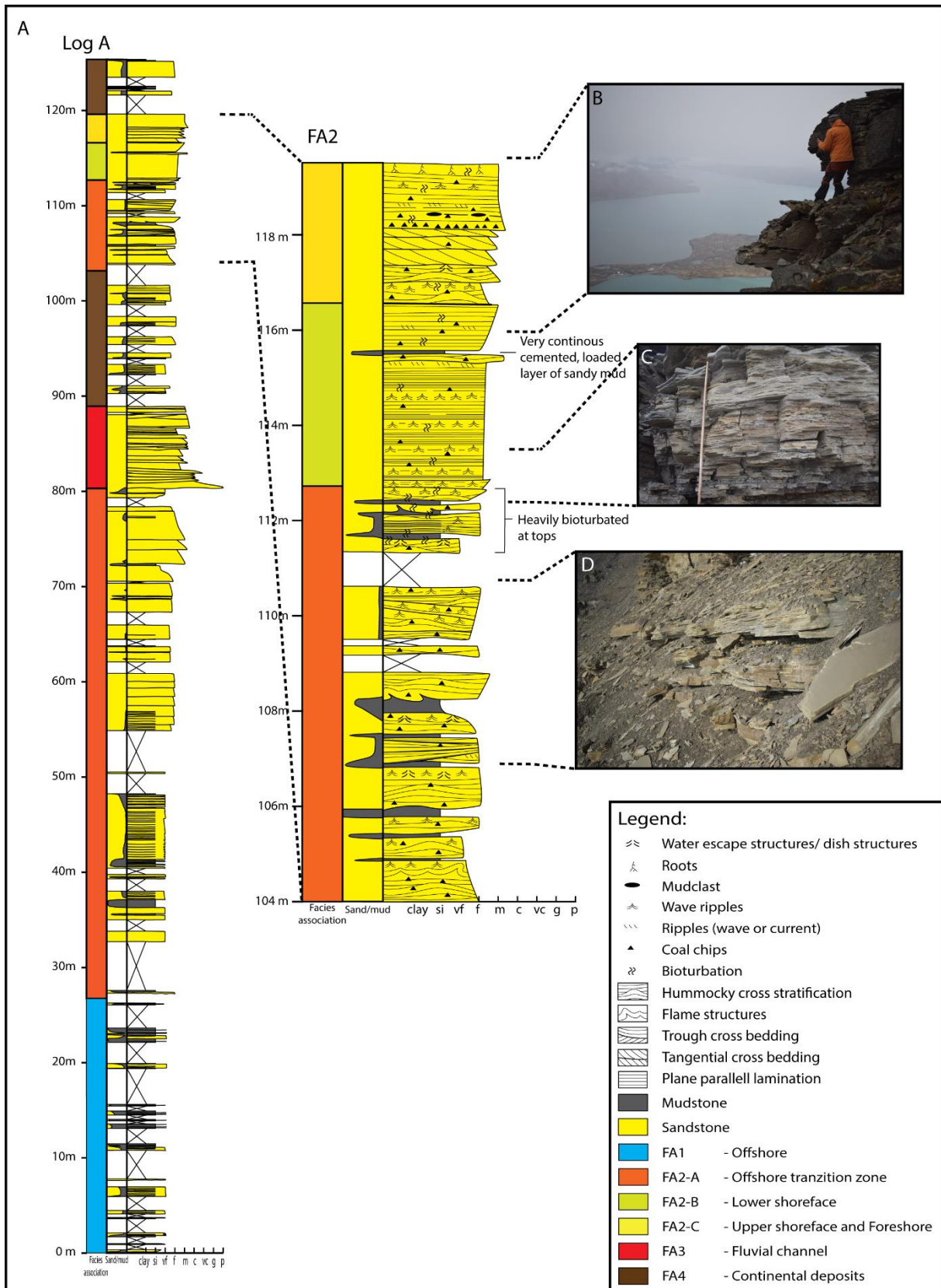


Figure 4.3: (A) Detailed log interval of FA2: Prograding wave-dominated delta deposits, from Log A. (B) Upper shoreface and shoreface deposits. (C) Lower shoreface deposits. (D) Offshore transition zone deposits.

4. Lithofacies and Facies Associations

Facies association 2-A (FA2-A): Offshore transition zone deposits (Figure 4.4)

Description:

FA2-A varies in thickness from 10–55 m in the study area. It consists mostly of thin to thick units (10 cm – 1 m) of fine to very fine sandstone (F3), either amalgamated or separated by siltstone (1-10 cm) or heterolithics (F1 and F2). Siltstones are more abundant in the lower part of the facies, whereas the thicker sand-packages become more common and eventually more amalgamated towards the top, where the facies transitions into FA2-B (Lower shoreface deposits). The lower parts of FA2-A are also more scree covered than the upper parts meaning the lower part is most likely siltstone dominated. The thinly laminated siltstones (F1) in the lower part of FA2-A often have 1-5 cm tabular or lens shaped fine to very fine sandstone interbeds (F2). They are also bioturbated, but it is hard to tell the extent of bioturbation or type of trace fossil due to weathering. The thicker sandstone beds exhibit hummocky cross stratification (HCS) (Figure 4.4 C) as the most prominent sedimentary structure with a few centimeters thick ripples (mostly wave ripples, but also some combined flow ripples) (Figure 4.4 B) at top. A few of the thicker sandstone beds appear to have low angle dipping PPL, however these might be part of larger HCS. Additionally these beds exhibit thinning upwards, typically have few mudclasts, occasional siderite concreted layers (relatively fewer than in FA1) and scattered small plant fragments (<1 cm). The base of these sandstone beds have erosional structures and more abundant coal fragments. Tops are slightly undulating and exhibit bioturbation where they are not eroded by an overlying amalgamated sandstone bed.

Throughout FA2-A abundant water escape structures (dish structures and flame structures) (Figure 4.4 D) and occasional ball and pillow structures are present, especially in the thick sandstone layers which also have loading structures into the underlying siltstones.

4. Lithofacies and Facies Associations

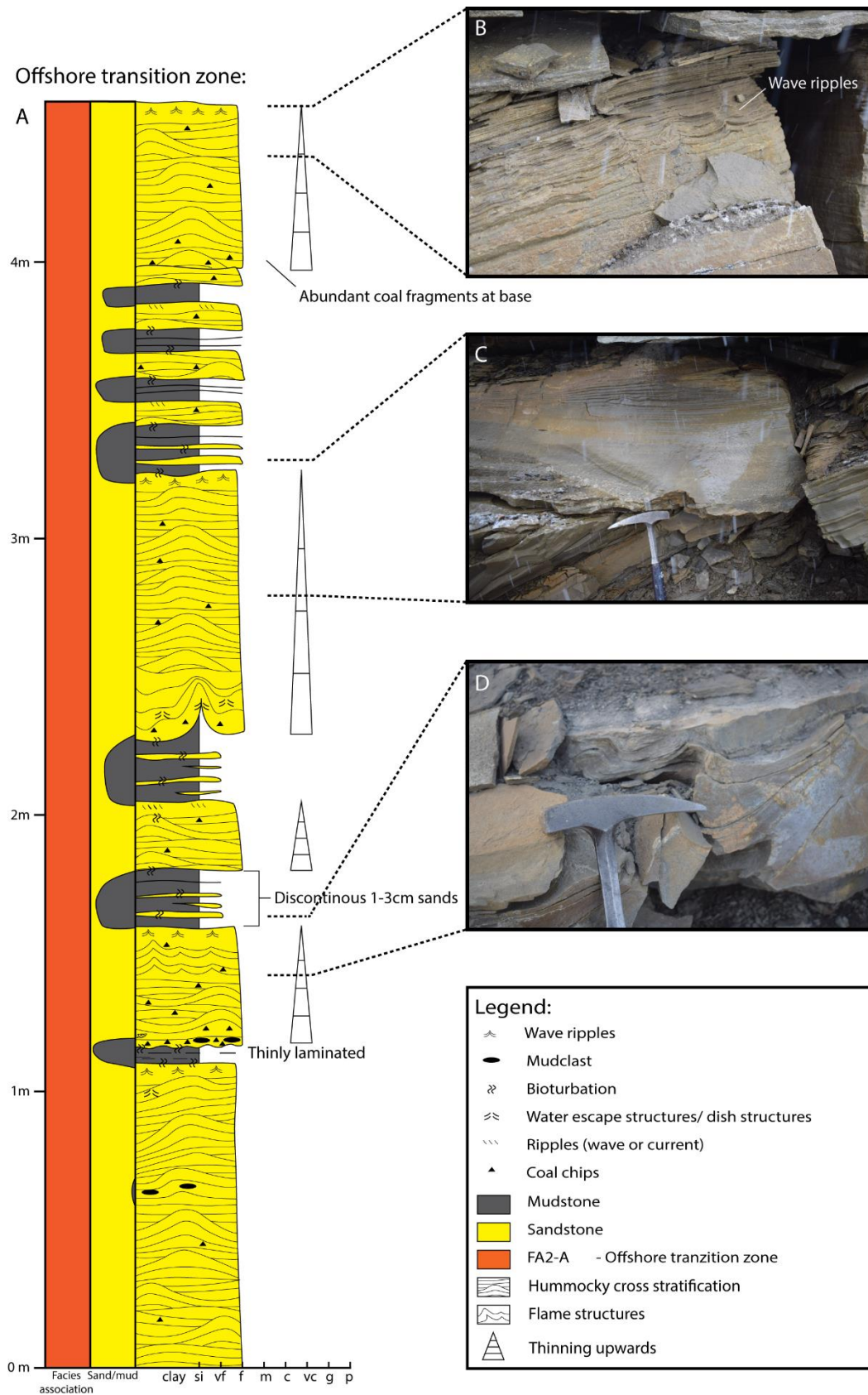


Figure 4.4: (A) Detailed log of the middle part of FA2-A: Offshore transition zone deposits (excerpt from Log A). (B-D) Photographs showing typical features of FA2-A. (B) Wave ripples. (C) Thick bed with hummocky cross stratification (HCS). (D) Water escape structures.

4. Lithofacies and Facies Associations

Interpretation:

The sandstone beds with HCS as the dominant sedimentary structure, and wave ripples (some combined flow ripples) at top are interpreted to be tempestites deposited during strong storms. Storms erode sediments from the upper shoreface and foreshore, and redistributes sands to the lower shoreface and beyond (Reading and Collinson, 1996). The siltstone beds are deposited as fallout from suspension during tranquil waters between these storms. Sandstone beds thus represents episodic depositional events, while the siltstone beds constitute the background sedimentation. Reading and Collinson (1996) suggested that such changes between low-energy background sedimentation and high-energy storm deposition characterizes a depositional environment between fair-weather wave base and storm-weather wave base, corresponding to the offshore transition zone.

There is an agreement in the literature that HCS is formed in relation to storms, but the exact processes that forms these structures has been thoroughly debated (Swift et al., 1983; Duke et al., 1991). Generally it is envisioned that HCS is either formed by complex oscillatory flows or storm wave-generated oscillations that are superimposed on a geostrophic flow (shore-oblique or to shore-normal geostrophic relaxation flow currents formed by costal buildup) (e.g. Héquette & Hill, 1993). High-velocity, continuous oscillatory or oscillatory-dominated combined-flows above storm wave base creating migrating and aggrading symmetrical to near-symmetrical 3D dunes are therefore considered responsible for the formation of HCS (Jelby et al., in prep). The wave ripples at the top of the storm beds were produced by oscillatory currents during the waning stages of the storm. At this point, the storm waves creating these oscillatory currents barely reached the seafloor (Stene, 2009). The thin tabular to lens shaped sandstone beds within the siltstones are interpreted to be storm sand layers deposited under similar conditions, but in deeper water. These tempestites are also containing few beds with low angle PPL leading to the interpretation of them being what Jelby and colleagues (Jelby et al., in prep) classifies as unsteadily generated tempestites.

The abundant soft-sediment deformation structures in the offshore transition zone deposits of the Battfjellet Fm were interpreted by Helland-Hansen (2010) to be a result of rapid deposition (perhaps also poor sorting-pressure build-up) of the tempestites.

Higher amount of siltstones in the lower parts of FA2-A and more amalgamated sandstone beds in the upper parts, show a general coarsening and shallowing upwards trend within the facies. This trend continues upwards where FA2-A is eventually gradually replaced by FA2-B (Lower shoreface deposits) in most areas.

4. Lithofacies and Facies Associations

Facies association 2-B (FA2-B): Lower shoreface deposits (Figure 4.5)

Description:

FA2-B varies from 1-14 m thickness in the study area. It consists mostly of fine to very fine sandstone with rare layers of laminated sandy siltstone (F2) of 1-10 cm thickness in the lower parts. In field, there is a clear transition from the scree covered mountain slopes and occasional outcrops of FA2-A, to the steep sandstone cliffs of FA2-B (Figure 4.5 D). The dominating feature of the sandstones (F4) are alternating layers of planar parallel lamination (PPL) and ripples (mostly wave ripples, but also some combined flow ripples) (Figure 4.5 C) with occasional small isolated trough cross beds (F5) truncating the PPL. The PPL beds are generally thicker (10-20 cm) than the rippled layers (5-10 cm), and sometimes erode the tops of underlying ripples leaving a sharp horizontal contact between the two (no relief on the truncation). This leaves both the wave rippled and PPL beds flat and laterally extensive. Additionally, thin siltstone drapes with very abundant coal fragments occur rarely throughout the PPL. Some sandstone beds appear more massive and are dominated by thicker low angle dipping PPL (Figure 4.5 B) rather than the alternating layers of PPL and ripples. Few beds show a clear fining up, from fine to very fine sandstone. Many of the sandstone beds have erosive bases and contain layers of abundant mudclasts (rip-up mudclasts) in the lowest parts, some of which are siderite concreted.

Water escape structures (dish structures, flame structures) (Figure 4.5 E) and occasional ball and pillow structures occur less frequently than in FA2-A, but is still common. Especially loading between the thin sandy siltstone and the sandstone is prevalent. Vertical burrows are present throughout FA2-B, though bioturbation seems less abundant than in FA2-A.

4. Lithofacies and Facies Associations

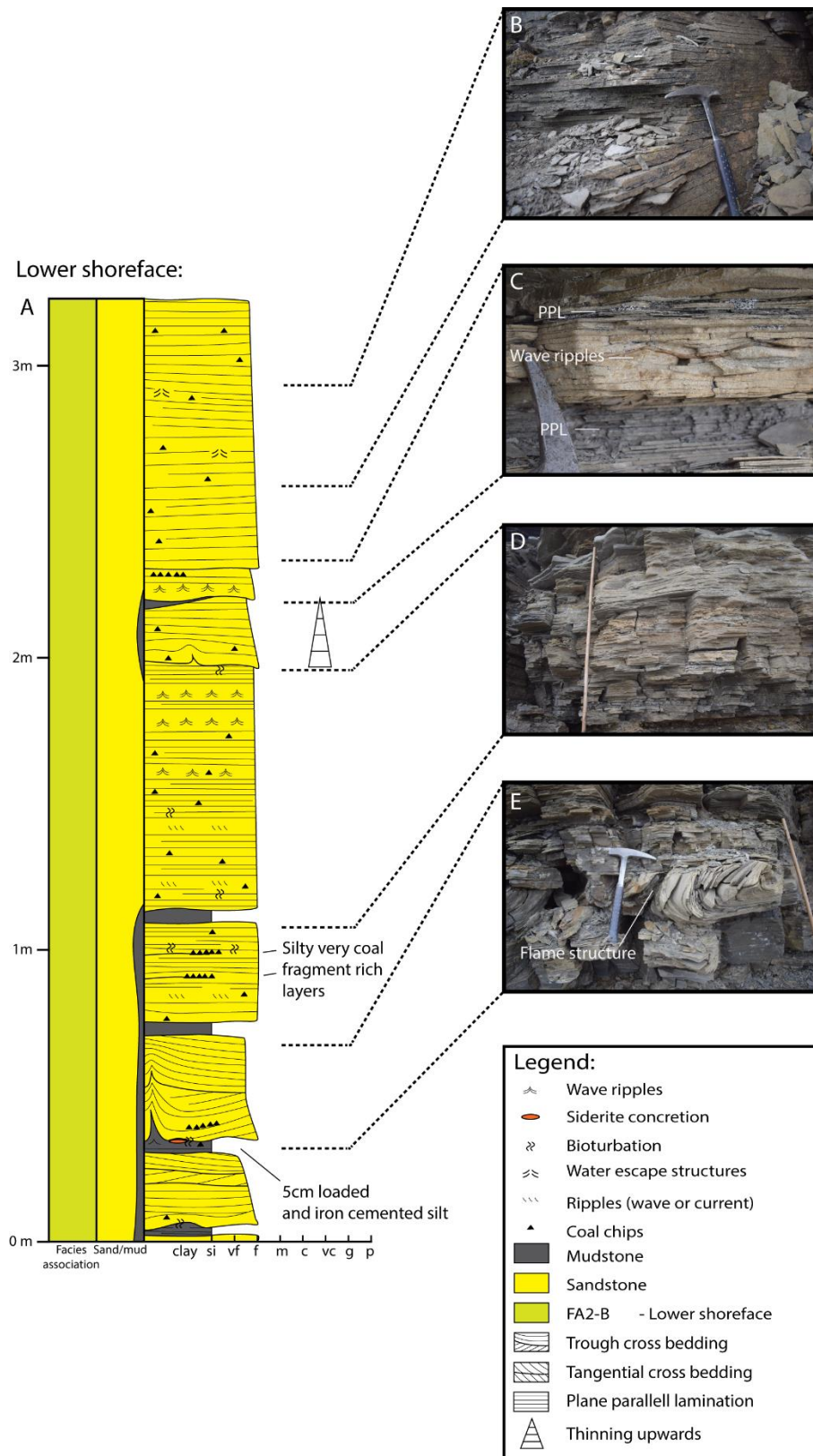


Figure 4.5: (A) Detailed log of FA2-B: Lower shoreface deposits (excerpt from Log C). (B-E) Photographs showing typical features of FA2-B. (B) Low angle planar parallel lamination (PPL). (C) Close up of alternating layers of planar PPL and wave ripples. (D) Overview of a vertical outcrop with several alternating layers of ripples and PPL. (E) Flame structure.

4. Lithofacies and Facies Associations

Interpretation:

The higher sand/mud ratio in FA2-B compared to underlying FA2-A, along with the lower amount of bioturbation, indicates a higher sedimentation rate with more persistent wave action. Being closer to the shore, this wave action inhibited deposition of silt and mud creating the amalgamated sandstone beds of FA2-B. This is indicative of a depositional setting above the fair-weather wave base (Helland-Hansen 2010). At the same time, the wave action and sedimentation rate was not too high, keeping habitable conditions for burrowing organisms.

The sandstones with alternating layers of PPL and wave ripples found in FA2-B are a common characteristic of lower shoreface deposits (Plink-Björklund et al., 2001). In combined flows where the unidirectional current component are even just a small fraction of the oscillatory component, PPL is created (Arnett and Southard, 1990). The PPL of Facies B is erosionally based and grades into wave ripples, suggesting that the PPL was deposited at the time when both the unidirectional and oscillatory components of the flow were at its strongest point (Cheel, 1991). The wave-orbital velocities then decreased from the upper flow regime, to the lower flow regime during more fair-weather conditions, favoring deposition of wave ripples. Hill et al., (2003) suggests that the PPL and wave-ripple couplets are a result of alternating high-energy storm and low energy fair-weather conditions. The absence of a dune bedform between the PPL and wave-ripples is likely due to the transition between them being too quick relative to the time needed for dune formation. Beds with low angle PPL, appearing more massive suggests continuous deposition in a high-energy environment, or superimposing PPL having fully eroded away previously deposited rippled sands. The occasional small trough cross-stratified beds truncating the PPL was identified by Helland-Hansen (2010) to reflect local erosion and deposition under larger than normal, and possibly breaking, waves.

Abundant carbonaceous detritus especially in the few thinner siltstone layers tells that sediments from terrestrial sources played an important role in deposition of FA2-B.

4. Lithofacies and Facies Associations

Facies association 2-C (FA2-C): Upper shoreface and Foreshore deposits (Figure 4.6)

FA2-C is divided into upper shoreface deposits and foreshore deposits, together making up 1.5–6 m thick successions. One of the criteria used to interpret deposits to be of upper shoreface is the transition into overlying foreshore deposits. It is therefore convenient to group them together into FA2-C. This facies association caps the sandstone cliffs in the study area where it transitions into the overlying FA4 (Aspelintoppen Fm). A transition that is easily distinguished in field by a flat mud and moss-covered plateau on top of the Battfjellet Fm sandstone cliffs.

Description:

The upper shoreface deposits consist of fine to medium sandstone beds. Dominating structures are tabular cross-stratification with a scattered dip orientation and ranging in thickness from 10-40 cm (F6) (Figure 4.6 C), and occasional of 7-20 cm thick trough cross-stratification (F5). The cross stratification show internal fining upwards, though the beds get overall thicker and coarser upwards. Wave-rippled horizons of 5-10 cm thickness exists between some of the smaller troughs.

The foreshore deposits lay immediately on top of the upper shoreface deposits, and consists of fine to medium sandstone beds (F7). They appear in the field as 0.5-1.5m thick lichen covered and heavily fractured vertical walls that caps the sandstone cliffs (Figure 4.6 B). The only structures observed are thick-bedded low angle PPL and abundant vertical roots of up to 5cm in the uppermost 5-10 cm.

4. Lithofacies and Facies Associations

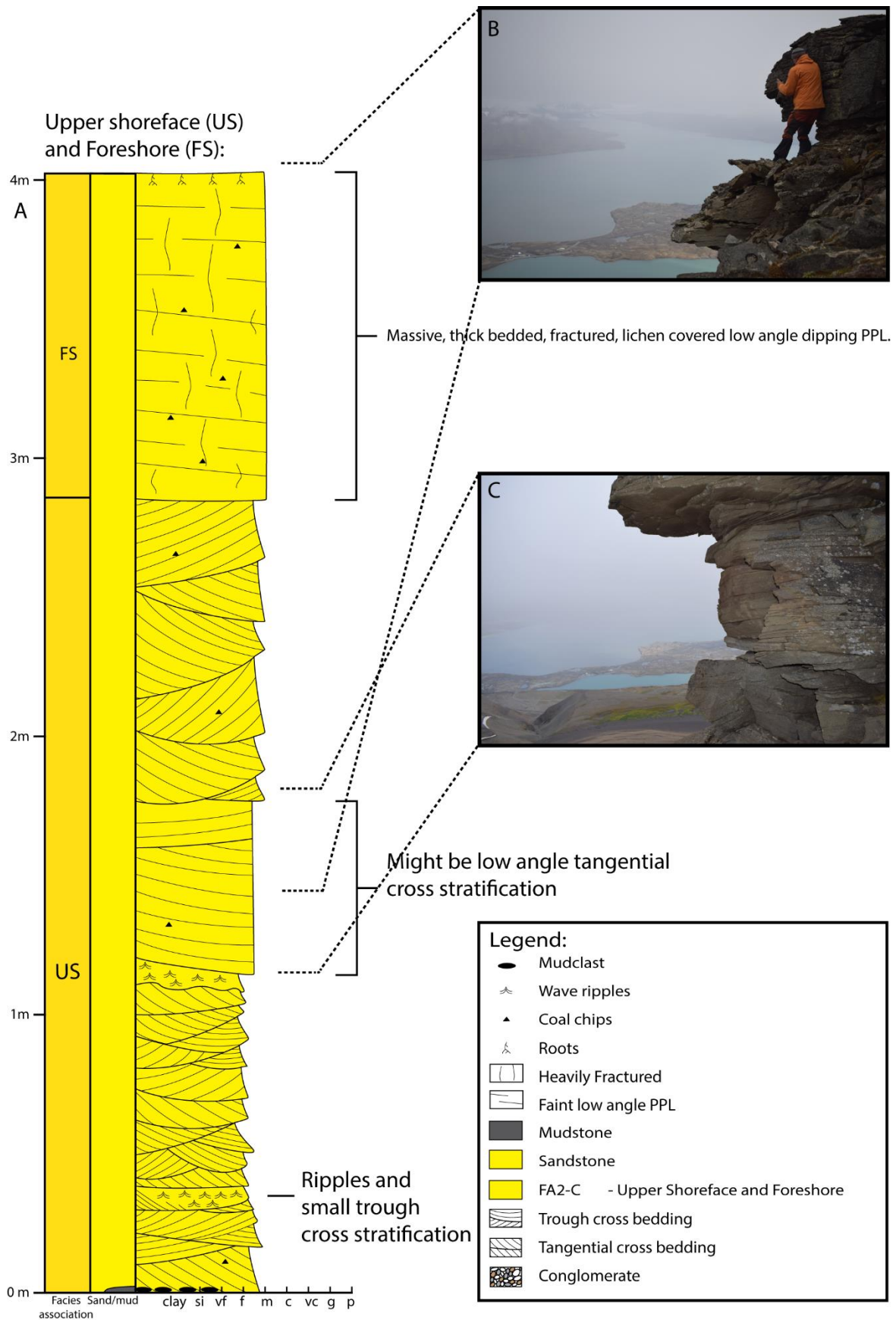


Figure 4.6: (A) Detailed log of FA2-C: Upper Shoreface and Foreshore deposits (excerpt from Log A). (B) Photograph of the top part of FA2-C. (C) Photograph showing the edge of tangential cross stratification.

4. Lithofacies and Facies Associations

Interpretation:

Position of the tabular cross-stratified sandstones immediately above FA2-B (lower shoreface deposits) and the occasional wave ripples, suggests marine deposition in a more proximal part of the shoreface environment. This is further supported by the close vertical distance to the rooted horizon at the top of FA2-C, a direct indicator of a nearshore environment. Tabular cross sets with a high spread of foreset dip-azimuths was by Helland-Hansen (2010) interpreted to indicate an environment where unidirectional shifting currents, capable of creating two-dimensional dunes, were operating. Longshore currents are known to produce such complex current patterns, especially in dissipative shorelines (Orton and Reading, 1993). Since longshore currents together with wave action are processes important to the upper shoreface (Niedoroda, A.W., and Swift, D.J.P. 1981) it is likely these processes were responsible for the formation of the tabular cross beds. The troughs are interpreted to reflect local erosion and deposition under larger than normal, and possibly breaking, waves.

The topmost 0.5-1.5 m of thick-bedded low angle PPL with a rooted horizon at top represents deposition in the upper flow regime. Clifton (1969) suggests an upper shoreface to foreshore environment with deposition by breaking wave's swash and backwash for such deposits.

Low amount of bioturbation in the upper shoreface and foreshore deposits imply a turbulent high-energy environment that inhibited the presence of burrowing organisms.

Interpretation of FA2 (Prograding wave-dominated delta deposits)

FA2 is interpreted to be a regressive depositional system, due to the overall coarsening upwards and shallowing upwards trend. This is also clearly reflected in the facies arrangement, with proximal facies stacked on top of more distal. With the absence of fluvial and tidal indicators, and an abundance of wave-generated structures (HCS, PPL and wave-ripple lamination) throughout FA2, it is safe to suggest that it was deposited in a highly wave-dominated environment. The facies successions also fit what, according to Hampson and Storms (2003), are very distinctive of a wave-dominated environment.

Although the succession shows no evidence of fluvial feeder points, the high amount of carbonaceous detritus throughout FA2 witnesses a steady terrestrial source of sedimentation. The abundance of water escape structures, especially in the lower parts of FA2 suggests a high depositional rate. This, coupled with the textural immaturity and high clay content of the sandstones within the Battfjellet Fm (Helland-Hansen, 2010), leads to the interpretation of a deltaic depositional setting, with short distance to the feeder points of a distributary fluvial channel. FA2 also show large similarities to the

4. Lithofacies and Facies Associations

storm-wave-dominated delta front successions in the Upper Cretaceous Dunvegan Formation, Alberta (Figure 4.6) described by Bhattacharya and Walker (1991), further supporting this interpretation.

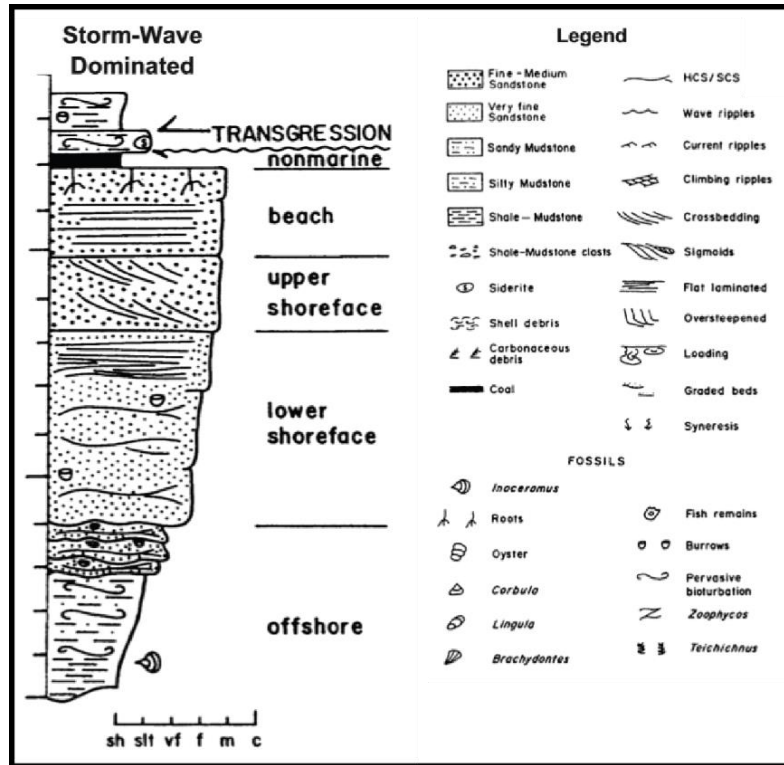


Figure 4.6: Wave-dominated delta-front succession from in the Upper Cretaceous Dunvegan Formation, Alberta, Canada. Modified from Bhattacharya and Walker (1991)

Previous work on the Battfjellet Fm has also reached the same conclusion of a wave-dominated delta front succession (e.g. Steel et al, 1985; Helland-Hansen, 1985; Steel et al, 2000; Deibert et al, 2003; Uroza and Steel, 2008; Helland-Hansen, 2010; Grundvåg et al., 2014b).

4. Lithofacies and Facies Associations

4.2.3 Facies association 3 (FA3): Distributary fluvial channel deposits (Figure 4.8 and Figure 4.9)

FA3 is exposed in the field as vertical sandstone cliffs with a thickness ranging from 9–14 m and was traced up 50 meter laterally. No distinct channel shaped geometries or lateral accretion were observed.

Description:

The most easily noticeable feature of FA3 is the erosive base cutting into FA2. This erosive base often have a 1-5 cm thick mudclast rich siderite-cemented layer at base, immediately overlain by conglomerate (F8) of varying thickness (5cm-40cm) (Figure 4.8 D). The conglomerate has abundant carbonaceous detritus, is clast supported, polymikt, with sub-rounded to sub-angular clasts and has a coarse to very coarse-grained sandy matrix. Laterally the grainsizes vary dramatically from pebbles to 10 cm cobbles, and the conglomerate extends upwards into the foresets of 15-30 cm thick tabular cross-beds. Each cross-stratified set fines upwards with conglomerate, abundant coal chips and plant fragments (up to 10 cm) at base, and coarse-grained sandstone at top. Above this, several stacked tabular cross-sets (F9) (Figure 4.8 C and Figure 4.9 C) and occasional trough cross-sets (F10) of 15 cm to 1 m thickness make up the bulk majority of FA3. Coal chips, plant fragments and pebbles (few single cobbles) are abundant in the foresets of these cross-sets. Some 1-5 cm thick lenses of loaded abundant coal chips and plant fragments exist between few of the cross-beds. At some level in the upper half of Facies E, trough cross-stratification becomes the dominant structure with rare beds of thick low angle PPL. Each trough has a thickness of 14-40 cm and contain scattered pebbles and coal chips throughout. The dominant structure changes to current ripples (F11) in the top 1-1.5 meters of FA3. Capping the facies association are a 5-10 cm rooted horizon.

Over all, there is a fining upwards trend throughout Facies E from conglomerates at base to fine sandstones at top. Water escape structures and mudclasts rich horizons are present in the uppermost 1-2 m.

Figure 4.8 below presents a detailed log of FA3 and pictures of the deposits, while Figure 4.9 presents FA3 from Log B, where it truncates into FA2-B, along with overview photos of typical outcrops from FA3.

4. Lithofacies and Facies Associations

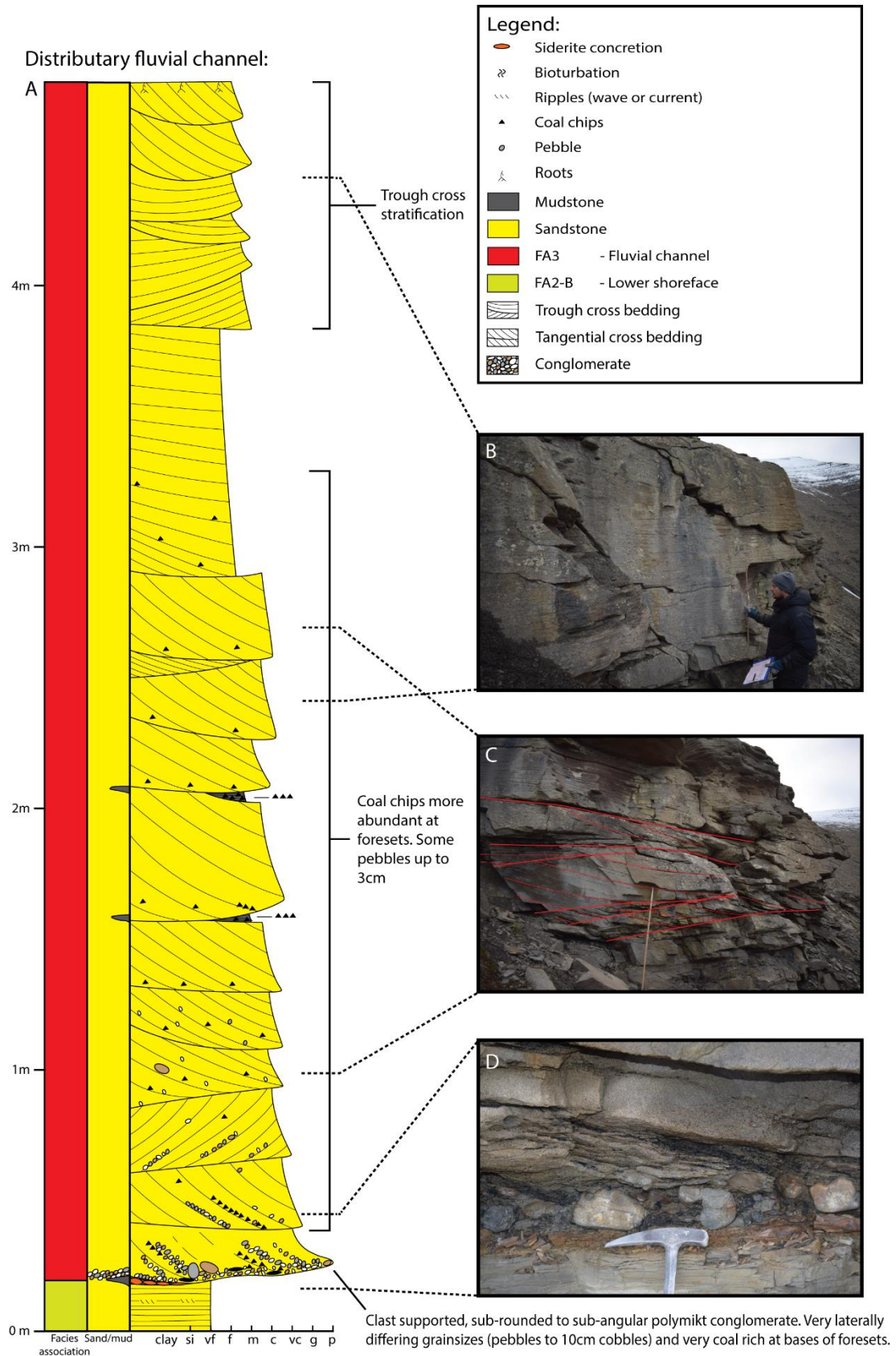


Figure 4.8: (A) Detailed log of FA3: Distributary fluvial channel deposits (excerpt from Log A). (B-D) Photographs showing typical features of FA3. (B) Stacked trough cross-stratification with meter-stick for scale. (C) Stacked tabular cross-stratification highlighted by red lines. Meter-stick for scale. (D) Erosive channel base with conglomerate lag on top of siderite cemented muddy sand horizon.

4. Lithofacies and Facies Associations

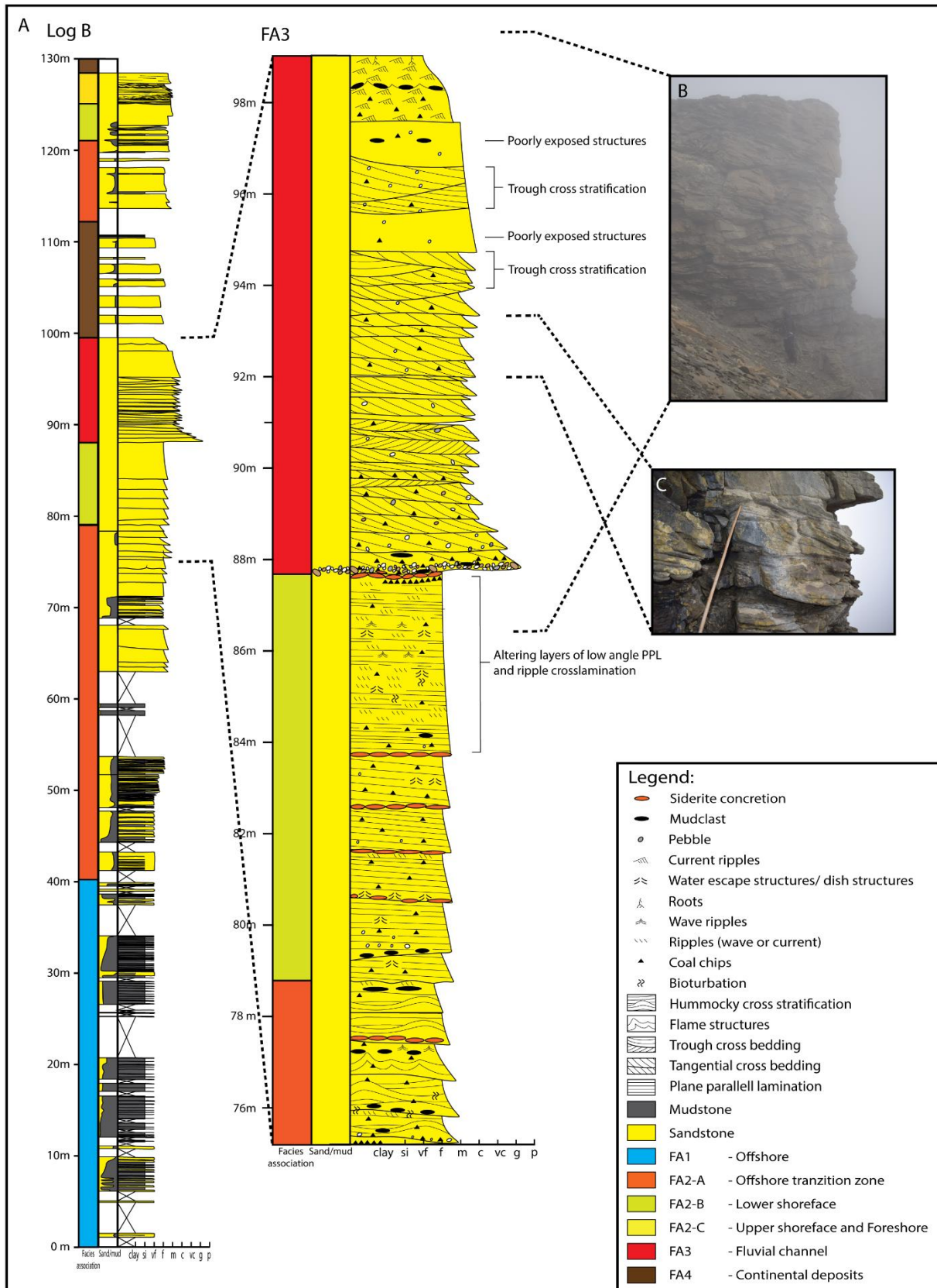


Figure 4.9: (A) Detailed log interval of FA3: Distributary fluvial channel deposits, from Log A, showing FA3 eroding into the shoreface deposits of FA2-B. (B) Overview photo of distributary fluvial channel deposits. (C) Tabular cross-stratification.

4. Lithofacies and Facies Associations

Interpretation:

The erosive base and the abrupt change from very fine- fine sandstone dominated shoreface deposits to conglomerates, at the base of FA3, indicates a change into a higher energy environment. This, together with a general fining upwards trend, abundant coal chips, plant fragments and cross stratification grading into current ripples at top, suggests that FA3 are fluvial channel deposits. Absence of marine trace fossils and absence of indicators of tidal influence suggests that these channels were fully continental.

Tabular and trough cross-stratified sandstones are interpreted to represent surfaces and 3D dunes that migrated downstream on the channel floor. The absence of lateral accretion surfaces suggests that the channels were straight to low sinuous (Ford and Pyles, 2014). The occasional units with low angle PPL is suggested to reflect temporary deposition under higher flow velocities in the upper flow regime. In contrast, the deposition of current ripples is suggested to represent lower flow velocities, favoring migration of 2D and 3D ripples. Given that these current-rippled beds only exists in some of the uppermost parts of Facies F, these beds are interpreted to be deposited at the inner turn of low sinuous fluvial meanders.

From what was demonstrated in the outcrops, the channel deposits of FA3 appear to be single-storey, but are present over a wide area (several km laterally) within the study area, leading to the interpretation that the fluvial channels are distributary. The channels also erode deep into the offshore transition zone (FA2-A) and shoreface deposits (FA2-B and FA2-C). This testifies to a low-gradient depositional environment favoring stable deep-eroding single-storey channels with a low-sinuosity. This is further supported by the previously mentioned lack of lateral accretion surfaces (Ford and Pyles, 2014).

The presence of distributary fluvial channel deposits superimposing the shoreface deposits further backs up the interpretation that the deposits of the Battfjellet Formation (FA2) must have been derived from a terrestrial source. As the shoreline progressed, the channels migrated across, and incised into the shoreface deposits. After deposition, the sediments were quickly reworked and redistributed along the shore by wave action within the basin.

4. Lithofacies and Facies Associations

4.2.4 Facies association 4 (FA4): Continental deposits (Aspelintoppen formation) (Figure 4.10)

The continental deposits of Aspelintoppen Fm is not the focus of this thesis, and is by convenience, therefore grouped into FA4: Continental deposits. No detailed log were taken from this facies, and emphasis was instead directed to demonstrating evidence for continental deposition. Logging in field were done up until the height of which enough evidence for continental deposits had been established, and that we were sure there could be no additional marine deposits above. These logged sections would range in thickness of 1-18 m. Abundant scree covers the more mud rich parts of FA4, meaning the sand/mud ratio is likely lower then what appears in the logs.

Description:

FA4 consists of mostly heterolithic 1-2 m deposits with 2-10 cm fine sandstones separated by thin 0.1–2 cm layers of siltstone (F12). Roots, abundant coal chips, plant fragments (up to 4 cm), some leafs (Figure 4.10 D) and bioturbation exists throughout. The dominant features of the sandstone beds are abundant current ripples (some climbing ripples, Figure 4.10 C), while the siltstones are finely laminated low angle PPL. The thickest sandstone beds (>8 cm) have erosive bases, occasional few pebbles and some climbing current ripples.

Occasionally, heterolithic deposits of 30 cm to 1 m thickness with 1-10 cm fine wave-rippled and some combined-flow-rippled sandstones separated by thin 0.1-1 cm siltstones are present (F14). These heterolithics also have bioturbation, abundant coal chips and plant fragments (up to 4 cm).

Some siderite-concreted horizons of massive very fine sandstone beds (10-30 cm) with ball and pillow structures and water escape structures exists throughout the facies association. 2-5 cm thick layers of coal (F13) are present with at least some centimeters of mudstones above and below, and the scree slopes are often covered with dark black coffee ground (Figure 4.10 B). Sandstone blocks in the scree slopes of FA4 also have abundant leafs, some with a width of up to 15 cm. Extensive weathering inhibits finding of distinct trace fossils or to what extent the beds have been bioturbated in FA4.

4. Lithofacies and Facies Associations

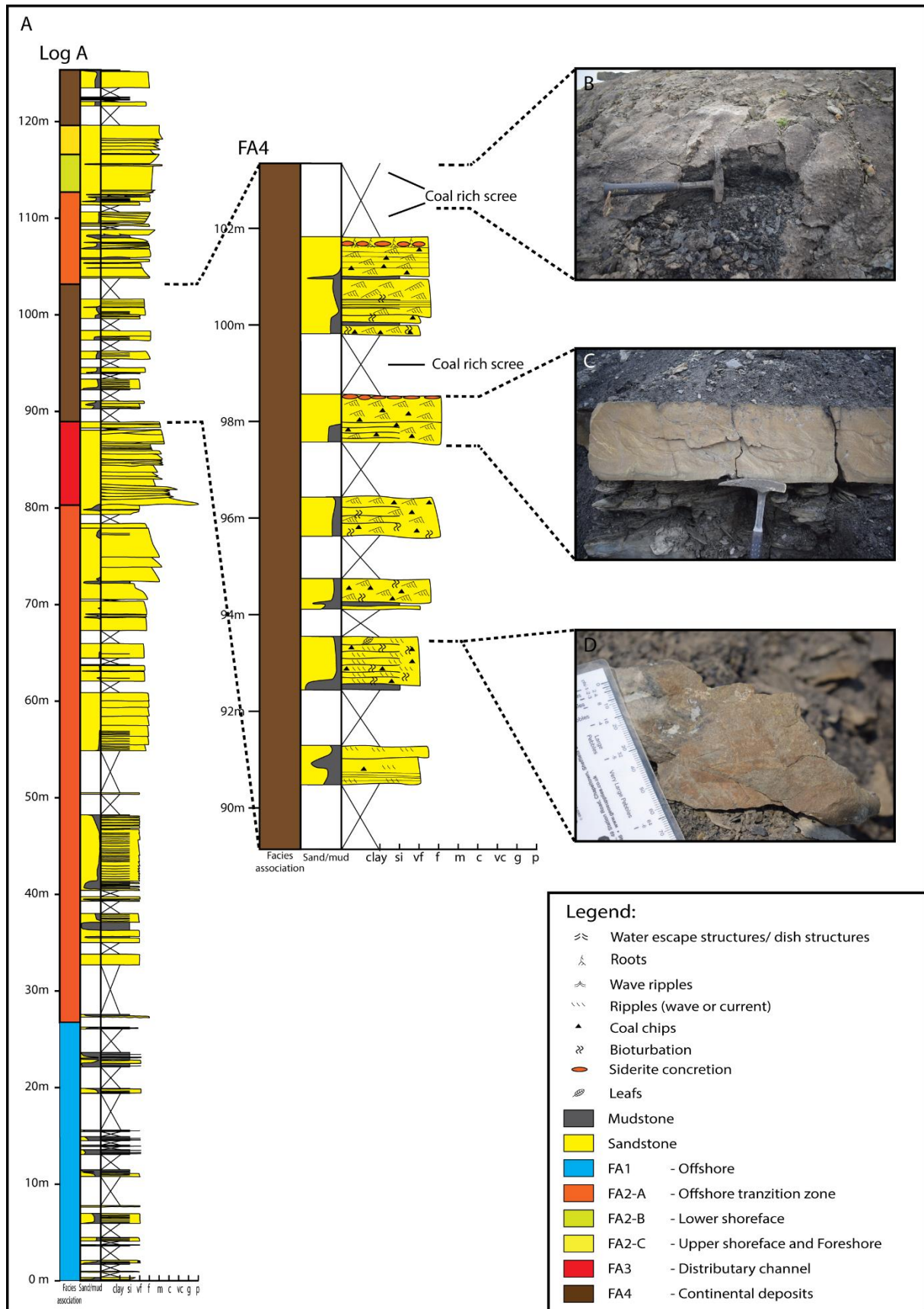


Figure 4.10: (A) Detailed log interval of FA4: Continental deposits, from Log A. (B) Coal layer in scree. (C) Typical FA4 outcrop. (D) Leaf.

4. Lithofacies and Facies Associations

Interpretation:

Generally, the abundant in situ growth of roots together with coal horizons (and coffee ground) fossilized leafs and abundant carboniferous detritus, leads to the interpretation of a continental depositional environment. FA4 laying immediately above FA3 (Distributary fluvial channel deposits) or FA2-C (Upper shoreface and Foreshore deposits) along with the lack of marine indicators further supports this interpretation. The large fossilized leafs are indicative of a floodplain with well established levees around fluvial channels, which allows for the growth of large trees.

The heterolithics with current rippled sandstones and PPL siltstones along with the coal horizons are interpreted to be floodplain deposits. The heterolithics are deposited during flooding of the distributary channels of FA3. Proximity to the breached distributary channel during deposition of the heterolithics are represented in the grain size and thickness of the sandstone beds. (Dreyer and Helland-Hansen, 1986) The thicker sandstone beds (>8 cm) with erosive bases, occasional pebbles and some climbing current ripples are interpreted to be crevasse splays deposited through crevasse channels. Though crevasse channels were not demonstrated in field, they are assumed to have extended across the levees creating their own channel pattern and system on the floodplain during floods (Reineck and Singh, 1980).

Heterolithics with abundant wave ripples and some combined flow ripples suggests a standing body of water. This body of water must have covered a sufficiently large enough area to generate waves, and the lack of distinct marine indicators along with the presence of underlying delta plain deposits suggests a lake setting. Additionally, abundant coal chips, plant fragments and leafs indicates a terrestrial source of sediments. These heterolithic beds are therefore interpreted to be interdistributary lake deposits. Distributary channels and crevasse channels interact with interdistributary basins. This creates crevasse splays that can establish small delta systems in standing water basins on the delta plain (Fielding, 1984)

5. Paleocurrent Data

5. Paleocurrent Data

5.1 Introduction

Several paleocurrent readings were retrieved from FA1, FA2 and FA3 in the study area. These measurements were obtained from symmetric wave ripple crests, solemarks, current ripples and tabular cross-stratification. The number of measurements taken are limited, and vary at each location, due to variable outcrop quality and abundant scree cover. Regardless, the measurements are believed to be solid evidence of the paleocurrents of the study area. A table of all the paleocurrent measurements taken is presented in Appendix 2.

5.2 Paleocurrent of FA1 (Offshore deposits) and FA2 (Prograding wave-dominated delta)

Measurements of symmetric ripple crest orientations and direction of solemarks (flutecasts and tool-mark lineations) was acquired from FA1 and FA2. The wave ripple crests were generally very subtle and hard to trace (Figure 5.1: C), leading to a substantial degree of uncertainty when measuring their orientations. This is likely the reason for the spread of measured orientations of these structures (Figure 5.1: A). Regardless, they show a clear SW to NE favoured orientation. Paleocurrent measurements of solemarks within FA1 and FA2 also have a clear northwest to southeast favoured orientation (Figure 5.1: B). This leads to the interpretation of a southwest to northeast oriented shoreline for the study area.

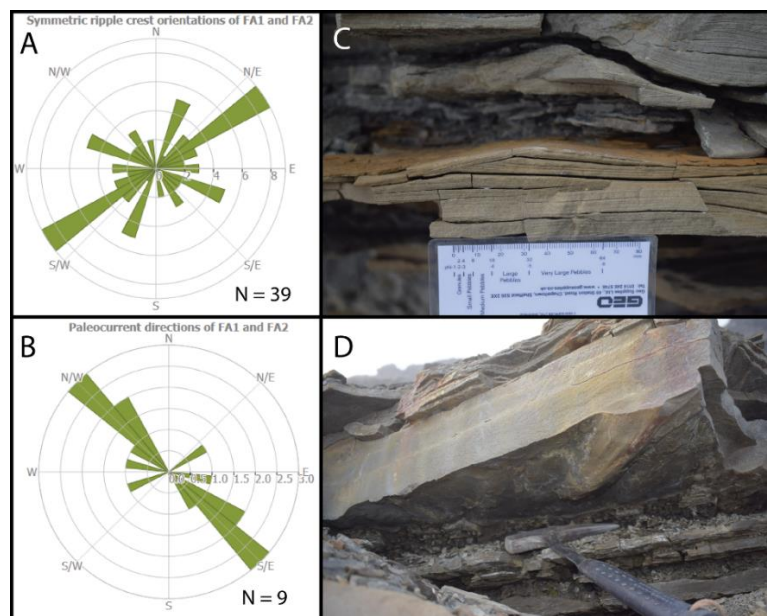


Figure 5.1: (A) Symmetrical ripple crest orientations of FA1 and FA2. (B) Paleocurrent directions of FA1 and FA2 measured from flutecasts and lineations. (C) Picture of a typical current ripple crest found in FA2 (from Log A). (D) Picture of currentmark at the sole of a sandstone bed in FA2 (from Log A).

5. Paleocurrent Data

Paleocurrent measurements from previous studies, compiled by Helland-Hansen and Grundvåg (in prep) (Figure 6.2), favours an interpretation of a north to south oriented shoreline and west to east buildout of the system within most parts of the basin. The paleocurrent measurements of the study area, favouring a northeast to southwest oriented shoreline, clearly deviates from this interpretation.

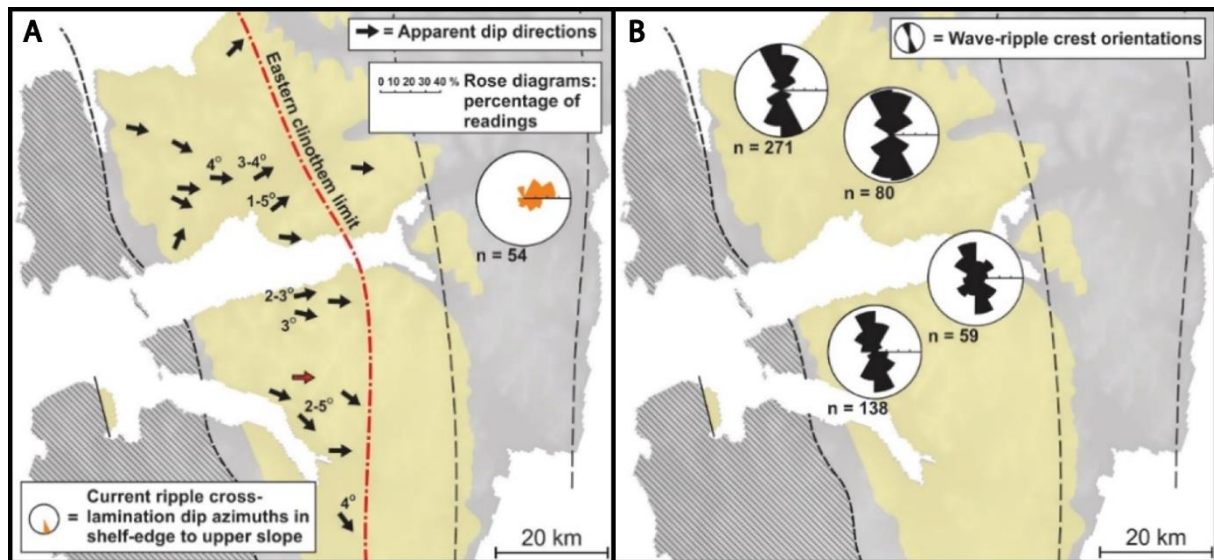


Figure 5.2: (A) Dip azimuths of current-ripple cross-lamination at shelf-edge to upper slope positions (rose diagram) and apparent clinoform dip directions/slope angles (arrows). (B) Wave-ripple crest orientations compiled from logged sections within the Battfjellet Formation, summarized for four sub-areas (modified from Helland-Hansen and Grundvåg, in prep).

Given the small size of the study area and most of the paleocurrent measurements having been taken in the lowestmost reaches of the Battfjellet Formation, this deviation could be due to a local change in the shoreline orientation due to a protruding delta lobe. This is however highly unlikely, as in order to change the orientation of the waves as far out as the offshore transition zone, the delta sandbody must have been substantially larger than the up to 10 km estimates for the Battfjellet Formation deltas (Helland-Hansen and Grundvåg, in prep).

The more likely explanation for the deviating shoreline orientation is that the system changed to a more southern progradational direction towards the later stages of basin infill. The reason for this could be that presence of a peripheral bulge northeast of the study area changed the drainage direction. This was suggested for the latest depositional stages of the Aspelintoppen Formation by (Helland-Hansen and Grundvåg, in prep), and could also be true for the Battfjellet Formation.

5. Paleocurrent Data

5.3 Paleocurrent of FA3 (Distributary fluvial channel deposits)

Paleocurrent measurements of current ripples and tabular cross-stratification was gathered from FA3 at Log B and Log E localities (Figure 5.3). All together, the measurements show a scattered pattern, favouring an east to southeast direction (Figure 5.3: A). The two locations separate, have quite different favoured orientations to each other. Measurements at Log B location points to an east to northeast directed river (Figure 5.3: B), while measurements at Log E points to a south to southeast directed river (Figure 5.3: C).

The difference in favoured orientations at the two localities might be due to the rivers fingering out at the delta front (spreading outwards), and/or having a more meandering shape towards the edge of the system than the low sinuous channels found elsewhere in the Aspelintoppen Formation (Ford and Pyles, 2014). However, as the paleocurrent measurements are only taken at two localities, these interpretations are quite far fetched.

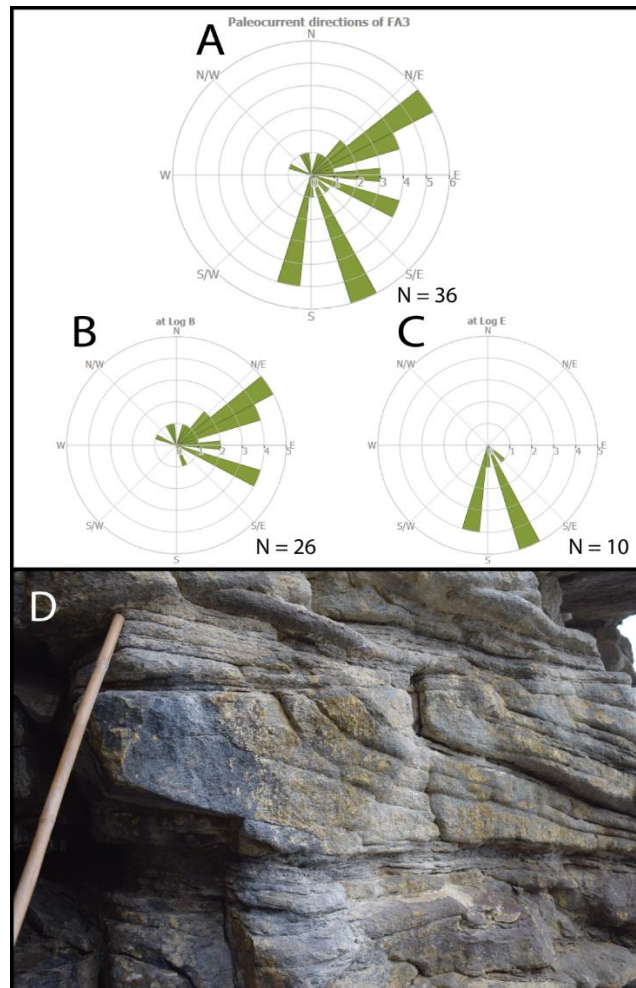


Figure 5.3: (A) Paleocurrent directions of FA3 measured from current ripples and tabular cross-stratification. (B) Paleocurrent directions of FA3 at Log B location. (C) Paleocurrent directions of FA3 at Log E location. (D) Typical tabular cross-stratification in FA3, of which paleocurrent measurements were taken.

6. Sandbody Geometry

6. Sandbody Geometry

6.1 Introduction

This chapter presents an interpretation of the sandbody geometry of the Battfjellet Formation within the study area, and ties it to interpretations done by Osen (2012) in the Urdkollidalen area, west of Liljevalchfjellet. Lithofacies and facies associations presented in Chapter 4, and by Osen (2012) show a specific stacking of depositional environments creating shallowing upwards parasequences of varying numbers (Figure 6.2). Based upon parasequence stacking patterns, one 2D correlation panel was constructed for the study area, and two more by including interpretations by Osen (2012). This provides coverage of the sandbody geometry in a combined area of approximately 66 km² (Figure 6.1). Though only constituting a small part of the approximately 12000km² basin, it provides a better understanding of the lesser-studied easternmost parts of the basin.

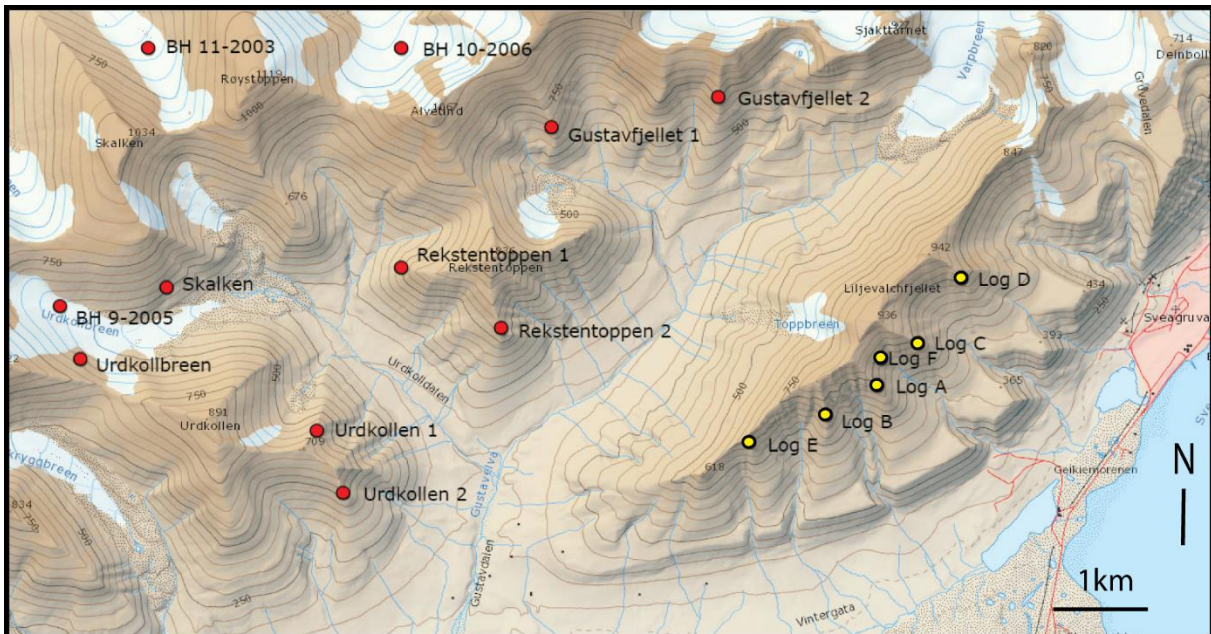


Figure 6.1: Map showing the combined study area. Red circles indicate logged sections by Osen (2012), and yellow circles indicate the sections logged in this study (Modified from Norsk Polarinstitutt).

6.2 Methods of correlation

One 2D correlation panel (Transect A, Figure 6.4) was constructed by placing logs A-E with the correct relative distance to each other, and using the lowest transition into the Frysjaodden Formation as a datum line. Field observations of lateral facies distribution was used to then correlate between the logs. Two more 2D correlation panels (Transect B, Figure 6.9 and Transect C, Figure 6.10) was constructed by redrawing correlation panels by Osen (2012), and extending his interpretations into the study area. This was done by placing the logs of the study area with the correct relative distance to the

6. Sandbody Geometry

redrawn Osen (2012) correlation panels, using the same datum line as in Transect A, and correlating between them.

Osen's (2012) correlations are based upon eight outcrops (Urdkollbreen, Skalken, Urdkollen 1, Urdkollen 2, Rekstentoppen 1, Rekstentoppen 2, Gustavfjellet 1 and Gustavfjellet 2), and three wells (cores: BH 9-2005, BH 10-2006 and BH 11-2003), in the Urdkollen, Rekstentoppen and Gustavfjellet areas, west of Liljevalchfjellet (Figure 6.1). He explains that his correlation panels are largely based upon sequence stratigraphic concepts, due to the difficulty of tracing the lateral extent of individual sandbodies in field. He further explains that in the logged outcrops, the exact position of the boundary between the Battfjellet Formation and the Aspelintoppen Formation were problematic to determine due to scree cover. Osen (2012) thus placed the boundary between the Battfjellet Formation and the Aspelintoppen formation as a horizontal datum line in his correlation panels. This is the same datum line used in the correlation panels made in this study.

In his logs and correlation panels, Osen (2012) interpreted the middle and upper shoreface into two distinct facies belts. For convenience, these facies have been grouped into FA2-C (Upper shoreface and foreshore deposits) when making the correlation panels for this study.

The number of parasequences are expected to change over short lateral distances in the Battfjellet Formation (Helland-Hansen, 2010). Therefore, correlations across large valleys such as Gustavdalen and Urdkolldalen should be taken lightly.

6.3 Correlation principles

Facies associations FA1 to FA5 presented in Chapter 4 are stacked conformably on top of each other following Walter's law with progressively more proximal depositional environments, until they are capped by a flooding surface, and superimposed by more distal facies. Correlation was largely based upon the stacking patterns of these parasequences. Van Wagoner et al (1990) defined a parasequence as: "...a succession of relatively conformable and genetically related beds or bedsets bounded by flooding surfaces or their correlative surfaces". Flooding surfaces representing rapid drowning and onset of more distal facies, violates Walter's law. They represent a timeline (isochronous line), while boundaries that does not violate Walter's law, such as facies belt boundaries, are considered diachronous.

Osen (2012) was only able to take a few paleocurrent measurements in his study area which pointed to a N to S oriented shoreline. He therefore suggested a west to east progradational direction for his study area, and backed up his claim by referring to paleocurrent measurements from Helland-Hansen

6. Sandbody Geometry

(1985), Helland-Hansen (1990), Johannesen and Steel (2005), Olsen (2008), Stene (2009), Skarpeid (2010), Gjelberg (2010) and Grundvåg et al (2014b). As outlined in Chapter 5, paleocurrent evidence in the study area of this thesis suggest that the system prograded towards a more SE direction. The parasequences are therefore expected to transition from continental deposits in the NW, to progressively more distal facies towards the SE. They are also expected to dip towards the E, where they also eventually pinch out. Furthermore, the Battfjellet Formation is expected to have a complex stacking pattern, where thicker parasequences have a greater lateral extent than thinner. Moreover, frequent terminations and onsets of parasequences occur.

Clinoforms pinching out into the fines of the Frysjaodden Formation, commonly found in the central and western parts of the Battfjellet Formation (Crabaugh and Steel, 2004; Helland-Hansen, 2010) was not observed in either this or Osen (2012) study. However, as much of the interpretations are concept based, one cannot rule out the possibility of such clinoforms in the area.

Transgressional deposits was only observed as minor contributions between stacked parasequences in the well cores of Osen's (2012) study, and was not observed in the study area of this thesis. Such deposits are therefore neglected in the correlation panels.

6.4 Parasequence stacking pattern

A total of six parasequences were defined. They vary in number, and their lateral extent is hard to determine due to the uncertainty factors mentioned above. Which parasequence was present at each location is presented in Table 6.1 below:

Table 6.1: The presence of parasequences at each of the logged section. The parasequences are ordered progressively from lowest (P1) to highest (P6) stratigraphic height. * = sections logged by Osen (2012). X = parasequence present. ? = parasequence might be present. "3(4)" refers to there being three confirmed parasequences, with a high probability of four being present.

Locality	P1	P2	P3	P4	P5	P6	P Σ
*BH 9-2005	X	X	X	X	X		5
*Urdkollbreen	?	?	?	?	?		0(5)
*BH 11-2003	X		X	X	X		4
*Skalken	X		X	X	X		4
*Urdkollen 1	X		X	X	X		4
*Urdkollen 2	X		X	X	X		4
*BH 10-2006	X		X	X	X		4
*Rekstentoppen 1	?		X	X	X		3(4)
*Rekstentoppen 2	?		X	X	X		3(4)
*Gustavfjellet 1	X		X	X	X		4
*Gustavfjellet 2	?		X	X	X		3(4)
Log A	X			X	X	X	4
Log B	X			X	X	X	4
Log C	X			X	X	X	4
Log D	X			X	X	X	4
Log E	?			X	X	X	3(4)

6. Sandbody Geometry

Helland-Hansen and Grundvåg (in prep) created a map with the number of parasequences present at each logged location within the Battfjellet Formation. This map is presented in Figure 6.3 below, with this study adding further data. The lateral change in number of parasequences reflects the limited lateral extent and overlapping of the parasequences (Helland-Hansen and Grundvåg, in prep).

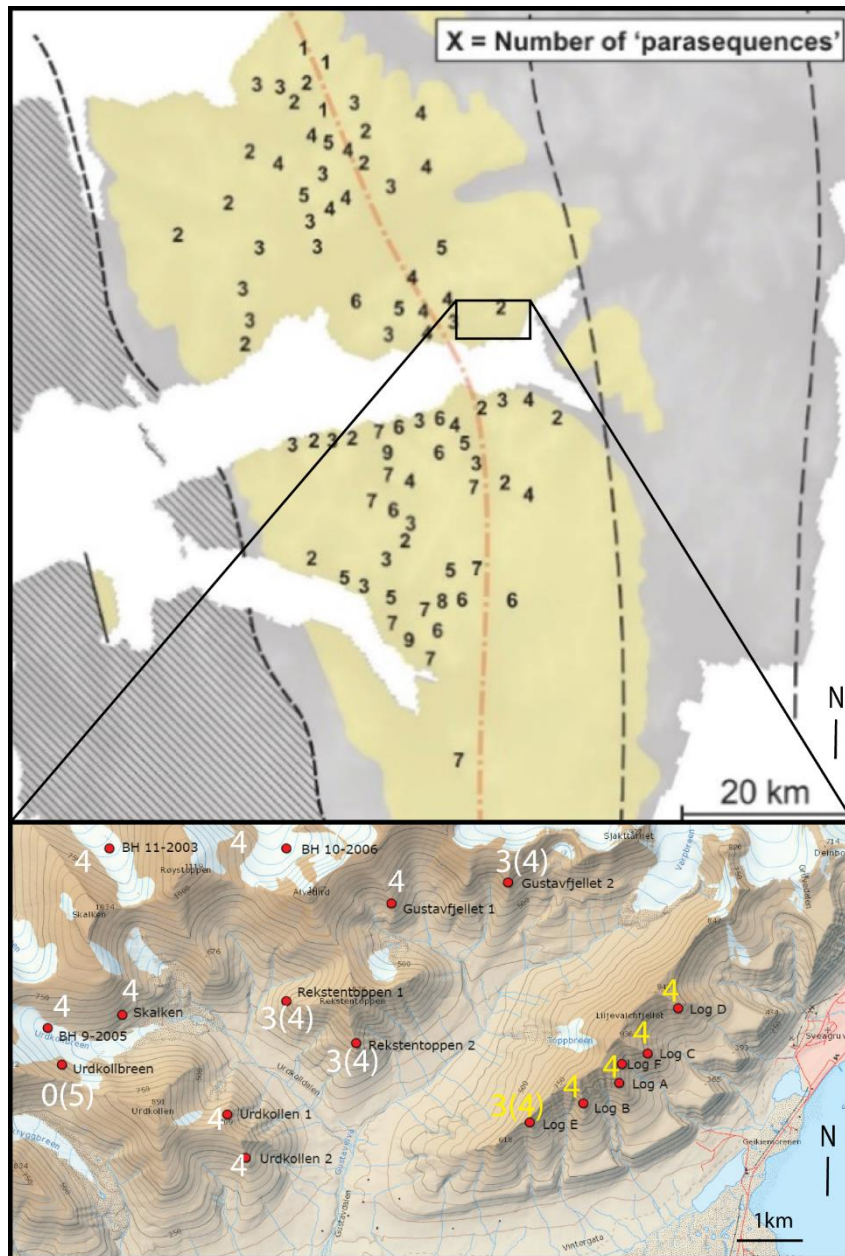


Figure 6.2: Map of the Central Basin showing number of parasequences at different studied locations (modified from Helland-Hansen and Grundvåg, in prep). Black numbers are provided from Helland-Hansen and Grundvåg (in prep). White numbers are from Osen (2012). Yellow numbers are from this study. “3(4)” refers to there being three confirmed parasequences, with a high probability of four being present.

6. Sandbody Geometry

The lowermost parasequence (P1), being the thickest parasequence in the study area, coincides with what is commonly demonstrated in the Battfjellet Formation. According to Helland-Hansen (2010), this is due to the first progradation building into deeper water than subsequent progradations. Accommodation space after each transgression therefore dictates the thickness of the next prograding parasequence.

In his study area, Osen (2012) only recorded continental deposits capping the top parasequence (P5), with no interfingering of the Aspelintoppen Formation and the Battfjellet Formation. He interpreted this to be because of a relatively short distance of flooding, during the intervening transgressive events, referring to (Helland-Hansen, 2010). Interfingering between the Aspelintoppen Formation and the Battfjellet formation was however recorded in this study, between P5 and P6. Thus, the transgressive event separating P5 and P6 must have had a much greater basinward extent compared to previous transgressions.

6.5 Correlation panels

One correlation panel covering the study area (Transect A), and two more panels (Transect B and C) connecting the study of Osen (2012), is presented in this chapter. The panels were chosen in a way that they capture the internal sandbody geometry of the Battfjellet Formation both along interpreted depositional strike and dip direction. An overview map of the three transects is presented in Figure 6.3 below:

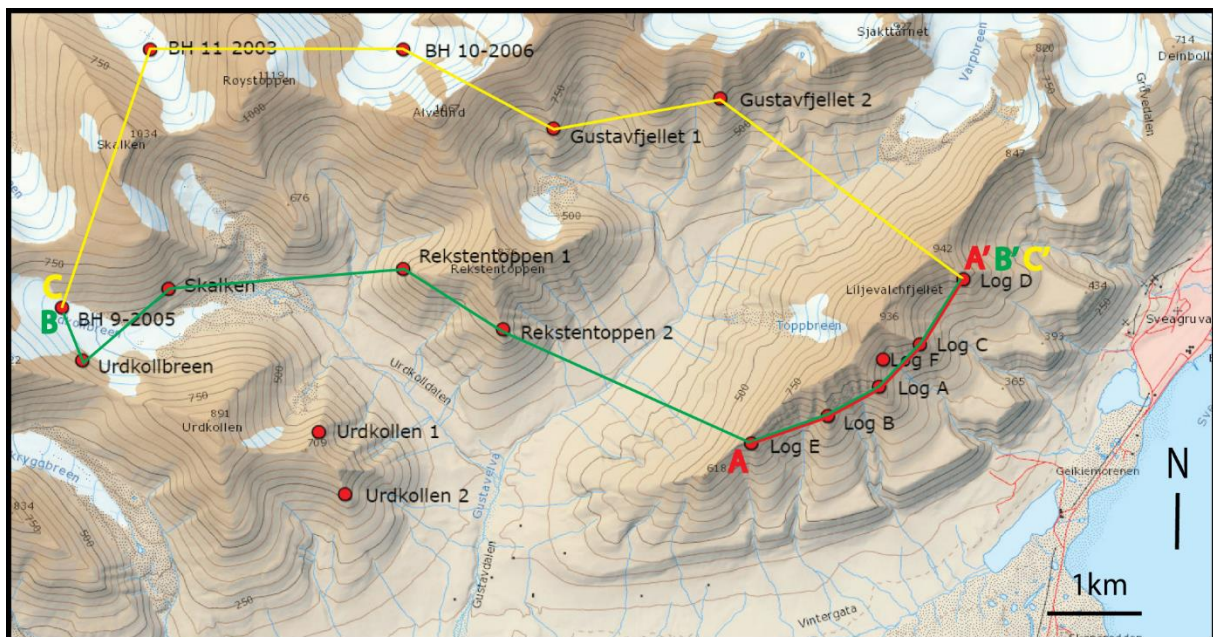


Figure 6.3: Overview map showing the correlation panel transects A (red), B (green) and C (yellow).

6. Sandbody Geometry

6.5.1 Transect A

Description:

Transect A (Figure 6.4) covers five logged outcrops in the study area, following a depositional strike direction through Log E, Log B, Log A, Log C and lastly Log D. A total of four parasequences was recorded at all five logged locations. These are P1, P4, P5 and P6.

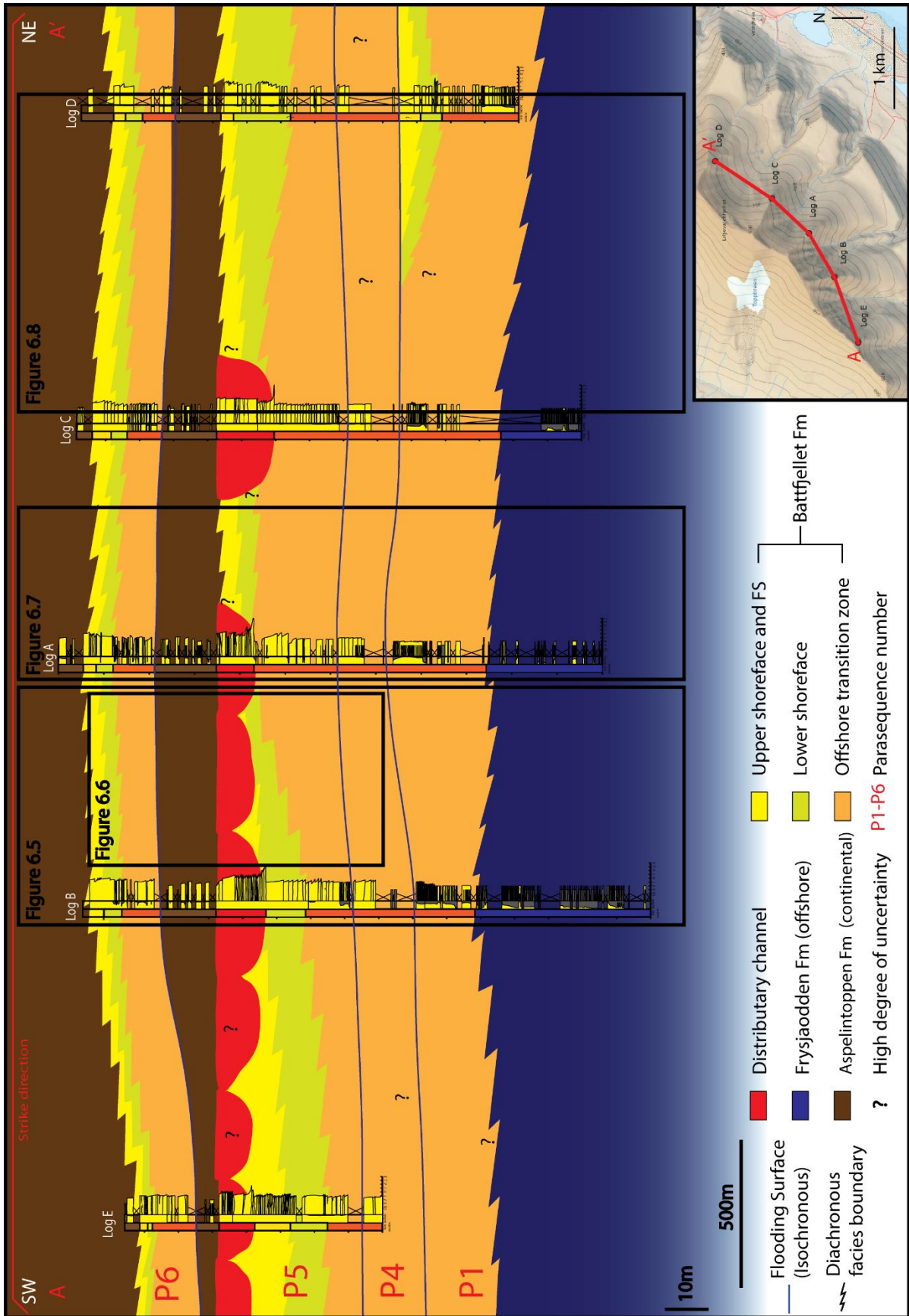
Parasequence 1 (P1) is the lowermost and the thickest of the parasequences, and the only parasequence that grades downwards into the Gilsonryggen Member shales. Along the transect, the top of P1 is represented as a correlative surface between stacked offshore transition zone deposits, except at the Log D location. There, P1 grades upwards into lower shoreface, upper shoreface and foreshore deposits, which is then capped by a flooding surface, overlain by offshore transition zone deposits. The flooding surface was not identified in the logs due to extensive scree cover, but can be recognized in field as a subtle laterally extending change from high to lower slope steepness (Figure 6.5, Figure 6.7 and Figure 6.8). The thickness of the total shallow marine packages of P1 also thickens around Log D location (towards the N).

Parasequence 4 (P4) is stacked on top of P1, and is the thinnest of the parasequences along the transect. Similar to P1, it is capped by a correlative surface between stacked offshore transition zone deposits, only recognizable in field (no in logs) as a subtle laterally extending change from high to lower slope steepness (Figure 6.5, Figure 6.7 and Figure 6.8).

Parasequence 5 (P5) is stacked on top of P4, and has an internal transition upwards from offshore transition zone deposits, all the way to continental deposits. At Log E, Log B, Log A and Log C locations, P5 is capped by distributary channel deposits eroding down into the Battfjellet Formation. The presence of channel fill deposits diminishes towards the NE, and is not present at Log D location (Figure 6.7 and Figure 6.8). The area between Log E and Log B is characterized by steep and inaccessible cliffs, which in combination with foggy weather during fieldwork inhibited the study of the channel geometries. The channel fill deposits were all located at approximately the same vertical level, with no stacked channel fills observed (Figure 6.6).

Parasequence 6 (P6) is positioned between continental deposits of the Aspelintoppen Formation, with a flooding surface at base, and an upwards grading from offshore transition zone deposits, to continental deposits.

6. Sandbody Geometry



6. Sandbody Geometry

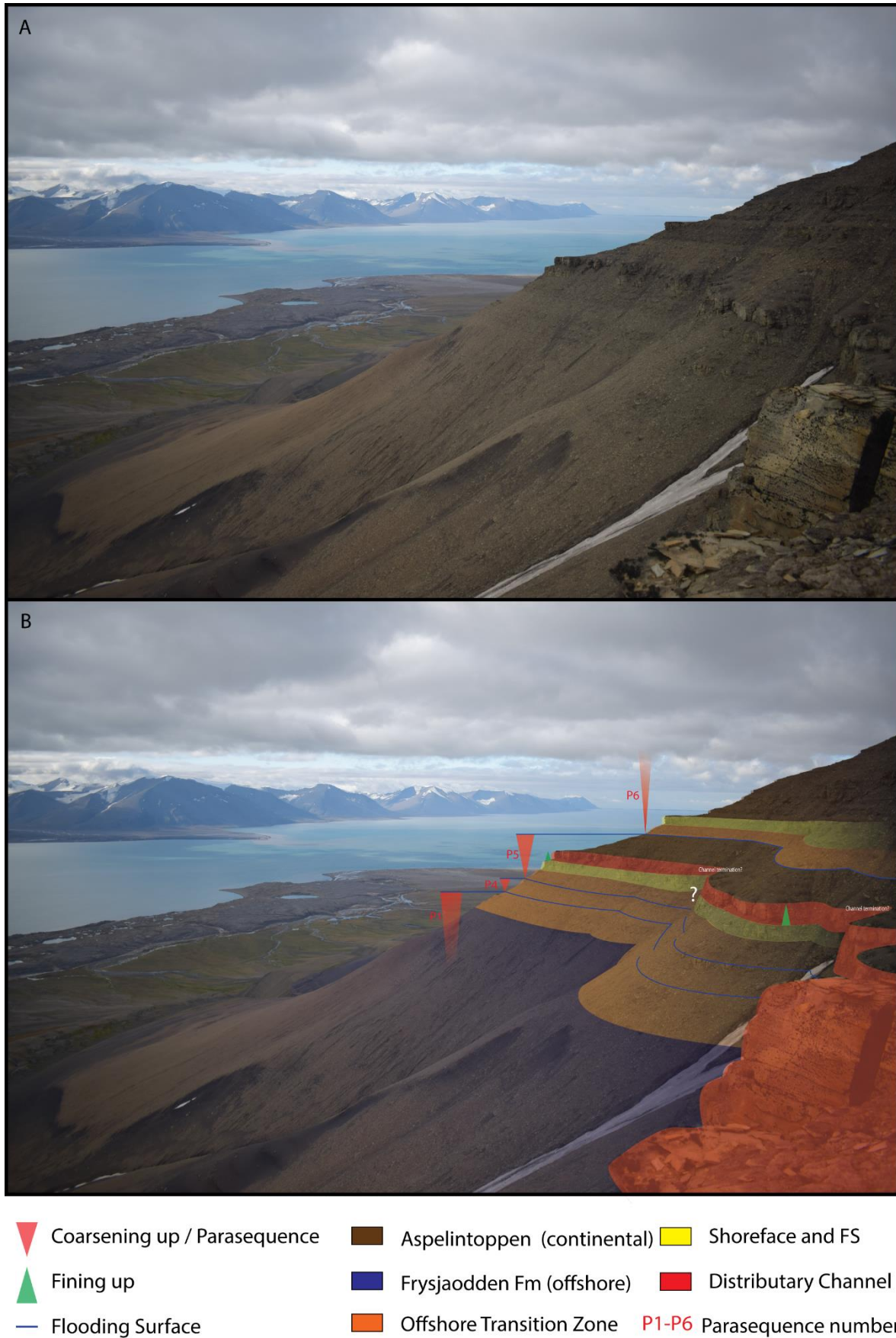


Figure 6.5: (A) Photograph taken from Log A location, directed towards Log B location. (B) Same photo as (A), with interpreted facies. FS = Foreshore.

6. Sandbody Geometry

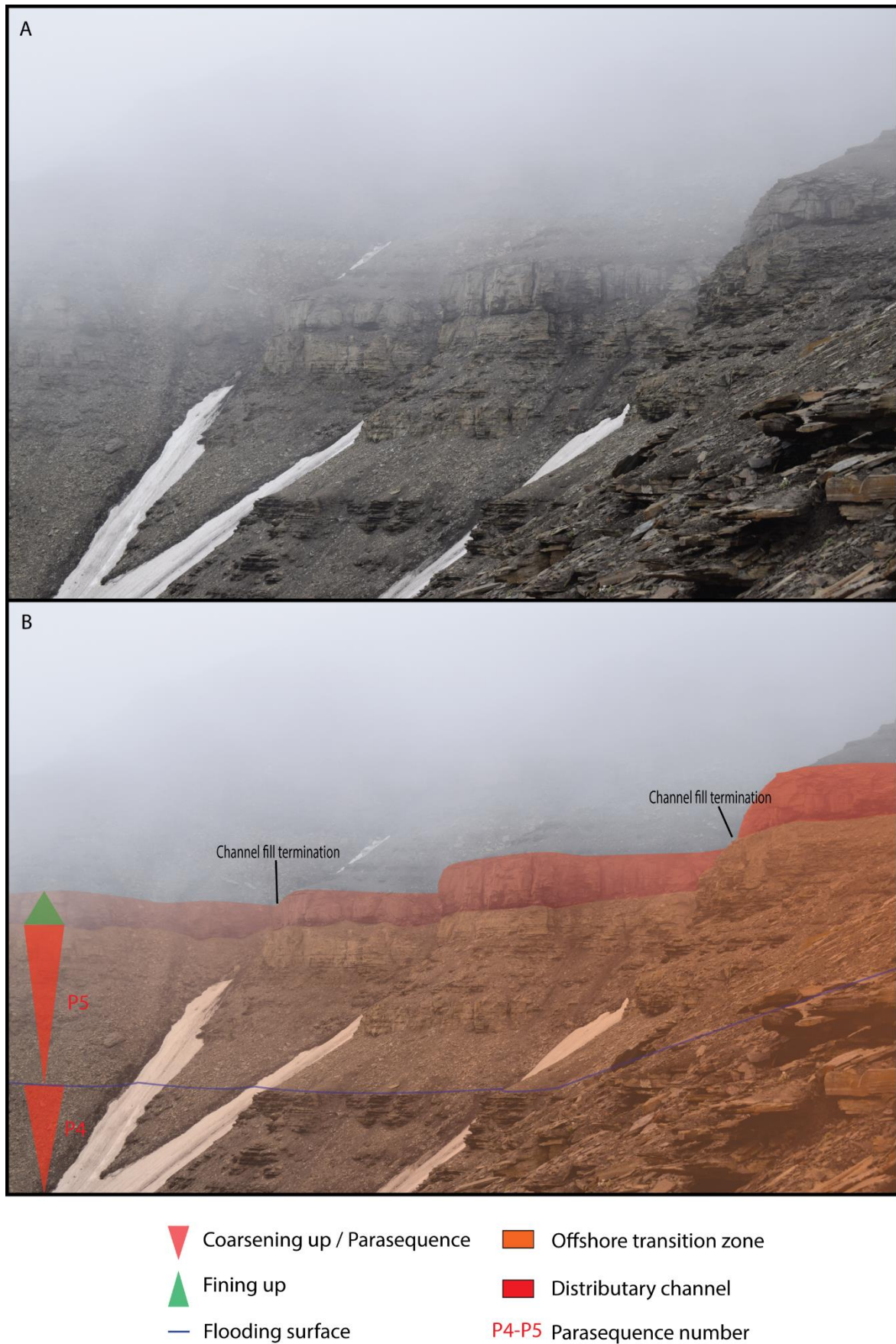


Figure 6.6: (A) Photograph of outcrop between Log A and Log B locations. (B) Same photo as (A), with interpreted facies.

6. Sandbody Geometry

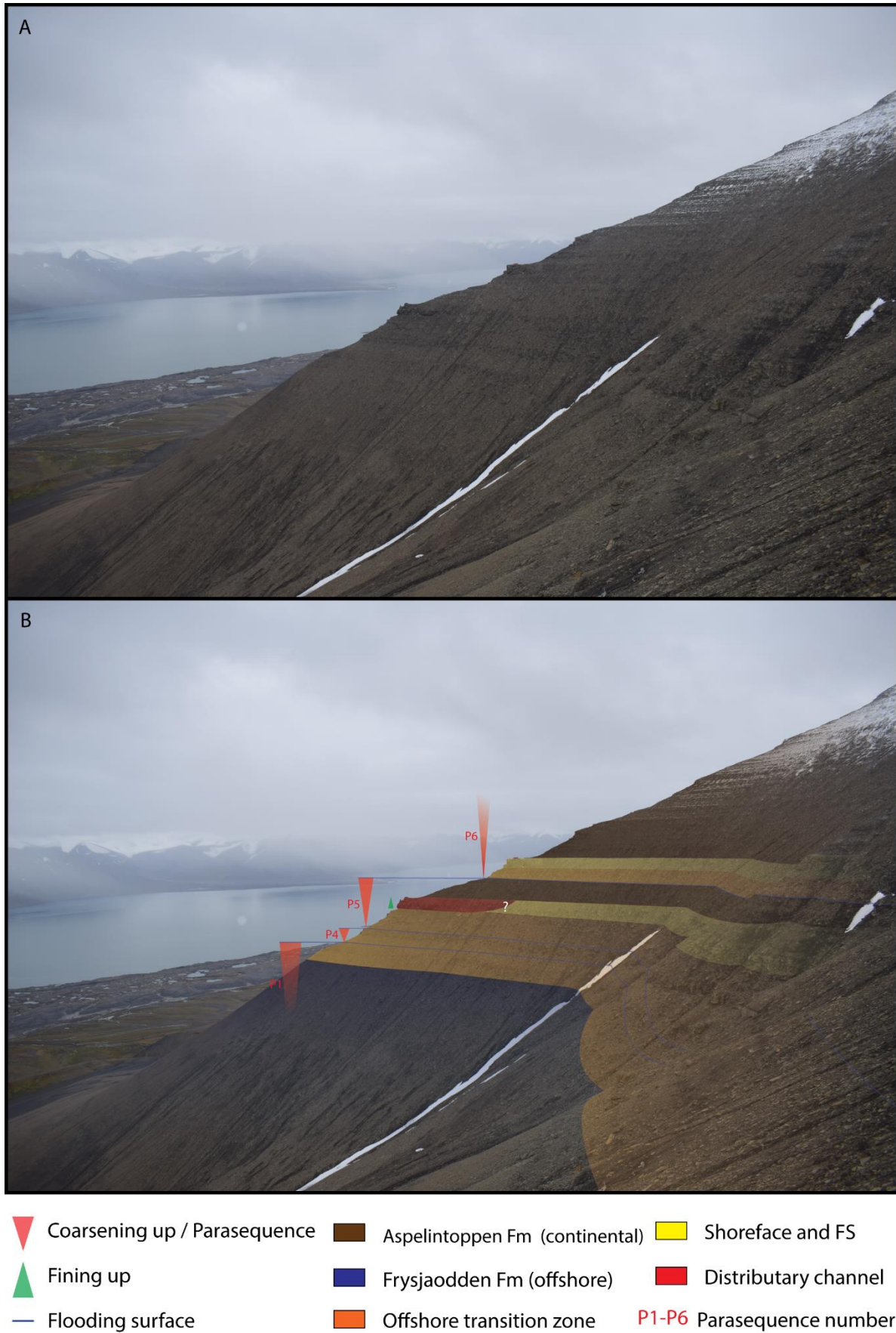


Figure 6.7: (A) Photograph taken from Log C location, directed towards Log A location. (B) Same photo as (A), with interpreted facies. FS = Foreshore.

6. Sandbody Geometry

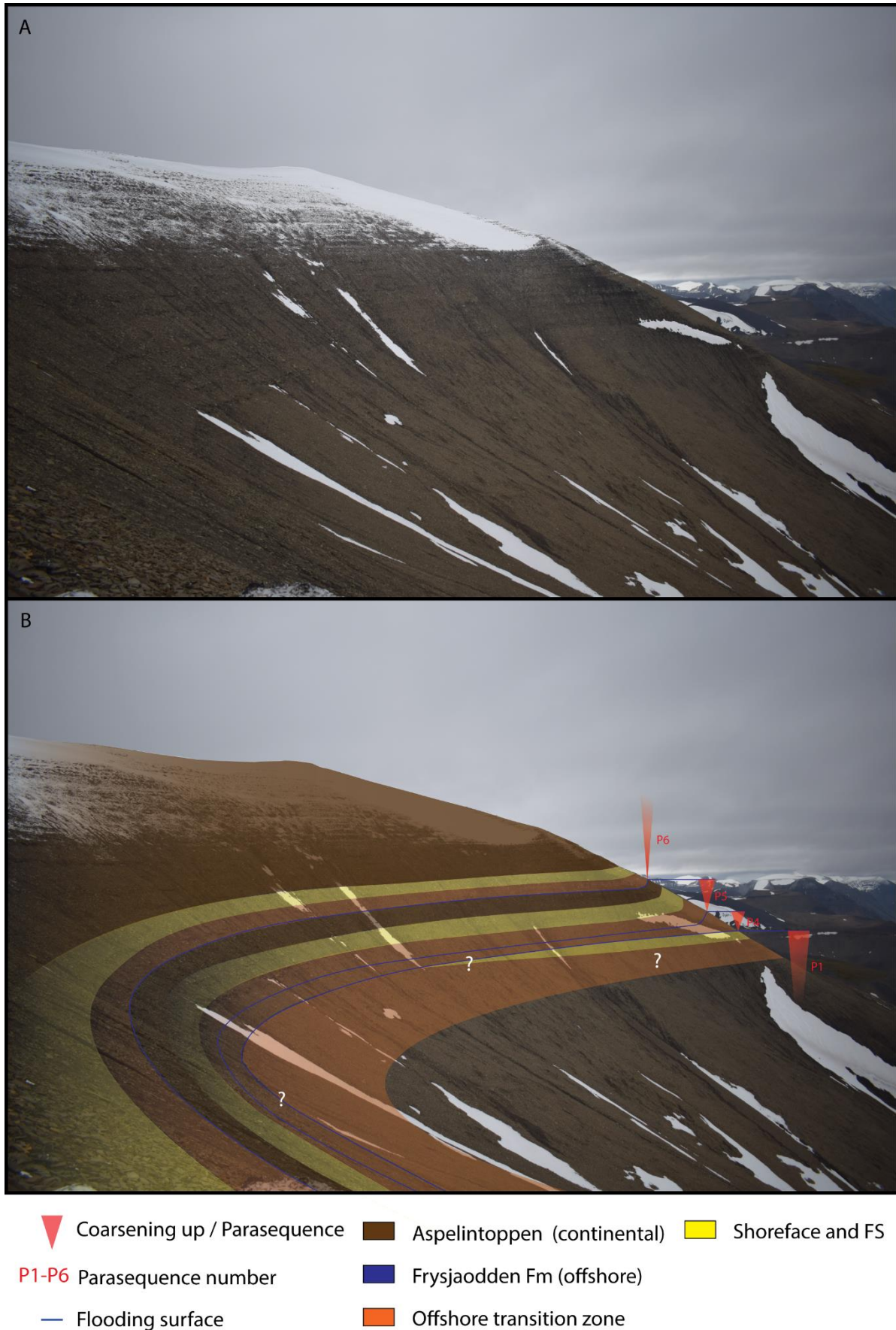


Figure 6.8: (A) Photograph taken from Log C location, directed towards Log D location. (B) Same photo as (A), with interpreted facies. FS = Foreshore.

6. Sandbody Geometry

Interpretation:

The internal change to shoreface and foreshore deposits towards the top of P1 at Log D location counteracting the regional trend of southeastwards progradation, is likely due to a delta lobe building out in that area. In this area, the northeastward decrease in distributary channel deposits (absent at Log D location) at top of P5, shows that the fluvial system capping the parasequence was localized rather than regionally extensive. Otherwise, Transect A show limited change in the lateral parasequence distribution along strike direction in the study area. This makes the local tabular nature of the sandbodies evident, and show that the lateral parasequence extent was greater than that of the study area.

7.5.2 Transect B

Description:

Transect B (Figure 6.9) starts at BH 9-2005 and follows the interpreted depositional dip direction to Urdkollbreen, then changes to depositional strike to Skalken, then back to depositional dip direction to Rekstentoppen 1, Rekstentoppen 2 and Log E, before it lastly switches back to following depositional strike direction along Transect A. A total of six parasequences are located along the transect which show an overall low-angle ascending shoreline trajectory. Osen (2012) referred to several uncertainty factors (scree cover, valleys and glaciers) which implicated interpretations of P1, P3 and P4's lateral extent stretching from BH 9-2005 to the rest of the logged sections.

As previously explained, P1 is the lowermost and the thickest of the parasequences, and the only parasequence that grades downwards into the Gilsonryggen shales. Along Transect B, it is capped by a flooding surface between BH 9-2005 and Skalken, and at Log D. Somewhere between Skalken and Log B, the shoreface and foreshore deposits at top of P1 cease to exist, and the flooding surface is represented as a correlative surface between stacked offshore transition zone deposits.

P1-P5 are present at BH 9-2005 location in the northwestern most parts of the combined study area. While P1, P4 and P5 stretches across the whole transect, P2 and P3 pinches out in the depositional dip direction, P2 between the BH 9-2005 and Skalken locations, and P3 between Rekstentoppen 1 and Log B locations. P5 increases in thickness in depositional dip direction. This might also be the case for P4, southeastwards from Skalken location, before it then thins towards Log E locations. P2 is the only parasequence recorded that counteracts the overall regressive low-angle ascending shoreline trajectory, by representing a significant backstepping of the system.

6. Sandbody Geometry

The distributary channel deposits at top of P5 dissipates towards the NW direction, with the channel fills being fewer and thinner with less erosion into the underlying shallow-marine deposits.

P6, which interfingers with the Aspelintoppen Formation in the SE, pinches out towards the NW before the Rekstentoppen 2 location.

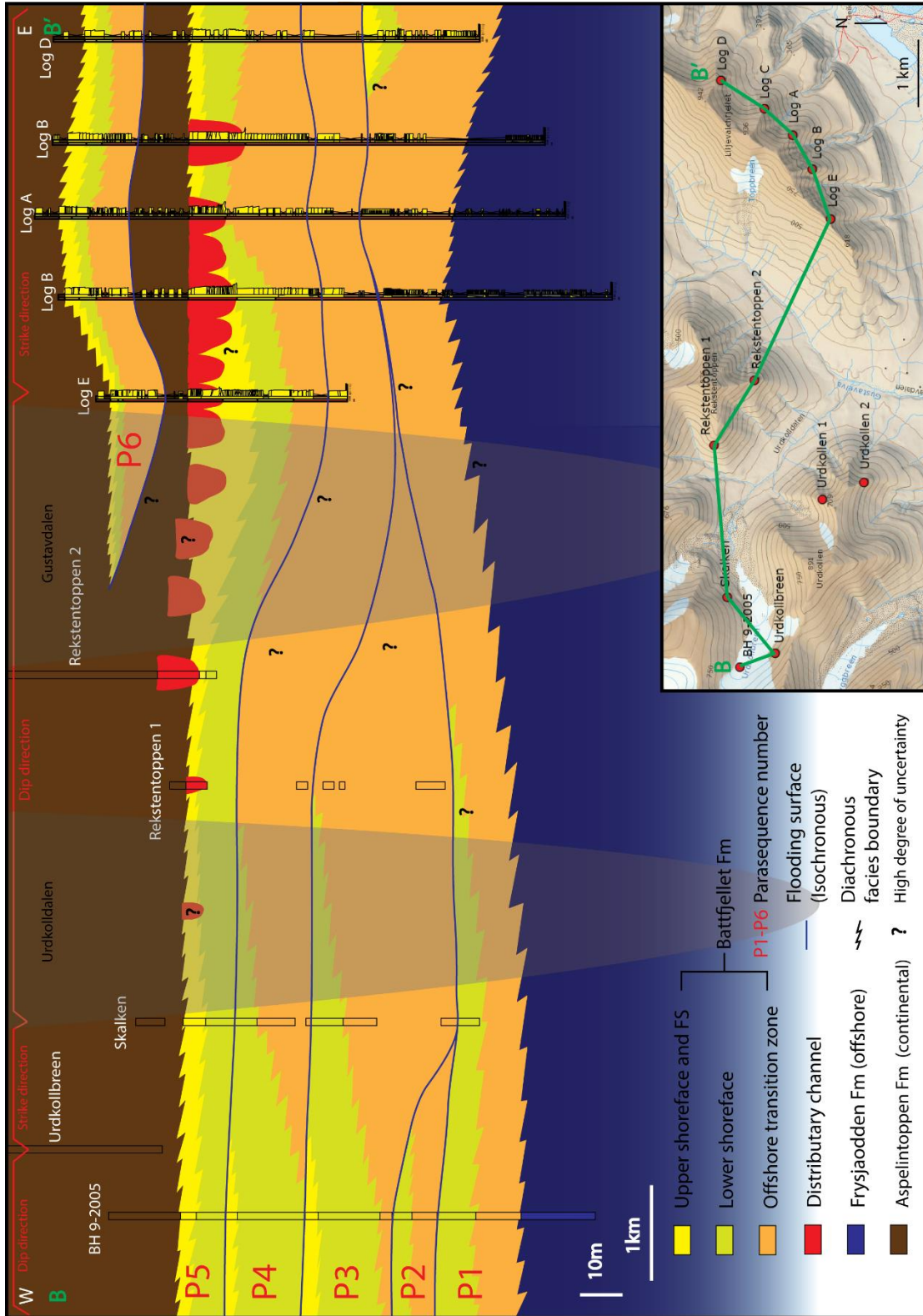


Figure 6.9: Correlation panel along Transect B. Gray area is a valley. The overview map shows position of Transect B in the study area.

6. Sandbody Geometry

Interpretation:

Along Transect B, a forward stepping parasequence pattern is evident, only interrupted by the intermittent backstepping of P2. This supports the regional depositional model of the Battfjellet Formation presented by Helland-Hansen and Grundvåg (in prep). The SE pinchout of P2 and P3 is the likely distal termination of these parasequences, which means that it is uncertain to know their maximum thickness and lateral extent towards the NW. This distal termination and thinning of P4 parallel to the dip direction, supports the interpretation of an SE oriented dip direction and buildout of the system. This is further supported by the distal development of the internal facies distribution towards the SE in P1-P4.

7.5.3 Transect C:

Description:

Transect C (Figure 6.10) starts at BH 9-2005 and follows depositional strike direction to BH 11-2003, then changes to depositional dip direction covering BH 10-2006, Gustavfjellet 1, Gustavfjellet 2 and Log D locations. The same six parasequences as in Transect B are present in Transect C, with P1, P4 and P5 having similar evolution as in Transect B. The same overall low-angle ascending shoreline trajectory is also evident.

P2 and P3 terminate in depositional dip direction, P2 between BH 9-2005 and BH 11-2003 locations, and P3 between Gustavfjellet 2 and Log D Locations. P3 also differs from the other parasequences in that it splits into in the lower shoreface deposits between BH 11-2003 and BH 10-2006 locations. As along Transect B, P2 is the only parasequence that violates the overall regressive low-angle ascending shoreline trajectory, by representing a local backstepping of the system.

P6 is only present at Log D location, and pinches out into the Aspelintoppen Formation somewhere between BH 10-2006 and Log D locations. It might be present in Gustavfjellet 1 and Gustavfjellet 2 locations, but then above the outcrops logged by Osen (2012).

Interpretation:

Osen (2012) pointed to the more distal character of the internal facies of P3 and P4 in Transect B relative to Transect A, to be a possible indicator of a strike directed wedging out of these units towards the north. He further suggested that the split of P3 in its distal reaches, to be of a parasequence bed-set origin, and not a flooding surface of parasequence scale. He backed up this interpretation by the

6. Sandbody Geometry

absence of a flooding surface candidate in nearby well BH 11-2003. Hampson et al (2008) suggests that such stratigraphic variation probably are a result of changes in wave climate, temporal and spatial variations in sediment supply, and relative sea-level fluctuations.

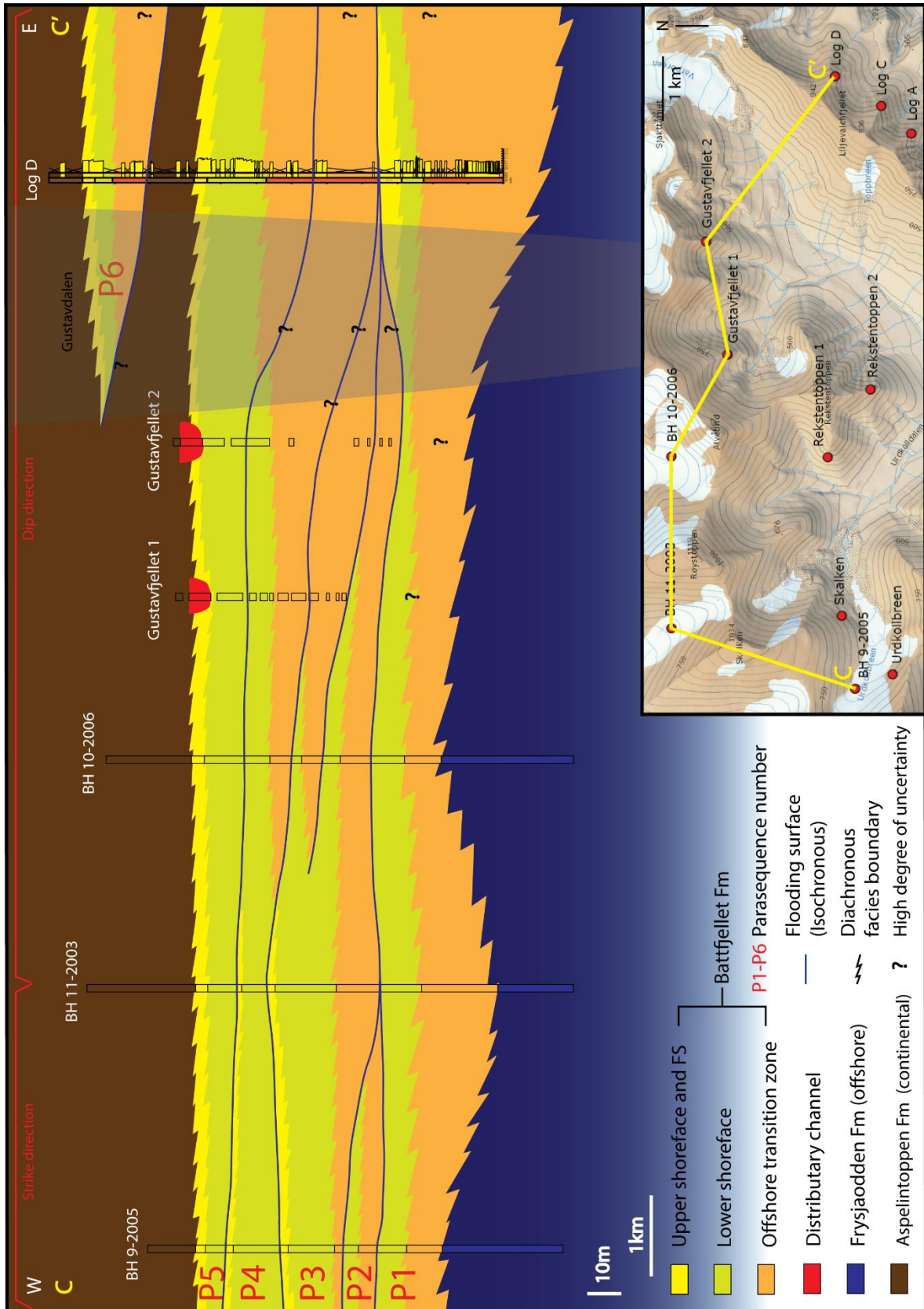


Figure 6.10: Correlation panel along Transect C. Gray areas are valleys. The overview map shows position of Transect C in the study area.

7. Digital 3D Reservoir Model

7.1 Introduction

This chapter presents a conceptual 3D reservoir model, which focuses on the Battfjellet Fm and covers an area of approximately 11 x 6 km. The model is the first of its kind made of the Central Basin deposits, giving a unique new look at the Battfjellet formation in 3D. It also enables volume estimations and serves as a basis for future work on the formation.

7.2 3D Modelling

The model was constructed in Petrel by importing interpreted lines and logs from Osen (2012) and this study. Osen (2012) logs are based on eight outcrops (Urdkollbreen, Skalken, Urdkollen 1, Urdkollen 2, Rekstentoppen 1, Rekstentoppen 2, Gustavfjellet 1 and Gustavfjellet 2), and three wells (cores: BH 9-2005, BH 10-2006 and BH 11-2003), in the Urdkollen, Rekstentoppen and Gustavfjellet areas, west of Liljevalchfjellet (Figure 8.1). When modelling, logs were positioned to account for the slightly ascending shoreline trajectory interpreted for the Battfjellet Formation (Grundvåg et al., 2014b; Helland-Hansen and Grundvåg, in prep).

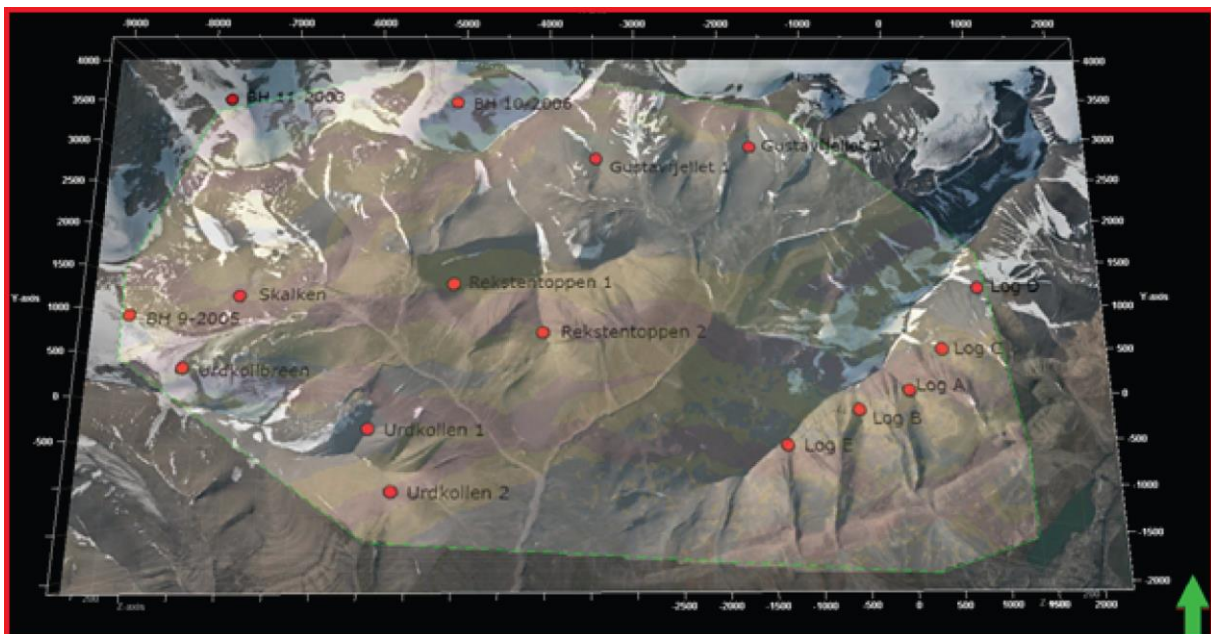


Figure 7.1: The reservoir model (outlined by green dotted line) extrapolated on top of the Urdkollaldalen and Liljevalchfjellet areas. The red dots show the position of the eight outcrops and three well cores logged and interpreted by Osen (2012), and the five outcrops logged and interpreted in this study. X and Y coordinates are given in meters, and uses the bottom of Log A as reference point.

7. Digital 3D Reservoir Model

To create a digital 3D reservoir model, the following steps were performed:

A. Transferred logs to Petrel (Figure 7.2: A):

- Converted interpreted logs into PNG-File format and imported them to Petrel E&P Software 2015.
- Used the distance-measuring tool on Topo Svalbard to create X and Y coordinates for the logs, using the bottom of Log A as reference point.
- Created Z values for the logs using the meters above sea level relative to the reference point, and adjusting heights to level out folding.

B. Created polygons (Figure 7.2: B):

- Created polygon points on the top of interpreted facies associations, added extra points that were dragged out to fit interpreted lines from correlation panels.

C. Made surfaces (Figure 7.2: C):

- Made surfaces from the polygons with automatic grid size and position from input data/boundary, and made boundary from input and extended it with 10 nodes.
- Copied the uppermost and lowermost surfaces, placed these a few meters above and below (by translating the Z-axis value by 50 points in operations) the upper and lowermost surfaces, to make zones for the overlying Aspelintoppen Formation and underlying Gilsonryggen Member.

D. Created a simple grid (Figure 7.2: D):

- Made simple grid from structural modelling, by inserting the surfaces and choosing automatic grid size and position from input data/ boundary. Grid increment was set to 25x25, which was suitable to capture the essential geometries of the facies. Used Insert surfaces in input data. Added these in sequence with the uppermost surface on top.

E. Created Zones (Figure 7.2: E):

- Selected the 3D model and used the Corner point gridding/Layering process. Followed base for all zones, except Zone 3: Interfingering Aspelintoppen Formation, which followed top. Cell thickness was set to 5.

F. Modelled Facies (Figure 7.2: F):

- Facies modelling was then performed by zone. Used the processes tab, property modelling, facies modelling. For settings used in each zone, see Table 7.1.

Due to issues with Petrel, the model was exported to RMS 2013.0.1 via Rescue format, to display cross-sections of the model and do volume estimations.

7. Digital 3D Reservoir Model

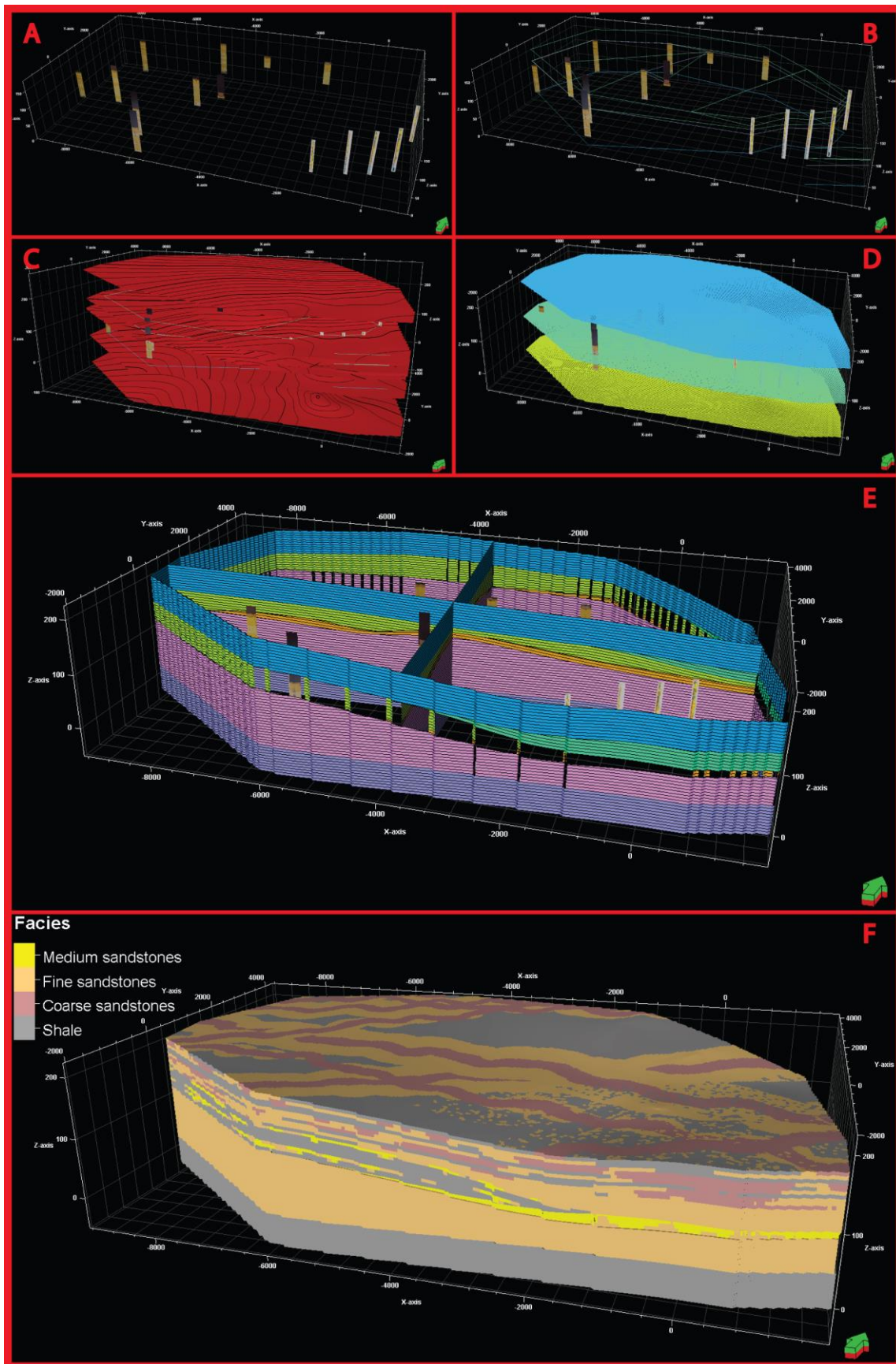


Figure 7.2: Steps performed to create the digital 3D reservoir model. (A) Logs transferred into Petrel. (B) Polygons created. (C) Surfaces made. (D) Created grid. (E) Created Zones. (F) Finished model with facies interpretations.

7. Digital 3D Reservoir Model

Numerical data used to create the model and a short description of the modelled zones is presented in Table 8.1. Boundaries between the zones are conformable, except the channel units (sand), which are allowed to erode downwards. The model length (X-axis) is 11,1km, width (Y-axis) is 6.3km, and height (Z-Axis) is 275m. Total number of grid cells are 7607046, and no faults are accounted for in the model.

Table 7.1: Facies modelling parameters. Parameters given in the format 0.5:1:1.5, refers to minimum:average:maximum values.

Zone #	Description	Modelling Method
1	Bulk Aspelintoppen Fm (floodplain shales, overbank sandstones and river channel sandstones)	Object modelling (stochastic) with shale background. "Coarse sand" fluvial channel bodies inserted with a 66 % volume fraction. "Fine sand" levees activated on the channels to model the overbank deposits. Channel layout: Orientation: 30:90:120, amplitude: 50:250:300, Wavelength: 1000:1500:2000. Section: width: 150:300:450, thickness: 3:4.5:16. Levee (values relative to channel width and thickness): width: 2:2.5:4, thickness: 0.2:0.25:0.8. Orientation layout is based upon the paleocurrent data collected in the study area, and the interpretation of low sinuous channels (Ford and Pyles, 2014). Section and levee layout is based upon the suggestion that roughly 2/3 of Aspelintoppen Fm is comprised of alternating floodplain sandstone sheets and shales (Steel et al., 1985), and that most of the fluvial channel fills are 4–5 m thick, with some reaching up to 16 m (Plink-Björklund, 2005).
2	P6 Battfjellet Fm (shallow marine sandstones)	Populated with only fine sand to represent the stacked sandstone beds of the Battfjellet Formation.
3	Interfingering Aspelintoppen Fm (floodplain shales, overbank sandstones and river channel sandstones)	Object modelling (stochastic) with shale background. "Sand" fluvial channel bodies inserted with a 20 % volume fraction. "Fine sand" levees activated on the channels to model the overbank deposits. Channel layout: Orientation: 30:90:120, amplitude: 50:250:300, Wavelength: 1000:1500:2000. Section: width: 150:300:450, thickness: 0.5:1:1.5. Levee (values relative to channel width and thickness): width: 0.3:0.5:0.7, thickness: 0.2:0.7:0.9. This layout is based upon the same concepts as Zone 1, but adjusted to suit FA3.
4	Erosive Channel Belt (shallow marine sandstones and distributary fluvial channel sandstones cutting down into the Battfjellet Fm)	Object modelling (stochastic) with fine sand background. "Sand" fluvial channel bodies inserted with a 60 % volume fraction. Channel layout: Orientation: 30:90:120, amplitude: 50:250:300, Wavelength: 1000:1500:2000. Section: width: 150:300:450, thickness: 9:13:16. This layout is based upon the geometry of the channels as observed in field, and interpreted by Osen (2012).
5	P1-P5 Battfjellet Fm (shallow marine sandstones)	As Zone 2
6	Gilsonryggen Member (offshore shales)	Populated with only shales, this unit represents a homogenous bottom seal that will not affect flow simulation.

7. Digital 3D Reservoir Model

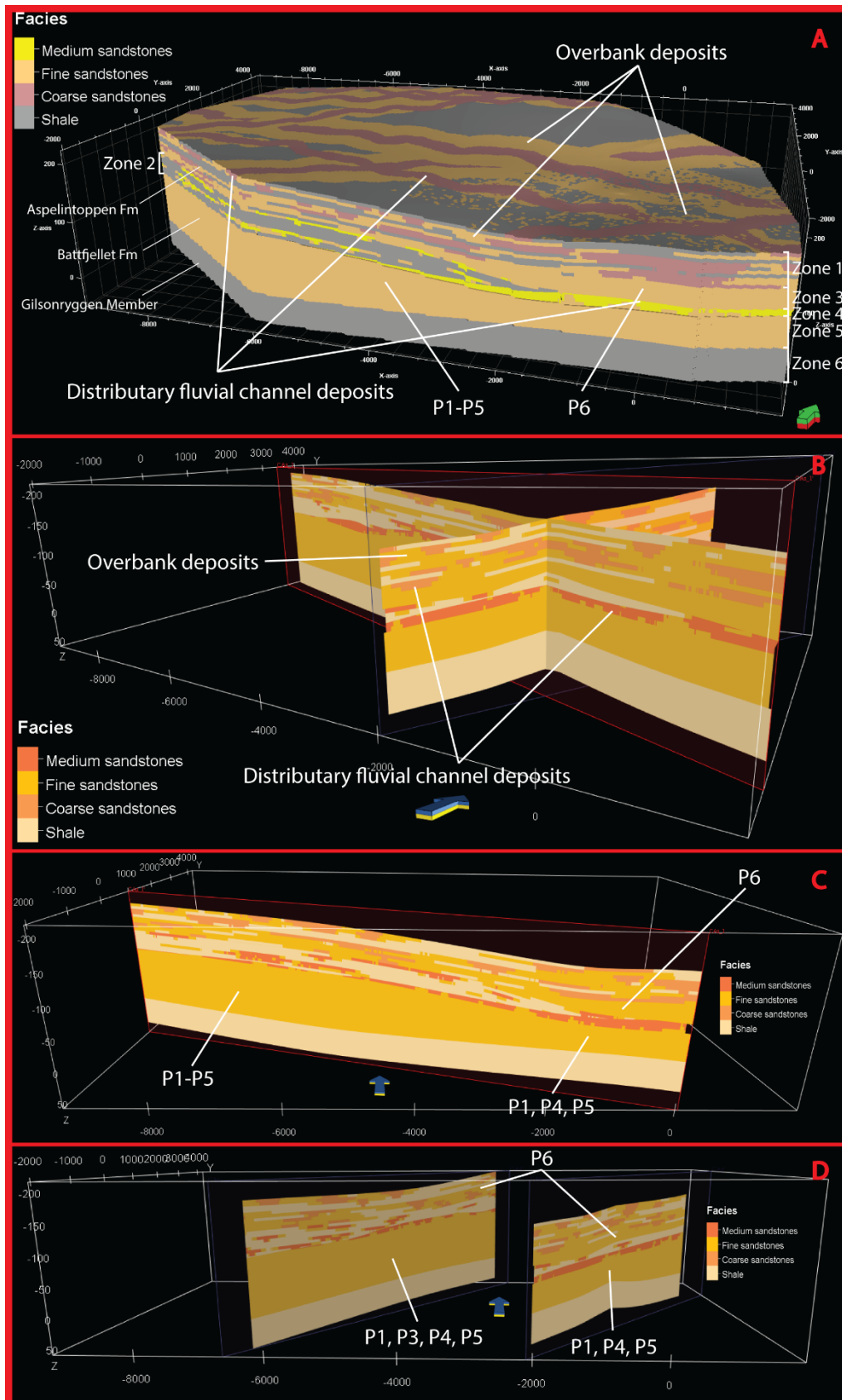


Figure 7.3: Reservoir model focusing on the Battfjellet Formation, built in Petrel (cross-sections are visualized in RMS). (A) Three-dimensional view of the model. (B) Vertical cross-sections through the center of the model, following depositional strike and dip directions. (C) Vertical cross-section following depositional dip direction. (D) Vertical cross-sections following depositional strike direction.

7. Digital 3D Reservoir Model

The reservoir model is presented as a whole and through a series of cross-sections in Figure 7.3 above. It is clear that Zone 5 (consisting of P1-P5) thins and descends in the depositional dip direction. Zone 2 (consisting of the part of the Aspelintoppen that interfingers into the underlying Battfjellet Formation) thins and eventually pinches out in depositional dip direction. In return, Zone 3 consisting of P1, thickens in depositional dip direction, where it is interpreted to eventually superimpose Zone 5 (P1-P5).

8.3 Volumetrics

Reservoir thickness and volume estimates were calculated from the reservoir interval of the model (Zone 2 – Zone 5). When calculating the net reservoir volume and net-to-gross (NTG) ratio, sandstones were regarded as rocks that can store and flow hydrocarbons/CO², while shales were regarded as rocks that cannot store or flow hydrocarbons/CO². The resulting estimates are listed in Table 7.2 below:

Table 7.2: *Volumetrics of reservoir model.*

Volumetrics	
Reservoir thickness	90 m
Gross rock	2 909 425 m ³
Net reservoir	1 763 344 m ³
Net-to-gross (NTG)	0.6

7.4 Reservoir Modelling Errors:

The 3D modelling is based upon interpreted logs and correlation panels. This provides a high level of uncertainty. The 3D model should therefore only be used as a conceptual model giving a general view of the facies distributions, and sandbody geometries.

X and Y coordinates of the logs used for building the reservoir model was determined by measuring their relative distances from Log A (reference point) using the measuring tool on Topo Svalbard. These measured distances likely have up to tens of meters of inaccuracy. Z coordinates of the logs are determined by how thick the logs are, and repositioned by eye measurement to fit the right height of the interpreted facies. This provides uncertainties in the exact height of the interpreted facies which is further enhanced by the logging errors mentioned in Chapter 3.1.

The thin sand lenses in the Gilsonryggen Member, the thin siltstones in the lower parts of the Battfjellet Fm and faults was not accounted for in the modelling. This might further increase uncertainties.

8. Discussion

8.1 Introduction

This chapter discusses the depositional environment and paleogeography of the study area, based upon the interpretation of facies associations, paleocurrent directions and parasequence stacking patterns presented in the previous chapters. A paleogeographical model for the Battfjellet formation during the late stage of basin infill, which accommodates the interpretations of this study, is also presented (Figure 8.2).

8.2 Depositional environment

A deltaic depositional setting for the succession is evident from the distributary fluvial channels (FA3) cutting into the shallow marine deposits (FA1), the upwards change in depositional environment from shallow marine to delta plain deposits and the immature sediments of the Battfjellet Formation (Helland-Hansen, 2010) (Figure 8.1). This interpretation is supported by previous studies (Steel, 1977; Helland-Hansen, 1990, 2010; Steel et al., 2000; Uroza & Steel, 2008; Pontén & Plink-Bjørklund, 2009; Gjelberg, 2010; Skarpeid, 2010; Osen, 2012; Grundvåg et al., 2014b; Helland-Hansen and Grundvåg, in prep).

The dominance of wave generated sedimentary structures in the Battfjellet Formation, points to deposition in a wave-agitated basin. Storm-weather-wave-base and fair-weather-wave-base thus determined the extent of the shallow marine deposits of FA2-A (Offshore transition zone deposits), FA2-B (Lower shoreface deposits) and FA2-C (Upper shoreface and Foreshore deposits). The interpreted paleo-latitude during these late stages of basin infill, points to a temperate climate (Worsley and Aga 1986; Clifton, 2012), meaning the storms were likely related to seasonal events. Limited lateral extent of the parasequences (<20 km in any direction) recorded in other parts of the Battfjellet Formation, indicates that the sandy sediments were not dispersed far out along the shore. However, longshore currents must have been present, as longshore bars and locally deflected river mouths are present in the formation (Grundvåg et al., 2014b). Helland-Hansen (2010) referred to the abundant soft sediment deformation structures and immature sandstone composition as evidence of rapid deposition and high sediment supply. He explained that the rapid deposition limited the time for wave action to mature the sediments and spread out the sands.

Distributary channels with a large capacity (Helland-Hansen, 2010), cut deep into the delta, and deposited mouth bars at the delta front. Osen (2012) recorded such mouth bars being superimposed

8. Discussion

by distributary channel deposits, witnessing the rapid advancement of the distributary fluvial channels. He also recorded a common presence of interdistributary bay/lagoon deposits superimposing beach deposits, evidence of barrier island presence. The complex stacking pattern of the parasequences in the Battfjellet formation suggest a frequent switching of delta lobes (Grundvåg et al., 2014b). This switching was likely driven by infilling of topographically lower interdistributary bays or lagoons situated between previously deposited lobes (Figure 8.1).

Though no apparent tidal reworking was recorded in the study area, some tidal influence must have been present in the basin, as e.g. tidal inlets and tidal-reworked distributary channel deposits has been recorded in previous studies (Steel, 1977; Helland-Hansen 1985, 2010; Mellere et al., 2002; Plink-Björklund, 2005; Løseth et al., 2006; Uroza and Steel, 2008; Pontén and Plink-Björklund, 2009; Stene, 2009; Skarpeid, 2010; Gjelberg, 2010; Grundvåg et al., 2014, Naurstad, 2014).

In situ coal deposits at the delta plain, and the presence of large leafs suggests a vegetated delta plain with presence of large trees.

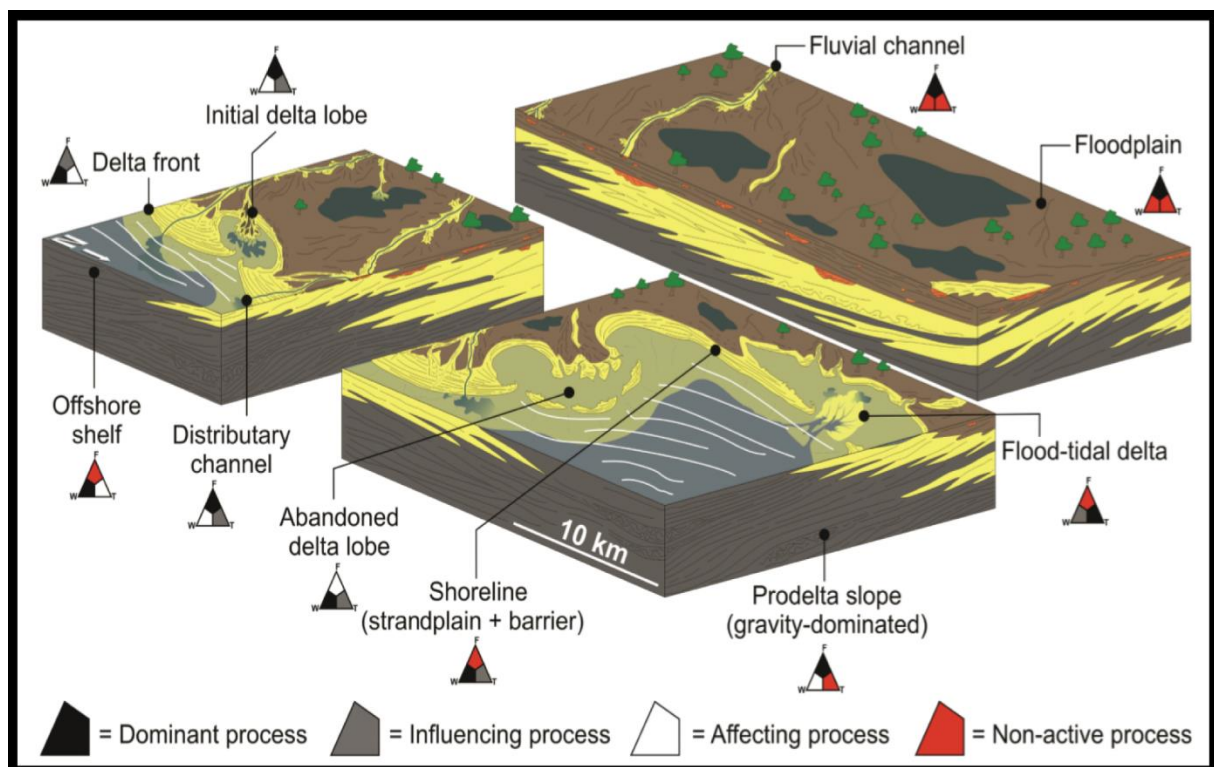


Figure 8.1: Schematic block diagram of the depositional environments and architecture of the Battfjellet Formation (modified from Grundvåg et al, 2014b), showing how process regimes changed laterally. The deltaic shoreline environment had a wave-dominated delta front, and delta lobes were reworked mostly by waves, but also by some tidal action.

8. Discussion

The easterly-located deltaic deposits of the Battfjellet Formation lack the clinoforms and submarine fans of the shelf edge deltas in the western and central parts of the basin. The parasequences also show a gentler depositional dip and have a close to tabular geometry, which indicates that they were deposited in a ramp-like setting with no pronounced shelf-slope break physiography (Helland-Hansen, 1990; Grundvåg et al., 2014).

8.3 Sequence stratigraphy

8.3.1 Introduction

The small size of the combined study area, coupled with the general absence of major basinward facies dislocations and major flooding events within the Battfjellet Formation (Grundvåg et al., 2014b), makes division into different systems tracts difficult. The focus of this sub chapter is therefore mainly on the shoreline trajectory within the Battfjellet Formation, and intervening transgressive episodes. Worth noting though, is Uroza and Steel's (2008) interpretation of a highstand systems tract for the Battfjellet Formation shelf edge deltas and associated clinoforms in the western part of the basin. This interpretation is most likely transferable across the basin, as greenhouse conditions lead to eustatic highstand conditions through most of the Eocene epoch (Miller et al., 2005).

8.3.2 Shoreline trajectory

Shoreline trajectory is dependent on several factors, such as basin topography, sediment supply, eustasy and subsidence rate (Helland-Hansen and Gjelberg, 1994; Helland-Hansen and Mart, 1996). The Central Basin, being a foreland basin, experienced a high subsidence rate (Helland-Hansen and Grundvåg, in prep), but in regards to the buildout of the individual parasequences, tectonic subsidence can be ignored (Helland-Hansen and Grundvåg, in prep). This is because delta progradation in such basins happens at a much faster rate than of the tectonic subsidence (Aadland and Helland-Hansen, 2016).

Helland-Hansen and Grundvåg (in prep) proposed that the system as a whole demonstrates a flat to low-angle ascending shoreline trajectory. Grundvåg et al (2014b) estimated the overall angle of the ascending progradational system to be around 1° . This is however a rough estimate, which does not take into account factors such as local variations in shoreline trajectory and differential compaction. The parasequences studied in this thesis also built out with an overall slightly ascending shoreline trajectory. As mentioned in Chapter 6, P2 is the only exception to this trend, representing a local backstepping of the system. This backstepping is however not evidence of an overall retreating

8. Discussion

shoreline, as it is likely related to lateral lobe shifting. Further, fluvial channels cutting into the shoreface, such as FA3, are often an indicator of a descending regression (Bhattacharya, 2006). However, as there are no other evidence for a descending regression in these parasequences, and since fluvial channels in general have the capacity to erode below sea level, such an interpretation is rejected.

The overall ascending shoreline trajectory within the Battfjellet Formation suggests that deposition took place during a continuous rise in relative sea level. According to Grundvåg et al (2014b) this was due to a combination of a high rate of tectonically induced basin subsidence (Steel et al., 1985; Müller Spielhagen, 1990), the Eocene eustatic highstand conditions (Miller et al., 2005) and sediment compaction.

8.3.3 Cause of transgressions

The regressively stacked parasequences of the study area are separated by intervening transgressive episodes represented as flooding surfaces and their correlative surfaces. In Osen (2012) study area, a neglectable amount of transgressive deposits separates the parasequences, something which is common within the Battfjellet Formation (Helland-Hansen, 2010). The effect of a limited lateral extent of the deltas, and the frequent delta lobe switching are suggested to best explain these transgressions (Helland-Hansen, 1895, 1990, 2010; Olsen, 2008; Stene, 2009; Skarpeid; 2010; Gjelberg, 2010; Osen, 2012; Grundvåg et al., 2014b). In this scenario, there was a simultaneous variation along the coastline, where protruding deltas underwent a regressive outbuilding, while the areas of topographic low between were subject to transgressive rework.

It should not be rejected that the complex parasequence stacking pattern of the Battfjellet Formation could be a result of tectonically induced transgressions and alternating supply-driven regressions (Helland-Hansen, 2010). This is however less likely, as the delta deposits were probably backed by a low-gradient coastal plain, that would have been flooded far inland during a rise in relative sea-level. Transgressive deposits from such a flooding are as mentioned, not present in the study area.

8.5 Delta type

The dominance of wave generated structures in FA1, point to a strongly wave-dominated deltaic setting. However, previous studies all point to a limited lateral extent of the sandbodies, and a lobate shoreline morphology for the Battfjellet Formation, commonly found in river-dominated deltaic settings (Olsen, 2008; Stene, 2009; Gjelberg, 2010; Helland-Hansen, 2010; Skarpeid, 2010; Grundvåg

8. Discussion

et al., 2014b; Helland-Hansen and Grundvåg, in prep). Due to the limited size of the study area, the total lateral extent of the sandbodies are uncertain, but looking at the findings of the previous studies, a similar low lateral extent of the sandbodies and lobate shoreline morphology is inferred. Given the evidence for both wave and fluvial influence, the Battfjellet deltaic system is interpreted as a fluvio-wave interaction delta. A classification first given by Helland-Hansen (2010), which was later supported by Grundvåg et al (2014b), and Helland-Hansen and Grundvåg (in prep).

A paleogeographic model of the Battfjellet deltaic system is presented in Figure 8.2 below. The model illustrates the large-scale shoreline morphology and sub environments of the deltaic setting.

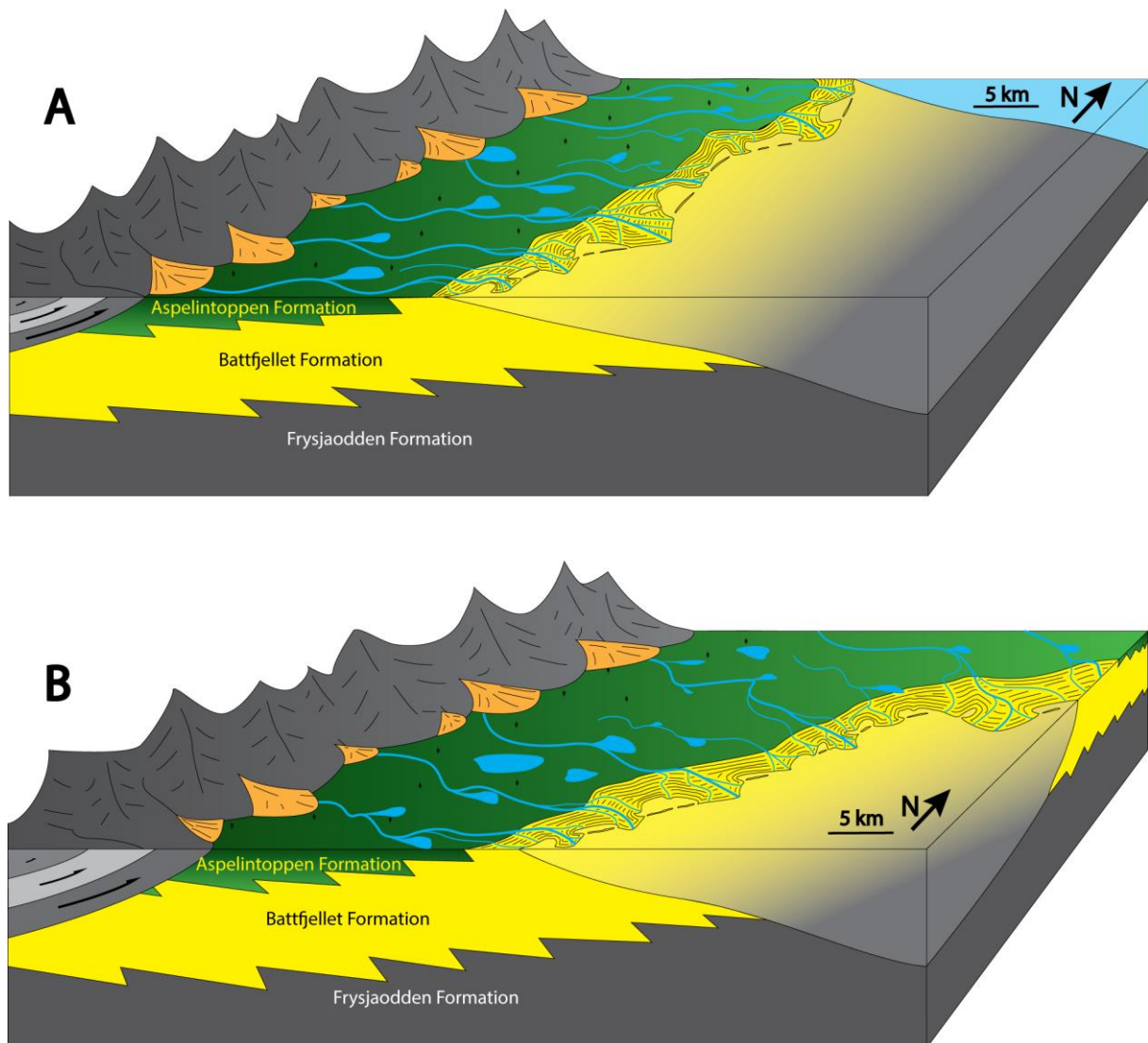


Figure 8.2: Proposed paleogeographic maps inferred from the deposits of the Battfjellet Formation (figure is vertically exaggerated). (A) Battfjellet Formation as proposed by other studies (B) Late development of the Battfjellet Formation in the eastern part of the basin, where the northern part of the basin has been gradually filled in, changing the shoreline outbuilding to a more southeastward direction.

8. Discussion

8.5.1 Modern Analogue

The Po delta in northeastern Italy (Figure 8.3) has been regarded as a possible analogue to the Battfjellet Formation deltas by several studies (Olsen, 2008; Helland-Hansen, 2010; Skarpeid, 2010; Gjelberg, 2010, Osen, 2012; Grundvåg et al., 2014b). This late Holocene delta, builds out into the Adriatic Sea, which similar to the Central Basin, is regarded as largely wave-influenced with some tidal influence (Amorosi and Milli, 2001). Using the classification scheme by Galloway (1975), Helland-Hansen (2010) classified the Po delta as a fluvio-wave interaction delta. Additionally, the presence of several parasequences have been attributed to autogenic lobe switching (Amorosi and Milli, 2001; Correggiari et al., 2005). However, though the Po delta have similarities to the deltas of the Battfjellet Formation, its size is significantly larger.

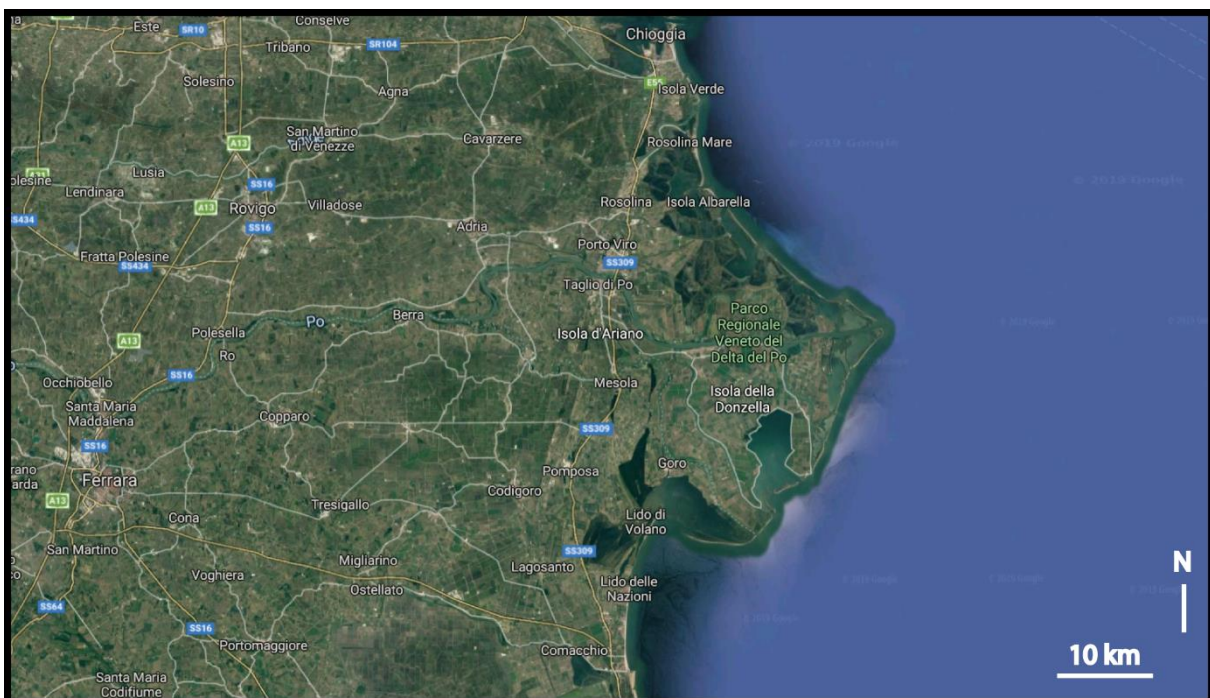


Figure 8.3: Picture of the Po delta, a fluvio-wave interaction delta similar to the deltaic lobes of the Battfjellet Formation, only larger. (Google Earth).

The 30 x 30 km Rhone deltaic headland (Kruit, 1955) and the 50 x 50 km Danube delta (Giosan et al., 2005) has been mentioned as other relevant fluvio-wave interaction delta analogues to the Battfjellet Formation (Helland-Hansen 2010). As a size comparison analogue to the Battfjellet deltas, the 9 x 8 km elongated wave dominated Williams delta in the Canadian Arctic (Smith et al., 2005) has also been used (Helland-Hansen 2010).

8. Discussion

8.5.2 Delta size

As previously mentioned, the lateral extent of the individual parasequences could not be determined based upon the data obtained in the study area. Getting an estimation of the size of the individual delta lobes in the study area is therefore complicated. It is however certain that the delta lobes that created P1, P4 and P5 must have at least been wider than the study area in strike direction (>6 km), since they extend laterally across the whole study area.

Helland-Hansen (2010) explained that the small size of the basin of approximately 200 x 60 km, indicated short distances to the catchment area and minor tributary joining, which lead to the formation of small deltas. He further proposed that the cost-parallel extension of the deltas must have been about the same magnitude as the lateral extent of the sandbodies in strike direction. These range from a few kilometers up to 20 km in any given direction (Helland-Hansen, 2010; Grundvåg et al., 2014b). Based upon the size of the parasequences in the study area and previous work, it is therefore suggested that the delta lobes in the study area must have been in the order of a few km to 20 km in any given direction.

9. Summary and Conclusions

Fieldwork carried out on Liljevalchfjellet, Svalbard, formed the basis of a detailed facies analysis for the study area. Work by Osen (2012) in the adjacent Urdkolldalen area was then incorporated, to interpret sandbody geometry, reconstruct paleogeography and create a digital 3D reservoir model for the combined study area. Abundant scree cover, glaciers and large valleys in this combined study area lead to difficulties when interpreting and correlating.

The Battfjellet Formation constitutes the delta front of a regressive megasequence (the GBA-unit) prograding eastward into a foreland basin (the Central Basin). In the western and central parts of the basin, the Battfjellet Formation is characterized by shelf edge deltas, clinofolds and basin floor fans. In the eastern part, subject to this study, shelf deltas built out in a low angle ramp setting.

The main results and conclusions of this study are presented below:

1. The studied deposits have been subdivided into fourteen lithofacies, and grouped into four facies associations based upon their interpreted depositional environment. The facies associations are stacked on top of each other in a shallowing upwards fashion, from the prodelta/offshore deposits (FA1) of the Gilsonryggen Member, through the prograding wave dominated delta deposits (FA2) of the Battfjellet Formation, and lastly the distributary fluvial channel deposits (FA3) and continental deposits (FA4) of the Aspelintoppen Formation.
2. Paleocurrent measurements from the study area suggests a NE to SW oriented paleo shoreline, and a subsequent NW to SE outbuilding of the system. This means a shift towards a more southward direction of progradation in the later stages of basin infill relative to what has been previously interpreted for the Battfjellet Formation.
3. A total of six stacked parasequences is recorded in the combined study area. They are separated by flooding surfaces and their correlative surfaces, and build out with an overall slight ascending shoreline trajectory. The deposition thus took place during a continuous rise in relative sea-level.
4. A digital 3D reservoir model focusing on the Battfjellet Formation, covering an area of 11 x 6 km was constructed, by incorporating the results of this study with work from Olsen (2012). Though conceptual, it gives a better view of the possible sandbody geometries and a better understanding of the facies associations.
5. High rates of sediment supply and rapid deposition is evident from the immature sandstones, abundant soft sediment deformation structures and the overall regressive ascending shoreline trajectory.

9. Summary and Conclusions

6. Abundant wave-generated structures coupled with a complex delta lobe stacking pattern due to frequent allogenic delta lobe switching, leads to the interpretation of a fluvio-wave interaction delta.
7. Transgressive reworking of interdistributary bay/lagoons between delta lobes took place simultaneous to the rapid progradation of the delta lobes.
8. The Po delta in northeastern Italy is suggested as a possible analogue to the Battfjellet deltas. However, its size is larger than the deltas of the Battfjellet Formation, which are estimated to have a lateral extent of few km up to 20 km.

Suggestions for further work

The apparent change to a more southward progradation of the Battfjellet Formation in the later stages of basin infill should be further investigated, as it is different to what has been previously interpreted. Emphasis should therefore be put on collection of paleocurrent measurements, and interpretation of sandbody geometries of The Battfjellet Formation in the eastern part of the Central basin.

As mentioned in Chapter 7, the 3D reservoir model constructed in this thesis should be used for further reference. Given the seal potential of the overlying mud prone delta plain deposits, a more thorough and extensive 3D modelling of the formation could help to better understand the extent of similar subsurface reservoirs, in regards to both petroleum exploration and CO² injection. Modern technology such as Lidar, or drone footage could be used to better map the lateral extent of the sandbodies, and height maps of the area could be imported into the reservoir model from GIS (Geographical Information System) softwares. Flow simulation of the model could also be conducted for various reasons, such as determining the most optimal sweep and estimating production/injection rates. If such work is performed, petrophysical parameters from the wave-dominated delta sandstones of the Sognefjorden Formation could be used for the Battfjellet Formation.

10. References

- Aadland, T. and Helland-Hansen, W.** (2016) Global compilation of coastline change at river mouths. *EGU General Assembly Conference Abstracts*. **18**. 3915.
- Aagard, P., Dypvika, H., Hellevang, H., Miri, R., Nystuena, J.P. and Sundala, A.** (2014) Variations in mineralization potential for CO₂ related to sedimentary facies and burial depth - A comparative study from the North Sea. *Energy Procedia*. **63**. 5063-5070.
- Amorosi, A. and Milli, S.** (2001) Late Quaternary depositional architecture of Po and Tevere river deltas (Italy) and worldwide comparism with coeval deltaic successions. *Sedimentary Geology*. **144**. 357-375.
- Arnott, R.W. and Southard, J.B.** (1990) Exploratory flow-duct experiments on combined-flow bed configurations, and some implications for interpreting storm-event stratification. *Journal of Sedimentary Petrology*, **60**. 211-219.
- Bhattacharya, J.** (2006) Deltas. *SEMP*. **84**. 237-292.
- Bhattacharya, J. and Walker, R.G.** (1991) River-and-wave-dominated depositional systems of the Upper Cretaceous Dunvegan Formation, northwestern Alberta. *Bulletin of Canadian Petroleum Geology*, **39**. 165-191.
- Bergh, S. G., Braathen, A., and Andresen, A.** (1997) Interaction of basement-involved and thin-skinned tectonism in the Tertiary fold-thrust belt of central Spitsbergen, Svalbard. *AAPG Bulletin*. **81**. 637–661.
- Blythe, A. E. and Kleinspehn, K. L.** (1998) Tectonically versus climatically driven Cenozoic exhumation of the Eurasian plate margin, Svalbard: fission track analyses. *Tectonics*, **17(4)**. 621-639.
- Braathen, A., Bergh, S. G., and Maher, H. D.** (1999) Application of a critical wedge taper model to the Tertiary transpressional fold-thrust belt on Spitsbergen, Svalbard. *Geological Society of America Bulletin*. **111**. 1468–1485.
- Bruhn, R., and Steel, R.** (2003) High-resolution sequence stratigraphy of a clastic foredeep succession (Paleocene, Spitsbergen): An example of peripheral-bulge controlled depositional architecture. *Journal of Sedimentary Research*. **73**. 745–755.
- Charles, A.J., Condon, D.J., Harding, I.C., Pälike, H., Marshall, J.E.A., Cui, Y., Kump, L. and Croudace, I.W.** (2011) Constraints on the numerical age of the Paleocene-Eocene boundary. *Geochemistry, Geophysics, Geosystems*. **12**. 1-19.

10. References

- Cheel, R.J.** (1991) Grain fabric in hummocky cross-stratified storm beds: genetic implications. *Journal of Sedimentary Petrology*, **61**. 102-110.
- Clark, B.E. and Steel, R.J.** (2006) Eocene Turbidite-Population Statistic from Shelf Edge to Basin Floor, Spitsbergen, Svalbard. *Journal of Sedimentology*. **8**. 7-26.
- Clifton, A.J.** (2012) The Eocene Flora of Svalbard and its Climatic Significance. *PhD thesis, University of Leeds*.
- Clifton, H.E.** (1969) Beach lamination: nature and origin. *Marine Geology*, **7**. 553-559.
- Correggiari, A., Cattaneo, A. and Trincardi, F.** (2005) The modern Po Delta system: Lobe Switching and symmetric prodelta growth. *Marine Geology* **222-223**. 49-74.
- Crabaugh, J.P. and Steel, R.J.** (2004) Basin-floor fans of the Central Tertiary Basin, Spitsbergen; relationship of basin-floor sand-bodies to prograding clinoforms in a structurally active basin. *Geol. Soc. Spec. Publ.* **222**. 187–208.
- Dalland, A. (1977)** Erratic clasts in the lower Tertiary deposits of Svalbard-Evidence of transport by winter ice. *Norsk Polarinstitutt Årbok*. **1976**. 151-166.
- Dalland, A. (1979)** Structural geology and petroleum potential of Nordenskiöld Land, Svalbard. *Norsk Petroleumsforening, Norwegian Sea Synoposium*. 1-20.
- Dallmann, W.K.** (1999) Lithostratigraphic lexicon of Svalbard: review and recommendations for nomenclature use: Upper Paleozoic to Quaternary bedrock. Tromsø, *Norwegian Polar Institute*.
- Dallmann, W. K., and Elvevold, S.** (2015) Geoscience Atlas of Svalbard. In Dallmann, W. K., (ed.) Chapter 7: Bedrock geology. *Norsk Polarinstitutt, Tromsø, Norway, Report Series*. **148**. 133–174.
- Deibert, J.E., Benda, T., Løseth, T., Schellpeper, M. and Steel, R.J.** (2003) Eocene Clinoform Growth in front of a storm-wave dominated shelf, Central Basin, Spitsbergen: No significant sand delivery to deepwater areas. *Journal of Sedimentary Research* **73(4)**. 546-558.
- Dreyer, T. and Helland-Hansen, W.** (1986) Aspelintoppen Fm. (Paleogene), Spitsbergen: Aspects of deposition and contribution to basin development. *Norsk Hydro*.
- Duke, W.L., Arnott, R.W.C. and Cheel, R.J.** (1991) Shelf sandstones and hummocky cross-stratification: New insights on a stormy debate. *Geology*, **19(6)**. 625-628.

10. References

- Embry, A. and Johannesen, E.** (1992) T-R sequence stratigraphy, facies analysis and reservoir distribution in the uppermost Triassic – Lower Jurassic succession, western Sverdrup Basin, Arctic Canada: in Worren, T et al, eds., Arctic Geology and petroleum potential. *Norwegian Petroleum Society Special Publication*. **2**. 121-146.
- Faleide, J. I., Tsikalas, F., Breivik, A. J., Mjelde, R., Ritzmann, O., Engen, O., Wilson, J., and Eldholm, O.** (2008) Structure and evolution of the continental margin off Norway and the Barents Sea. *Episodes*, **31**. 82–91.
- Fielding, C.R.** (1984) A coal depositional model for the Durham Coal Measures of NE England. *Journal of the Geological Society*, **141**. 919-931.
- Ford, G.L. and Pyles, D.R.** (2014) A hierarchical approach for evaluating fluvial systems: Architectural analysis and sequential evolution of the high net-sand content, middle Wasatch Formation, Uinta Basin, Utah. *AAPG Bulletin*, **98**. 1273- 1304.
- Friend, P.F., Harland, W.B., Rogers, D.A., Snape, I. and Thornley, R.S.W.** (1997) Late Silurian and Early Devonian stratigraphy and probable strike-slip tectonics in northwestern Spitsbergen. *Geological Magazine* **134(04)**: 459-479.
- Galloway, W.E.** (1989) Genetic stratigraphic sequences in basin analysis. Architecture and genesis of flooding-surface bounded depositional units. *American Association of Petroleum Geologists Bulletin*. **73**. 125-142.
- Gee, E. R., Harland W.B., and McWhae J.R.H.** (1952) Geology of Central Vestspitsbergen: Part I. Review of the geology of Spitsbergen, with special reference to Central Vestspitsbergen: Part II. Carboniferous to Lower Permian of Billefjorden: *Royal Society of Edinburgh. Transactions*, v. *B.LXII, Part II*, **9**, 1951-1952: Edinburgh, Oliver & Boyd.
- Giosan, L., Donnelly, J., Vespremeanu, E. and Buonaiuto, F.S.** (2005) River delta morphodynamics: examples from the Danube delta. *River Deltas – Concepts, Models, and Examples (Eds L. Giosan and J. Bhattacharya)*, *SEPM Spec. Publ.* **83**. 393–411.
- Gjelberg, H.K.** (2010) Facies Analysis and Sandbody Geometry of the Paleogene Battfjellet Formation, Central Western Nordenskiöld Land, Spitsbergen. *University of Bergen, Bergen*. **117**.
- Gjelberg, J.G. and Steel, R.J.** (1995) Helvetiafjellet Formation (Barremian-Aptian), Spitsbergen: characteristics of a transgressive succession. *Norwegian Petroleum Society Special Publications*, **5**. 571-593.

10. References

- Golovneva, L.** (2010) Variability in epidermal characters of *Ginkgo tzagajanica* Samylnina (Ginkgoales) from the Paleocene of the Tzagayan Formation (Amur region) and the taxonomy of Tertiary species of *Ginkgo*. *Paleontological J.* **44**. 584-594.
- Grundvåg, S.-A., Johannessen, E.P., Helland-Hansen, W. and Plink-Björklund, P.** (2014a) Depositional architecture and evolution of progradationally stacked lobe complexes in the Eocene Central Basin of Spitsbergen. *Sedimentology*, **61**. 535-569.
- Grundvåg, S.-A., Helland-Hansen, W., Johannessen, E.P., Olsen, A.H. and Stene, S.A.K.** (2014b) The depositional architecture and facies variability of shelf deltas in the Eocene Battfjellet Formation, Nathorst Land, Spitsbergen. *Sedimentology*, **61**. 2172-2204.
- Hamblin, A.P. & Walker, R. G.** (1979) Storm-dominated shallow marine deposits: the Fernie-Kootenay (Jurassic) Note 217 transition, southern Rocky Mountains. *Can. J. Earth Sei*, **16**. 1673-1690.
- Hampson, G.J. and Storms, J.E.A.** (2003). Geomorphological and sequence stratigraphic variability in wave-dominated, shoreface-shelf parasequences. *Sedimentology* **50**. 667- 701.
- Hampson, G.J., Rodriguez, A.B., Storms, J.E.A., Johnson, H. D. and Meyer, C.T.** (2008) Geomorphology and high-resolution stratigraphy of progradational wave-dominated shoreline deposits: Impact on reservoir-scale facies architecture. Recent advances in models of siliclastic shallow-marine stratigraphy: *SEMP Special Publication*. **90**. 117-142.
- Harding, I.C., Charles, A.J., Marshall, J.E.A., Pälike, H., Roberts, A.P., Wilson, P.A., Jarvis, E., Thorne, R., Morris, E., Moremon, R., Pearce, R.B. and Akbari, S.** (2011) Sea-level and salinity fluctuations during the Paleocene–Eocene thermal maximum in Arctic Spitsbergen. *Earth Planet. Sci. Lett.* **303**. 97-107.
- Harland, W.B.** (1969). Contribution of Spitsbergen to understanding of Tectonic Evolution of North Atlantic Region. North Atlantic, *Geology and Continental Drift. Kay M., American Association of Petroleum Geologists. Memoir* **12**. 817-851.
- Harland, W.B., Anderson, L.M., Manasrah, D., Butterfield, N.J., Challinor, A., Doubleday, P.A., Dowdeswell, E.K., Dowdeswell, J.A., Geddes, I. and Kelly, S.R.A.** (1997) The Geology of Svalbard. *London, Geological Society*.
- Haq, B.U., Hardenbol, J. and Vail, P.P.** (1987) Chronology of fluctuating sea levels since the Triassic (250 million years ago to present). *Science*. **235**. 1156-1166.

10. References

- Helland-Hansen, W.** (1985) Sedimentology of the Battfjellet Formation (Paleogene) in Nordenskiöld Land, Spitsbergen. *Unpublished Cand. Scient. Bergen*, University of Bergen. 322.
- Helland-Hansen, W.** (1990) Sedimentation in Paleogene Foreland Basin, Spitsbergen (1): *AAPG Bulletin*. **74(3)**. 260-272.
- Helland-Hansen, W.** (1992) Geometry and facies of Tertiary clinothems, Spitsbergen. *Sedimentology*. **39**. 1013-1029.
- Helland-Hansen, W., Helle, H.B., Sunde, K.** (1994) Seismic modelling of Tertiary sandstone clinothems, Spitsbergen. *Basin Research*, **6(4)**. 181-191.
- Helland-Hansen, W.** (2010) Facies and stacking patterns of shield-deltas within the Paleogene Battfjellet Formation, Nordenskiöld Land, Svalbard: implications for subsurface reservoir prediction. *Sedimentology*, **57**. 190-208.
- Helland-Hansen, W and Gjelberg, J.G.** (1994) Conceptual Basis and variability in sequence stratigraphy: a different perspective. *Sedimentary Geology*. **92(1)**. 31-52.
- Helland-Hansen, W and Grundvåg, S.** (in prep) The Spitsbergen Eocene Central Basin succession: Sedimentation patterns and controls. *University of Bergen, The University Centre in Svalbard (UNIS) and The Arctic University of Norway*.
- Helland-Hansen, W and Mart, O.J.** (1996) Shoreline Trajectories and Sequences: Description of Variable Depositional Dip Scenarios. *SEPM Journal of Sedimentary Research*. **66**.
- Jelby, M.E., Grundvåg, S.A., Helland-Hansen, W., Olausen, S. and Stemmerik, L.** (in prep) Wave-modified hyperpynites and unsteadily generated tempestites across a 2 wide ramp: Towards a polygenetic model for hummocky cross-stratification. *The University of Copenhagen, The University Centre in Svalbard (UNIS), The Arctic University of Norway and The University of Bergen*.
- Johannessen, E.P. and Steel, R.J.** (2005) Shelf-margin clinoforms and prediction of deepwater sands. *Basin Research*. **17**. 521-550.
- Kellogg, H.E.** (1975) Tertiary Stratigraphy and Tectonism in Svalbard and Continental Drift. *AAPG Bulletin*. **59**. 465-485.
- Kruit, C.** (1955) Sediments of the Rhone Delta. Grain size and microfauna. *Ned. Geol. Mijnb. Genoot. Verh. Geol. Ser.* **15** 357-514.

10. References

- Kvaček, Z.** (1994) Connecting links between the Arctic Palaeogene and European Tertiary floras. In: Cenozoic plants and climates of the Arctic (Eds M.C. Boulter and H.C. Fisher). *NATO ASI Series*. **27**. 251-266.
- Ljutkevic, E.M.** (1937) Geologiceskji ocerk I problem ugljenosnosti gory Piramidy ostrova Spicbergena. (Geological survey and problems of the coal fields of mount Pyramiden, Spitsbergen). *Turdy Arktieeskogo Instituta Leningrad*. **76**. 25-38.
- Løseth, T.M., Steel, R.J., Crabaugh, J.P. and Shellpeper, M.** (2006) Interplay between shoreline migration paths, architecture and pinchout distance for siliclastic shoreline tongues: evidence from the rock record. *Sedimentology*. **53**. 735-767.
- Major, H., and Nagy, J.** (1972) Geology of Adventdalen map area. Norsk Polarinstitut, Skrifter. **138**. 1-58.
- Manum, S.B.** (1962) Studies in the Tertiary flora of Spitsbergen, with notes on Tertiary floras of Ellesmere Island, Greenland and Iceland. A Palynological investigation. Oslo, Norsk Polarinstitut.
- Manum, S.B. and Throndsen, T.** (1978) Rank of coal and dispersed organic matter and its geological bearing in the Spitsbergen Tertiary. *Norsk Polarinstitut Årbok*. **1977**. 159-177.
- Manum, S.B. and Throndsen, T.** (1986) Age of Tertiary formations on Spitsbergen. *Polar Research*. **4**. 103-131.
- Mellere, D., Plink-Björklund, P. and Steel, R.** (2002) Anatomy of shelf deltas at the edge of a prograding Eocene shelf margin, Spitsbergen. *Sedimentology*. **39**. 1189-1206.
- Miller, K.G., Kominz, M.A., Browning, J.V., Wright, J.D., Mountain, G.S., Katz, M.E., Sugarman, P.J., Cramer, B.S., Christie-Blick, N. and Pekar, S.F.** (2005) The Phanerozoic record of global sea-level change. *Science*. **310**. 1293–1298.
- Müller, R. D., and Spielhagen, R. F.** (1990) Evolution of the Central Tertiary Basin of Spitsbergen, towards a synthesis of sediment and plate tectonic history. *Palaeogeography, Palaeoclimatology, Palaeoecology*. **80**. 153–172.
- Nagy, J., Kaminski, M. A., Kuhnt, W., and Bremer, M.A.** (2001) Agglutinated foraminifera from neritic to bathyal facies in the Paleogene of Spitsbergen and the Barents Sea. Proceedings of the Fifth International Proceedings of the Fifth Workshop on Agglutinated Foraminifera: (Plymouth, U.K., September 6-16, 1997). *Grzybowski Foundation Special Publication*. **7**. 333-361.

10. References

- Nathorst, A. G.** (1910) Beiträge zur Geologie der Bäreninsel, Spitzbergens und des König-Karl-Landes. *Bulletin Geologiska Institutionen Universitetet I Uppsala*. **10(1910-1911)**. 261-416.
- Naurstad, O. A.** (2014) Sedimentology of the Aspelintoppen Formation (Eocene-Oligocene), Brogniartfjella, Svalbard. *University of Bergen. Bergen*. **124**
- Niedoroda, A.W. and Swift, D.J.P.** (1981) Maintenance of the shoreface by wave orbital currents and mean flow: observations from the Long Island Coast. *Geophys. Res. Letters*. **8**. 337 – 348.
- Osen, T.G.** (2012) Facies, Sandbody Geometry and Paleogeography of the Battfjellet Formation, Urdkollaldalen area, Nordenskiöld Land, Svalbard. *University of Bergen. Bergen*. **90**
- Olsen, A.H.** (2008) Sedimentology and Paleogeography of the Battfjellet Fm, Southern Van Mijenfjorden, Svalbard. *University of Bergen. Bergen*. **104**
- Orton, G.J. and Reading, H.G.** (1993) Variability of deltaic processes in terms of sediment supply, with particular emphasis on grain size. *Sedimentology*, **40**. 475-512
- Orvin, A.** (1940) Outline of the geological history of Spitsbergen. *Norsk Polarinstitut, Skrifter*. **78**.
- Petter, A.L. and Steel, R.J.** (2006) Hyperpycnal flow variability and slope organization on an Eocene shelf margin, Central Basin, Spitsbergen. *AAPG Bulletin*. **90**. 1451-1472
- Reading, H.G. and Collinson, J.D.** (1996) Clastic Coasts. *Sedimentary Environments: Processes, Facies and Stratigraphy*. *Blackwells, Cornwall*, 154-231.
- Reineck, H.E. and Singh, I.B.** (1980) Depositional sedimentary environments: With References to Terrigenous Clastics, (Second, Revised and Updated Edition): *Berlin, Springer-Verlag. New York*, **549**.
- Riis, F., Lundschieen, B.A., Høy, T., Mørk, A. and Mørk, M.B.E.** (2008) Evolution of the Triassic shelf in the northern Barents Sea region. *Polar Research*, **27**. 318-338.
- Plink-Björklund, P., Mellere, D. and Steel, R.J.** (2001) Turbidite variability and architecture of sandprone, deep-water slopes: Eocene clinofolds in the Central Basin, Spitsbergen. *Journal of Sedimentary Research*. **71**. 895-912.
- Plink-Björklund, P. and Steel, R.J.** (2004) Initiation of turbidity currents: outcrop evidence for Eocene hyperpycnal flow turbidites. *Sed. Geol.* **165**. 29–52.

10. References

- Plink-Björklund, P. (2005)** Stacked fluvial and tide-dominated estuarine deposits in high frequency (fourth-order) sequences of the Eocene Central Basin, Spitsbergen. *Sedimentology*. **52**. 391–428.
- Plink-Björklund, P. and Steel, R.J. (2006)**. Incised valleys on an Eocene coastal plain and shelf, Spitsbergen-part of a linked shelf-slope system. *SEPM Special Publication*. **85**. 281-307.
- Pontén, A. and Plink-Björklund, P. (2009)** Process regime changes across a regressive to transgressive turnaround in a shelf-slope basin, Eocene Central Basin of Spitsbergen. *Journal of Sedimentary Research*. **79**. 2-23.
- Roest, W., and Srivastava, S. (1989)** Sea-floor spreading in the Labrador Sea. A new reconstruction. *Geology*. **17**. 1000-1003.
- Seilacher, A. (2007)** Trace Fossil Analysis. *Berlin: Springer*.
- Senger, K., Tveranger, J., Ogata, K., Braathen, A. and Planke, S. (2014)** Late Mesozoic magmatism in Svalbard: A review. *Earth-Science Reviews*. **139**. 123-144.
- Skarpeid, S.S. (2010)** Facies Architecture and Paleogeography of the Battfjellet Formation, Rypefjellet, Spitsbergen. *University of Bergen. Bergen*. **85**.
- Skjærpe, K.T. (2017)** Sedimentological facies analyses of Clinothem 8C (Eocene), Battfjellet Formation, Brogniartfjella, Svalbard. University of Bergen, Bergen. **98**.
- Smith, D.G., Jol, H.M., Smith, N.D., Kostaschuk, R.A. and Pearce, C.M. (2005)** The wave-dominated William River Delta, Lake Athabasca, Canada: its morphology, radar stratigraphy, and history. *River Deltas – Concepts, Models, and Examples (Eds L. Giosan and J. Bhattacharya), SEPM Spec. Publ.* **83**. 295–318.
- Steel, R.J. (1977)** Observations on some Cretaceous and Tertiary sandstone bodies in Nordenskiöld Land, Svalbard. *Norsk Polarinstitutt Årbok*. **1976**. 43-68.
- Steel, R. J., Dalland, A., Kalgraff, K. and Larsen, V. (1981)** The Central Tertiary Basin of Spitsbergen: sedimentary development of a sheared-margin basin. *Canadian Society Petroleum Geology*. **7**. 647–664.
- Steel, R.J., Gjelberg, J., Helland-Hansen, W., Kleinspehn, K.L., Nøttvedt, A. and Rye-Larsen, M. (1985)** The Tertiary strike-slip basins and orogenic belt of Spitsbergen. *Strike-Slip Deformation, Basin Formation, and Sedimentation. SEPM Special Publication*. **37**. 339-359.


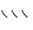










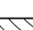


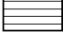
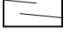

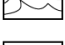
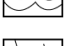
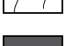










10. References

- Steel, R., Mellere, D., Plink-Björklund, P., Crabaugh, J.P., Deibert, J.E., Loeseth, T. and Shellpeper, M.** (2000) Deltas vs. Rivers on the Shelf Edge: Their Relative Contributions to the Growth of Shelf-Margins and Basin-Floor Fans (Barremian and Eocene, Spitsbergen). *GCSSEPM Special Publication*, **20**. 981-1009.
- Steel R.J., Worsley D.** (1984) Svalbard's post-Caledonian strata — an atlas of sedimentational patterns and paleogeographic evolution. In: Spencer A.M. (eds) *Petroleum Geology of the North European Margin*. Springer, Dordrecht.
- Stene, S.A.K.** (2009) Facies and architecture of the Battfjellet Formation, northern Nathorst Land, Spitsbergen. *University of Bergen. Bergen*. **104**.
- Swift, D.J.P., Figueiredo, A.G., Freeland, G.L. and Oertel, G.F.** (1983) Hummocky cross-stratification and megaripples; a geological double standard? *Journal of Sedimentary Research (1983)* **53(4)**. 1295-1317.
- Uroza, C.A., and Steel, R.J.** (2008) A highstand shelf-margin delta system from the Eocene of West Spitsbergen, Norway. *Sedimentary Geology*, **203**. 229-245.
- Van Wagoner, J.C., Mitchum, R.M., Campion, K.M. and Rahmanian, V.D.** (1990) Siliciclastic Sequence Stratigraphy in Well Logs, Cores and Outcrops: Concepts of High Resolution Correlation of Time and Facies. *AAPG Meth, Explor. Ser.* **7**. 55.
- Worsley, D.** (2008) The post-Caledonian development of Svalbard and the western Barents Sea: *Polar Research*, **27**. 298-317.
- Worsley, D. and Aga, O.J.** (1986) The geological history of Svalbard: evolution of an arctic archipelago: Stavanger, *Den norske stats oljeselskap* **121**.

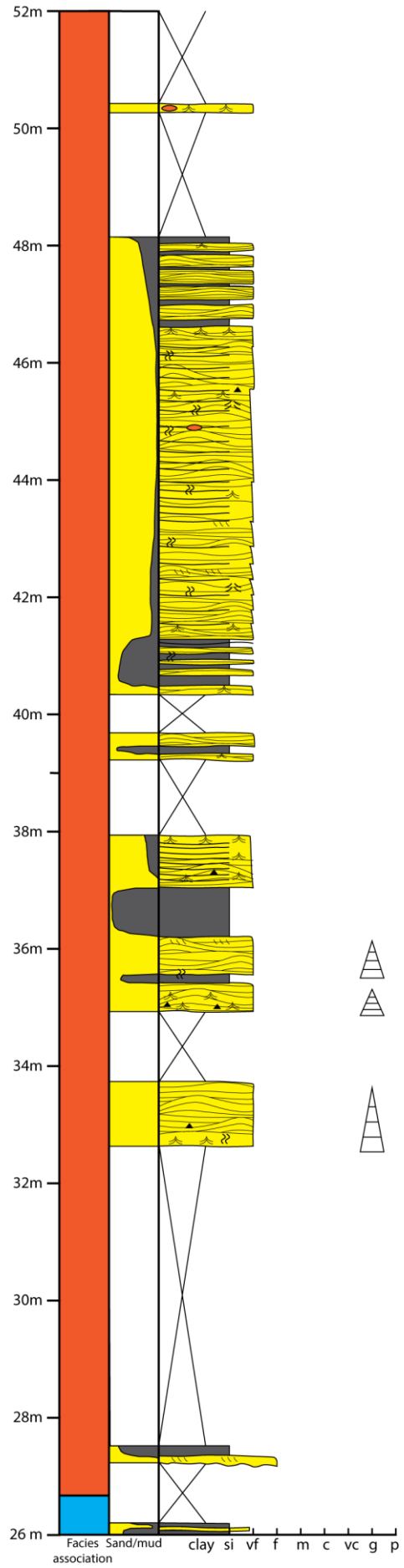
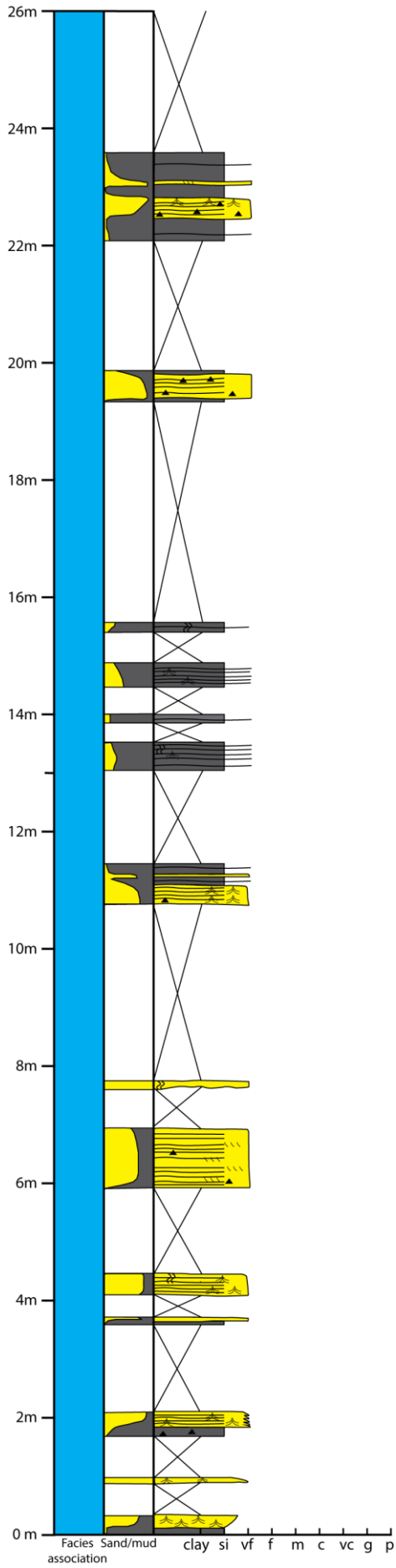
Appendix 1: Logs

Logs are:

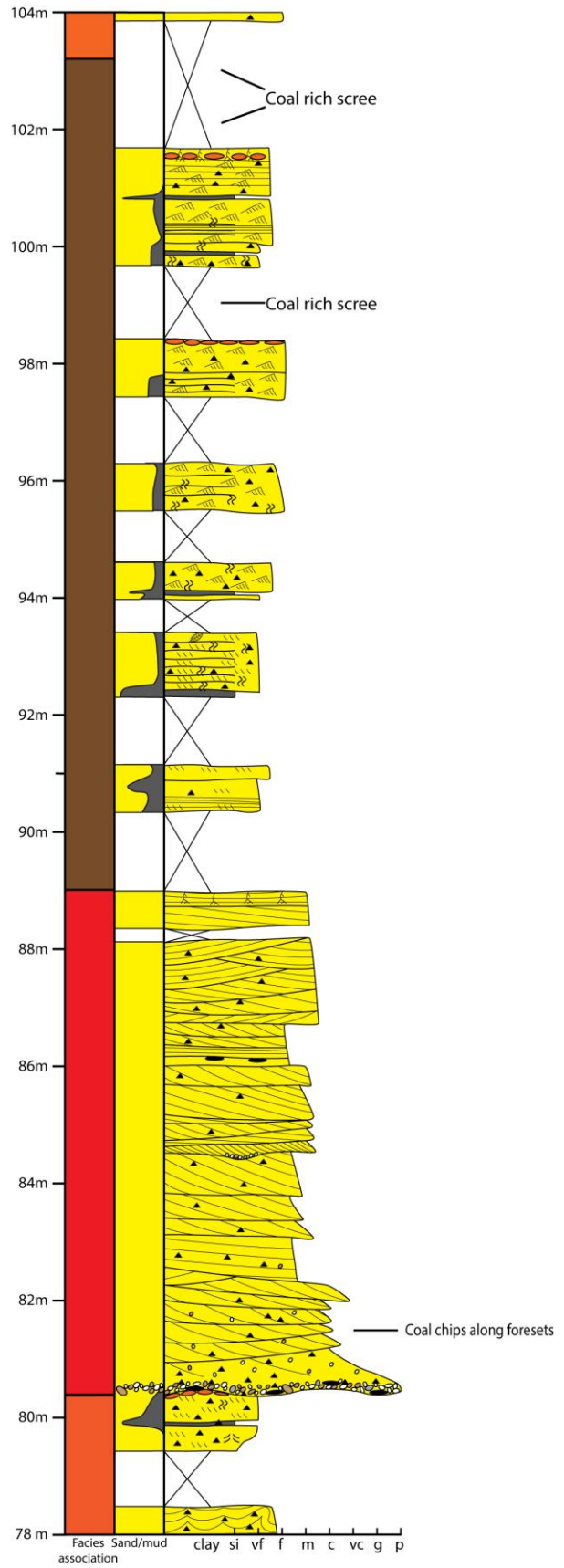
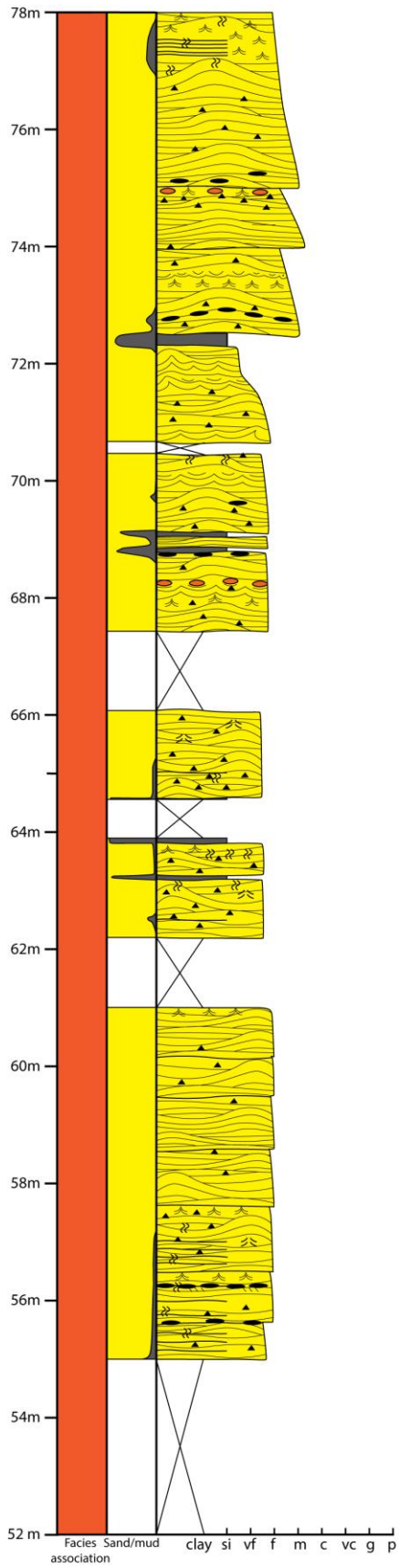
- Ordered from A-F
- Shown in a 1:50 scale

Legend:		
	Pebble	
	Ripples (wave or current)	
	Climbing Ripples	
	Current ripples	
	Wave ripples	
	Mudclast	
	Ciderite concretion	
	Bioturbation	
	Leaf	
	Water escape structures/ dish structures	
	Leaf	
	Roots	
	Coal chips	
	Tangential cross stratification	
	Trough cross stratification	
	Plane parallel lamination	
	Faint low angle PPL	
	Hummocky cross stratification	
	Flame structures	
	Ball and pillow	
	Heavily fractured	
	Mudstone	 FA1 - Offshore
	Sandstone	 FA2-A - Offshore tranzition zone
	Conglomerate	 FA2-B - Lower shoreface
	Thinning upwards	 FA2-C - Upper shoreface and Foreshore
		 FA3 - Fluvial channel
		 FA4 - Continental deposits

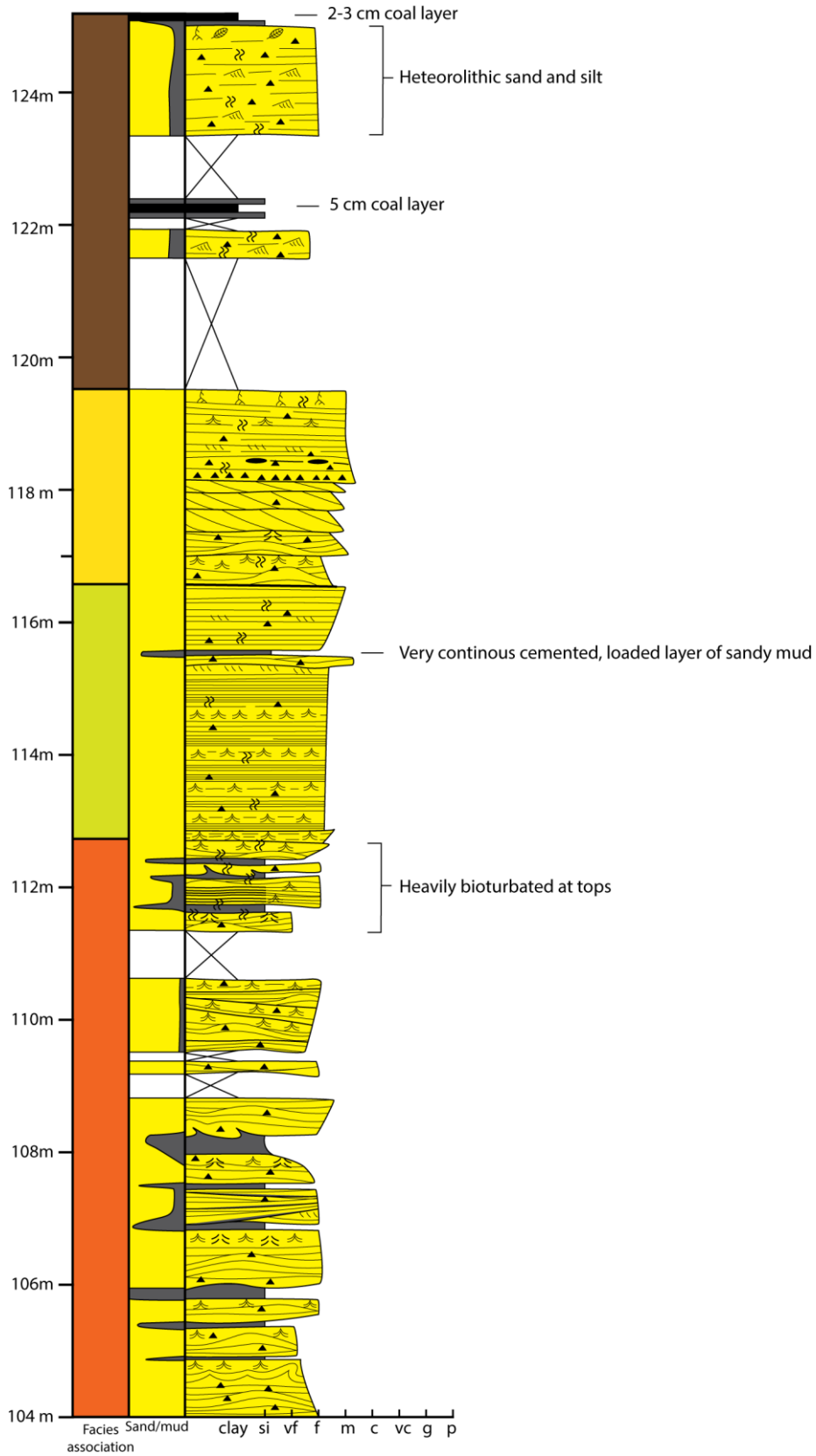
Log A



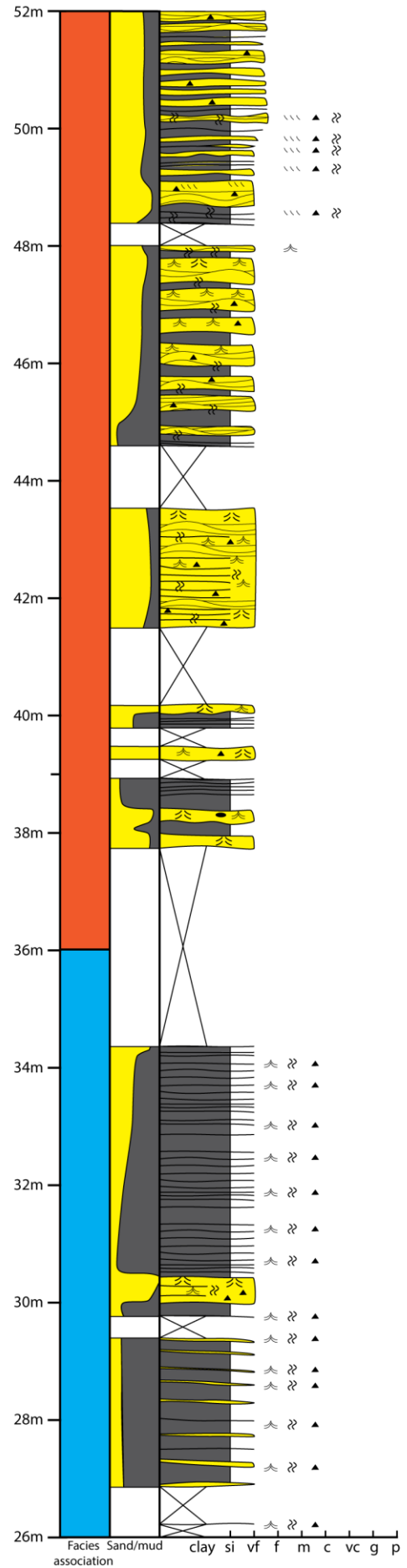
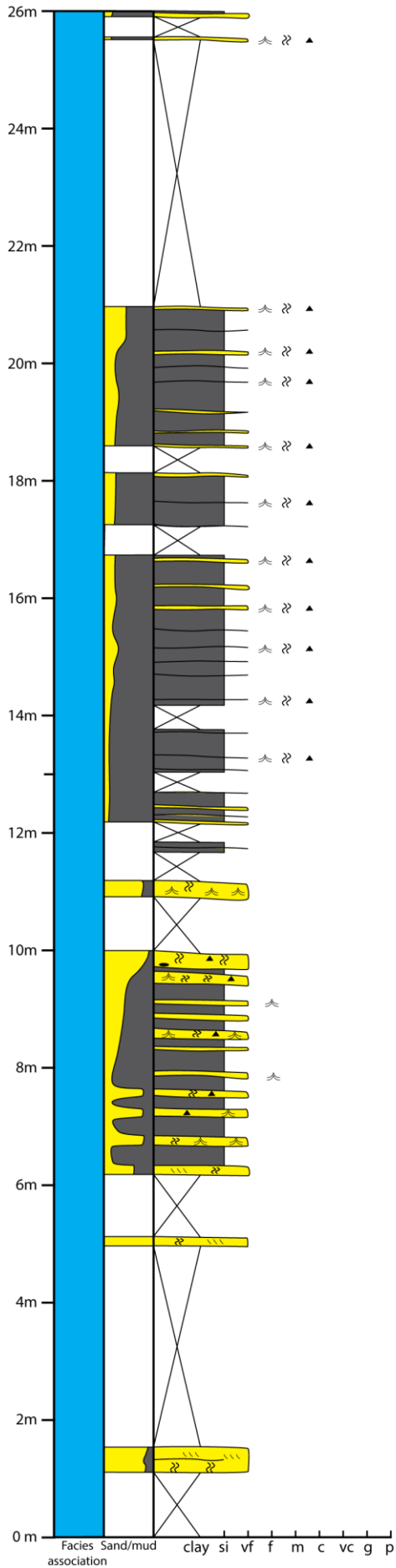
Log A



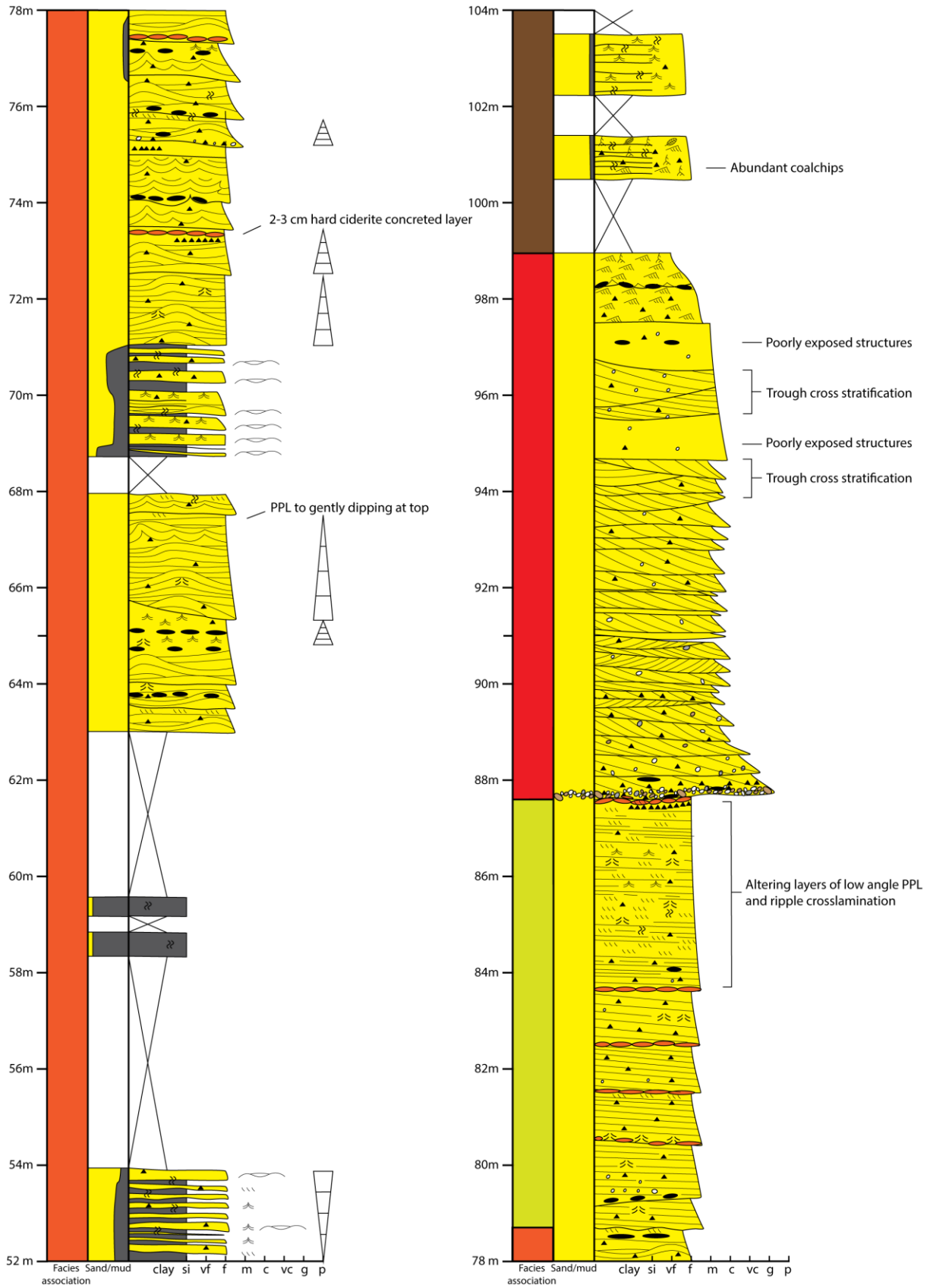
Log A



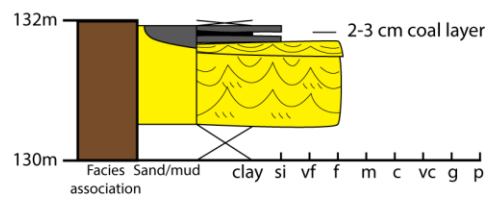
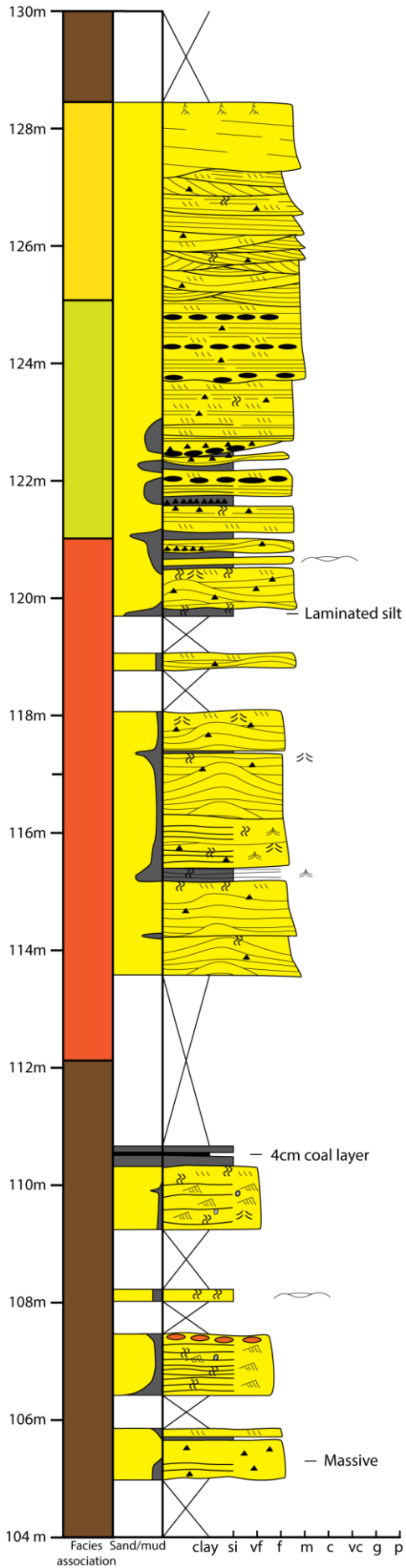
Log B



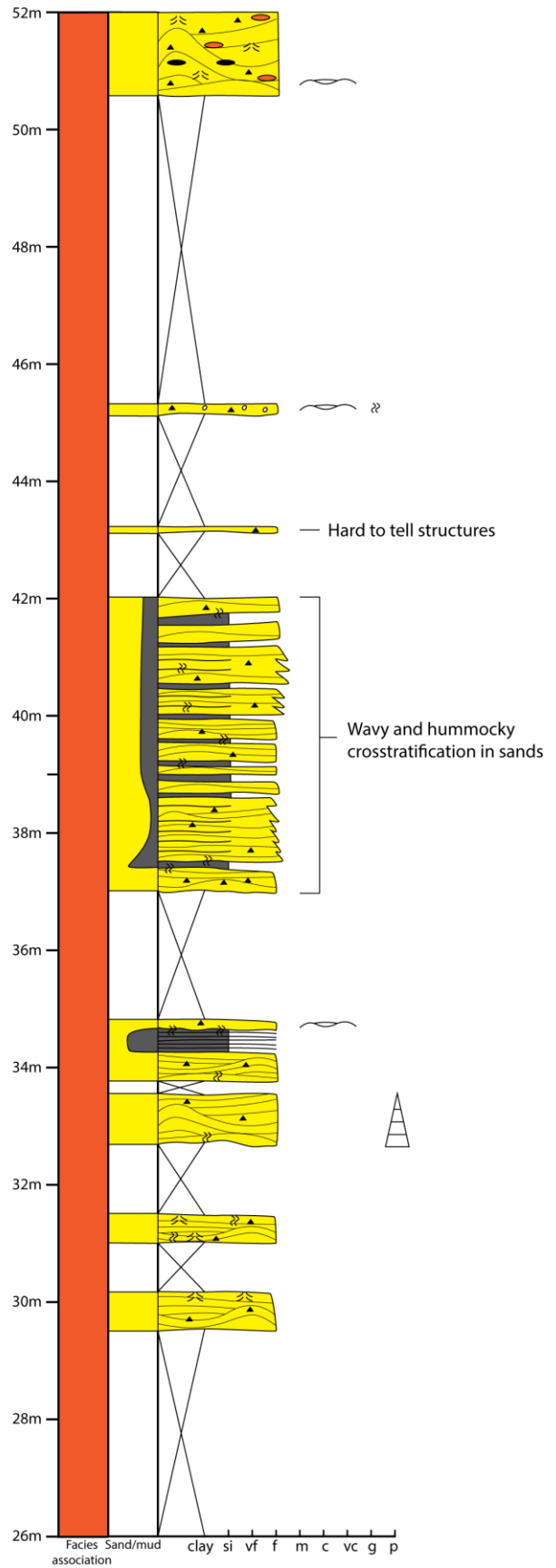
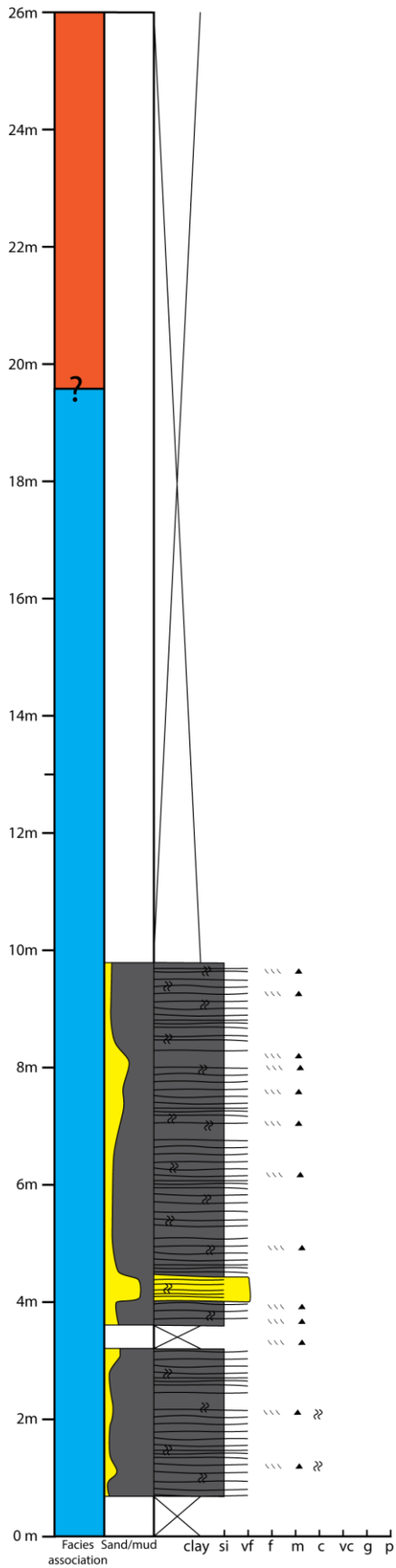
Log B



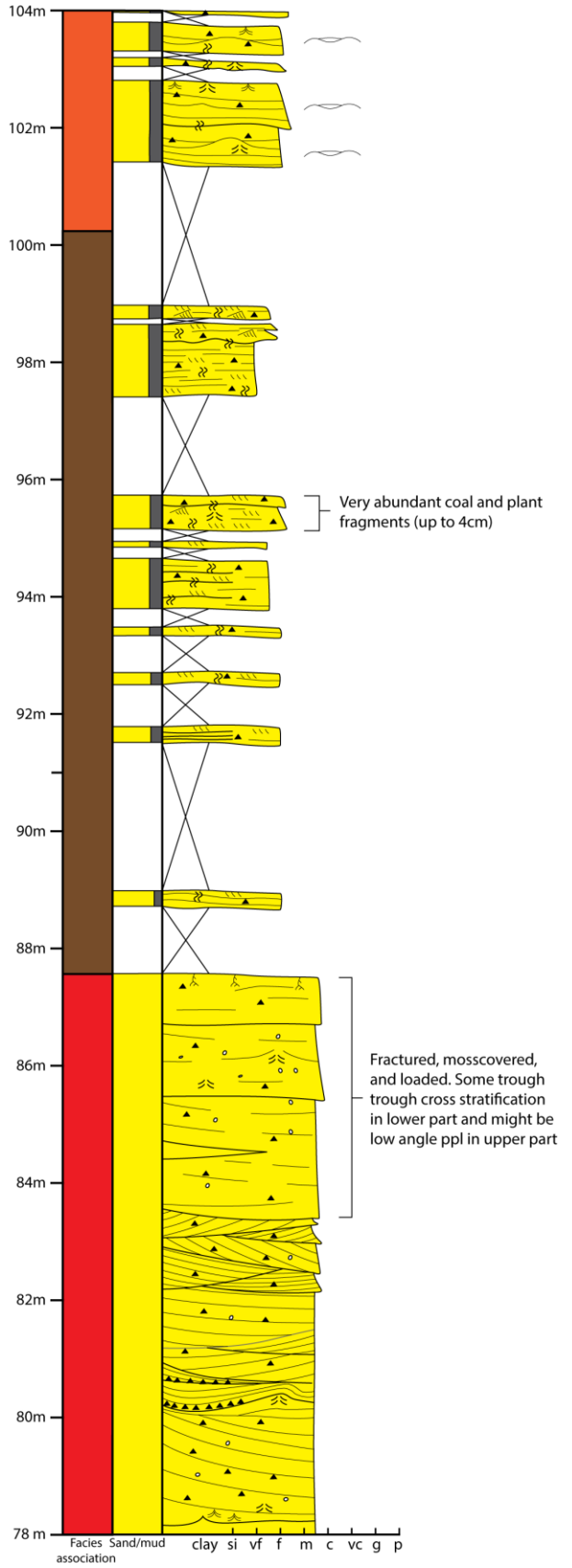
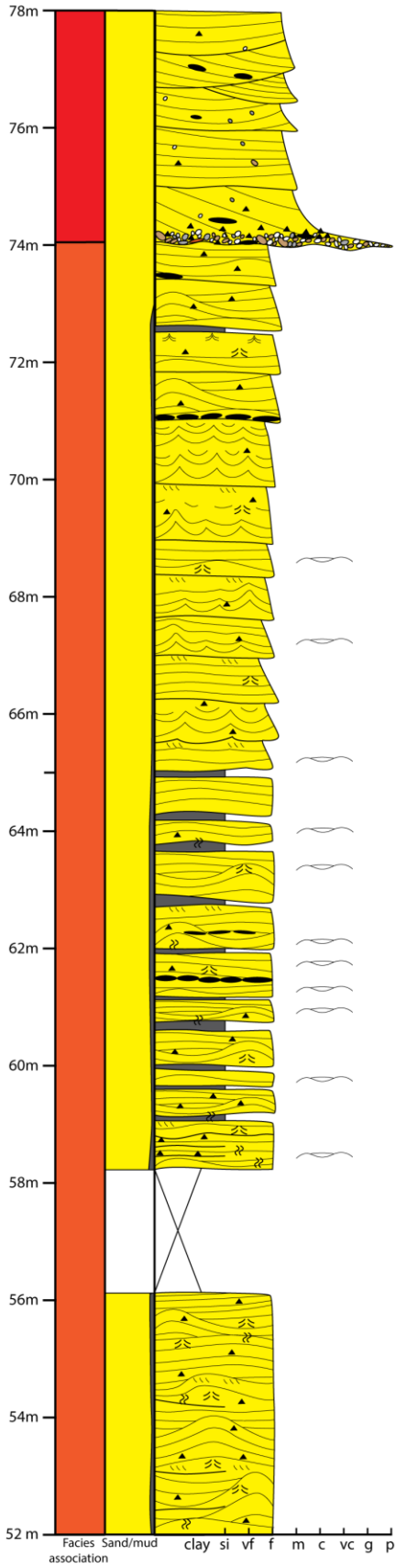
Log B



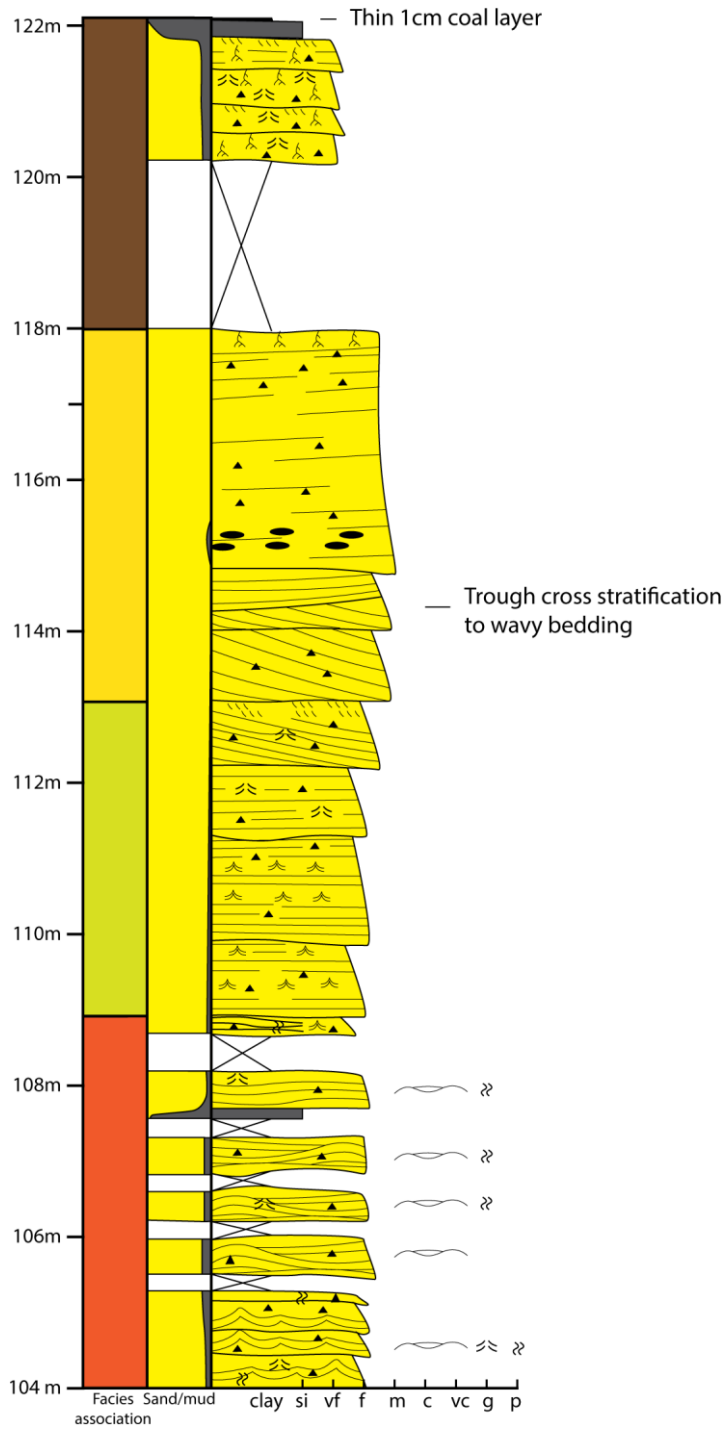
Log C



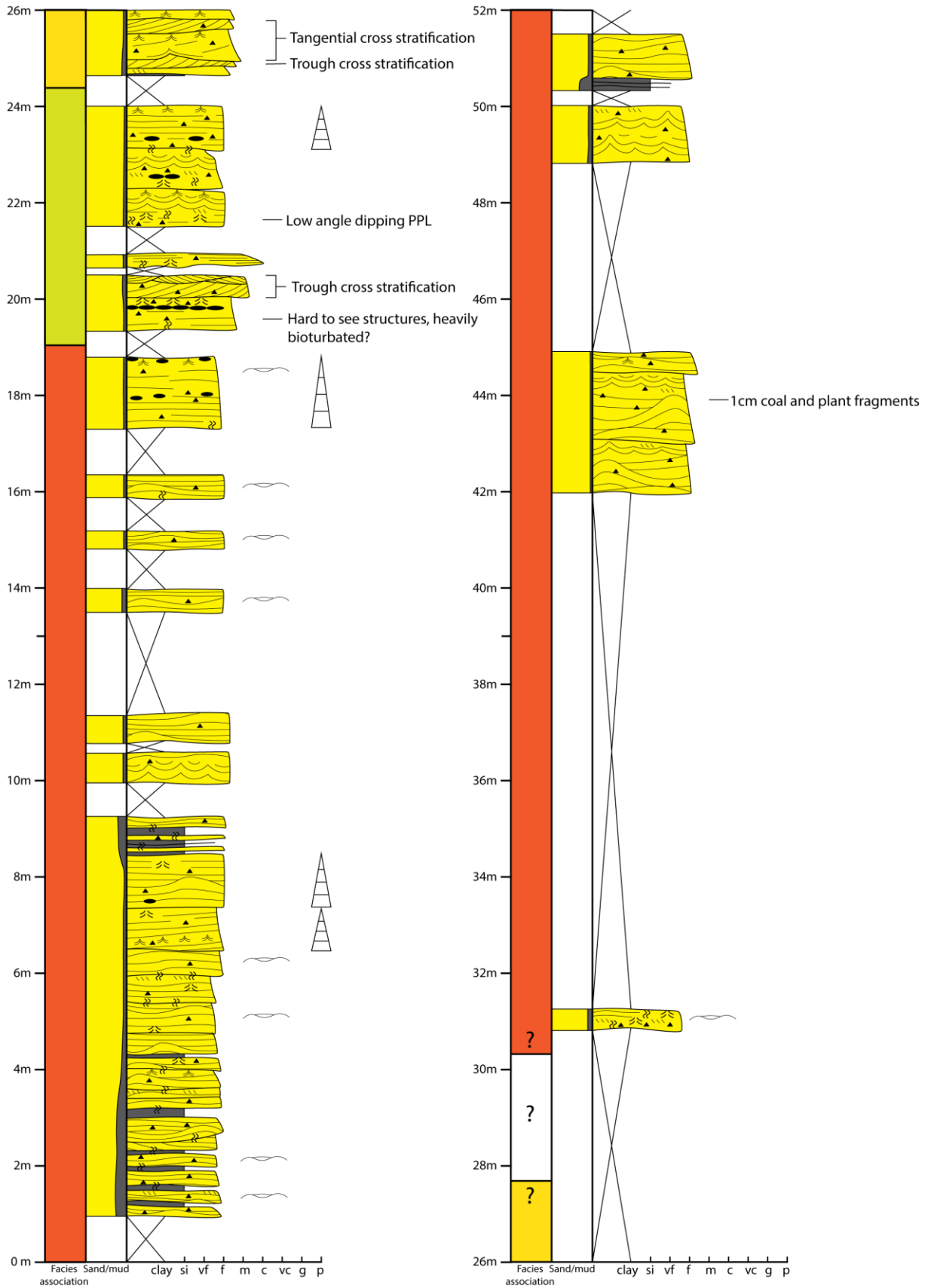
Log C



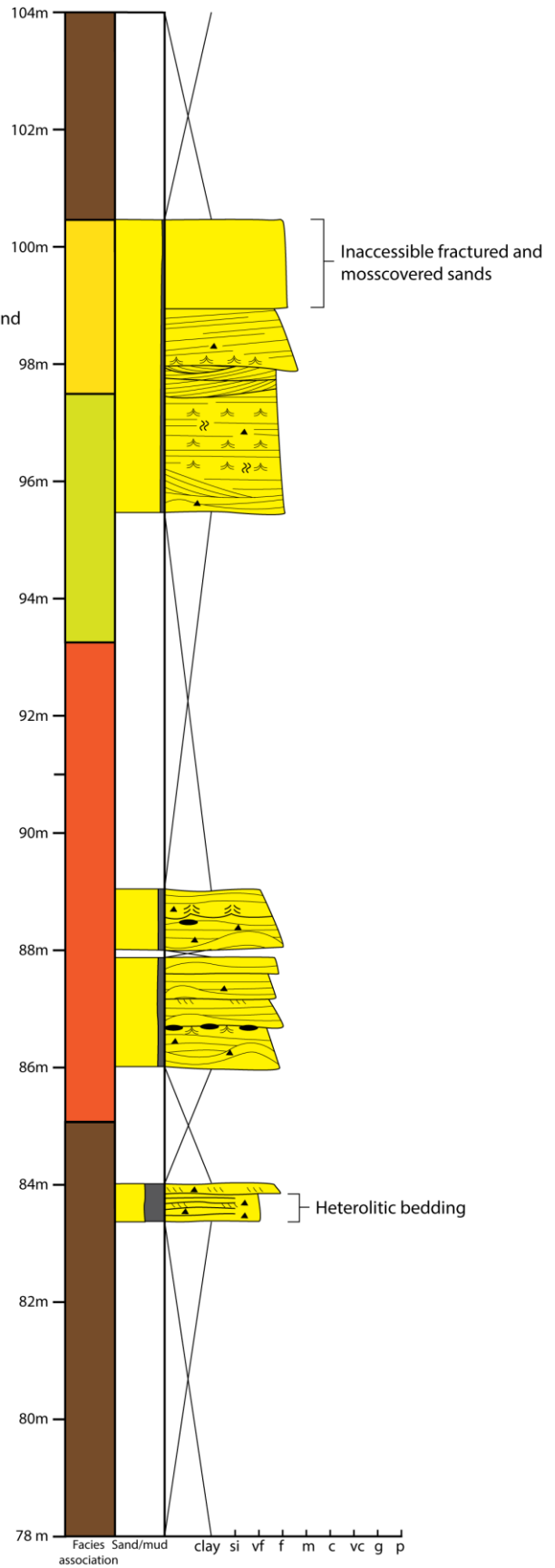
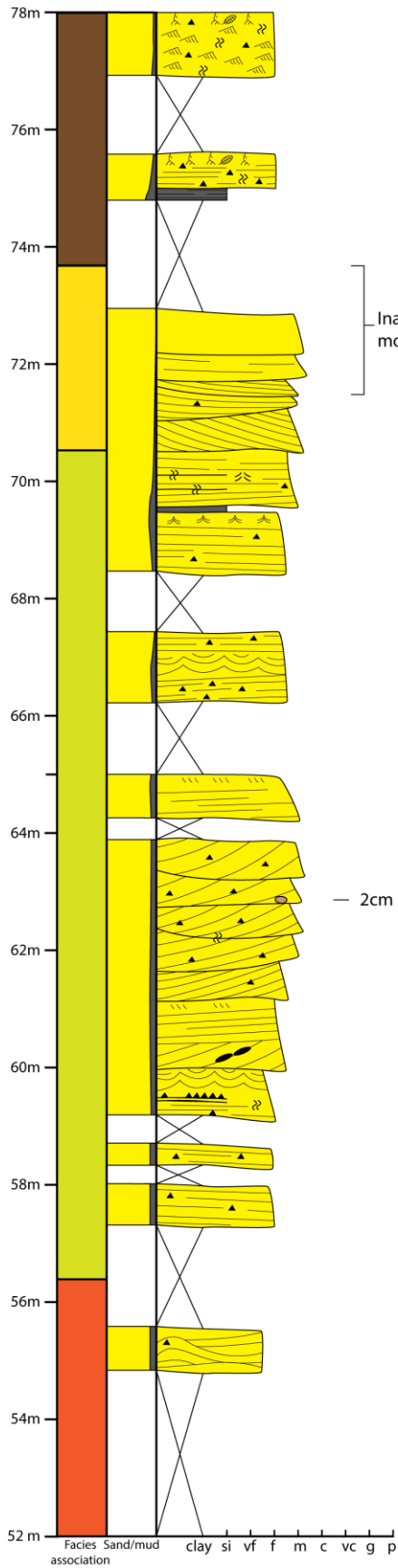
Log C



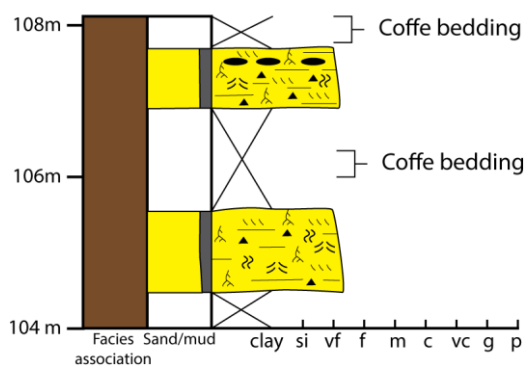
Log D



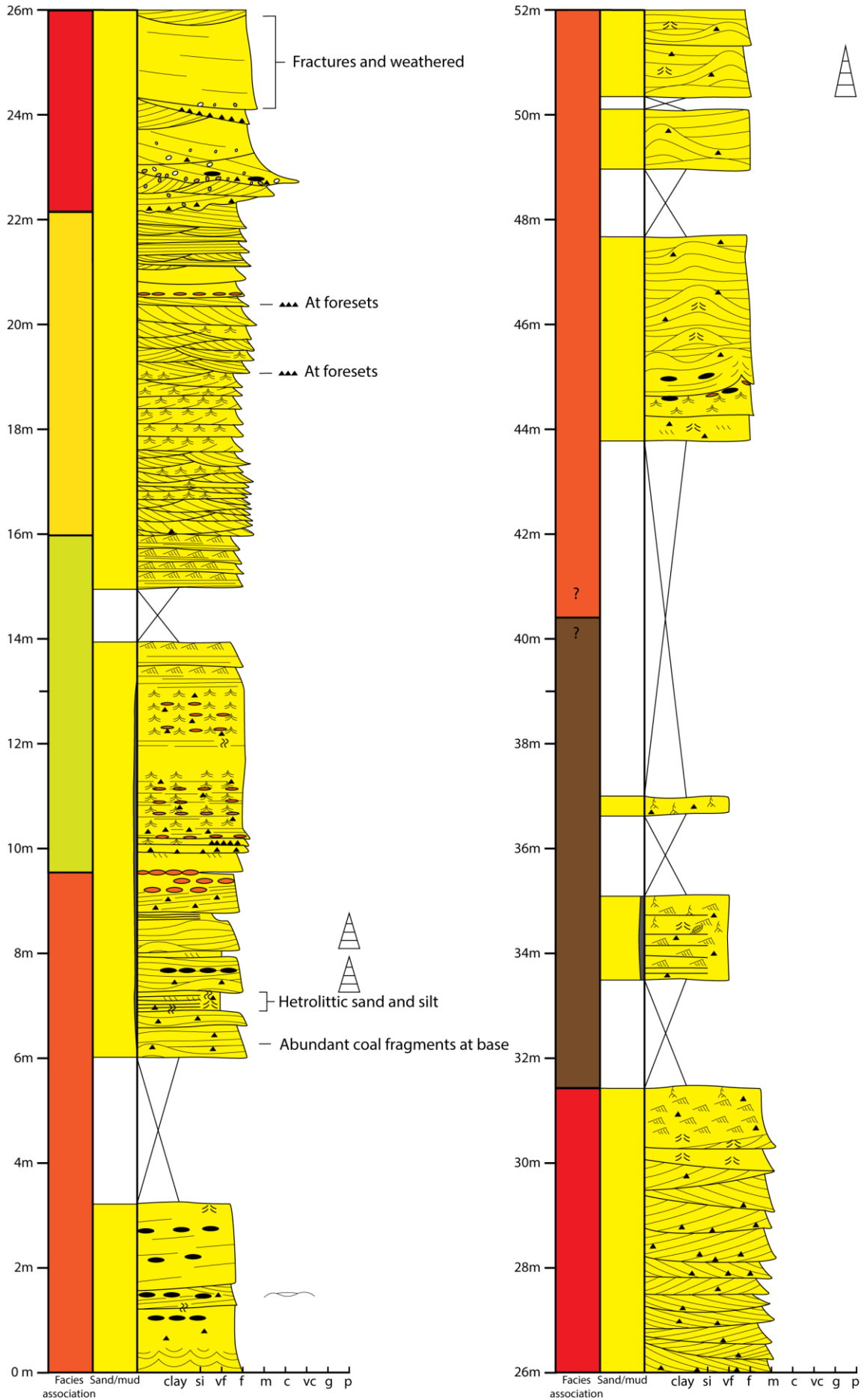
Log D



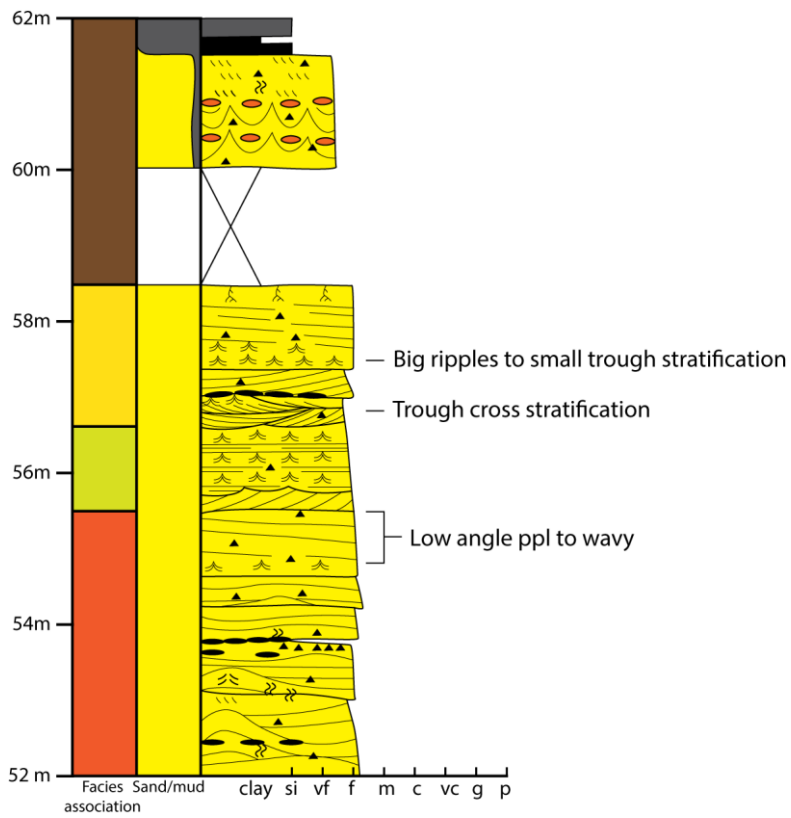
Log D



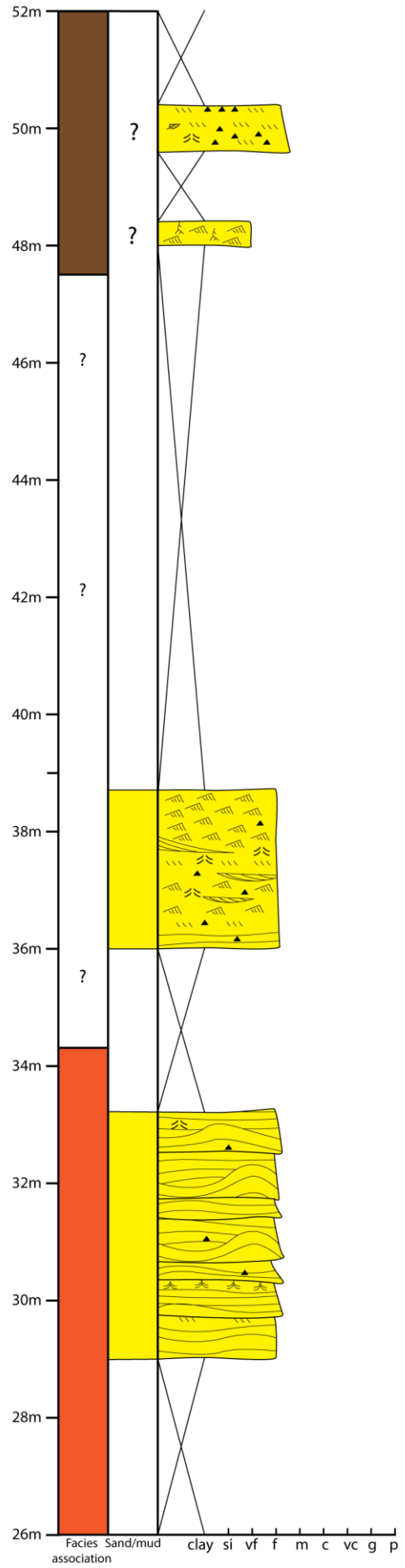
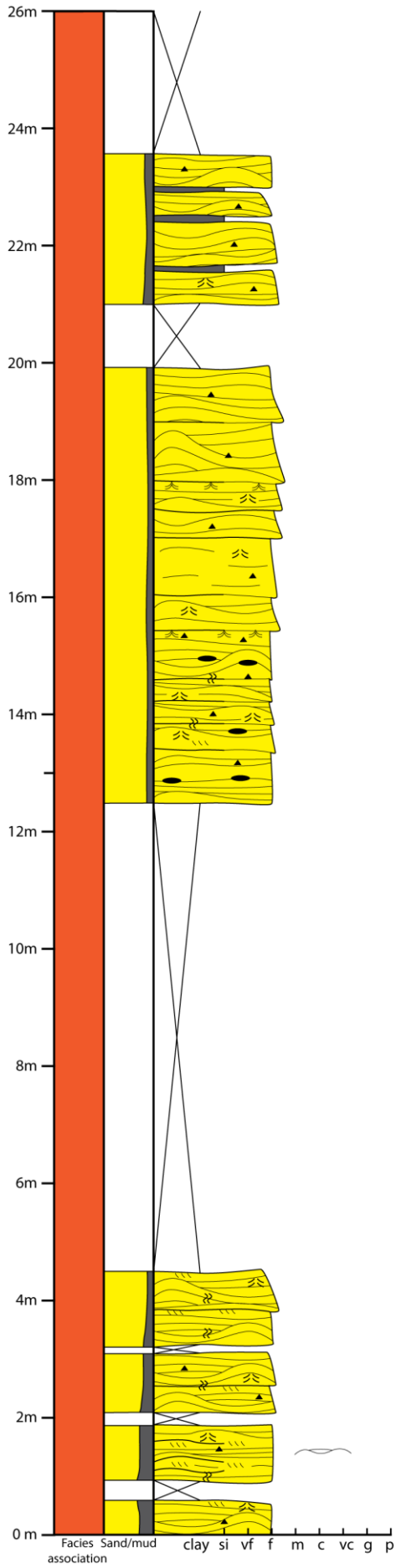
Log E



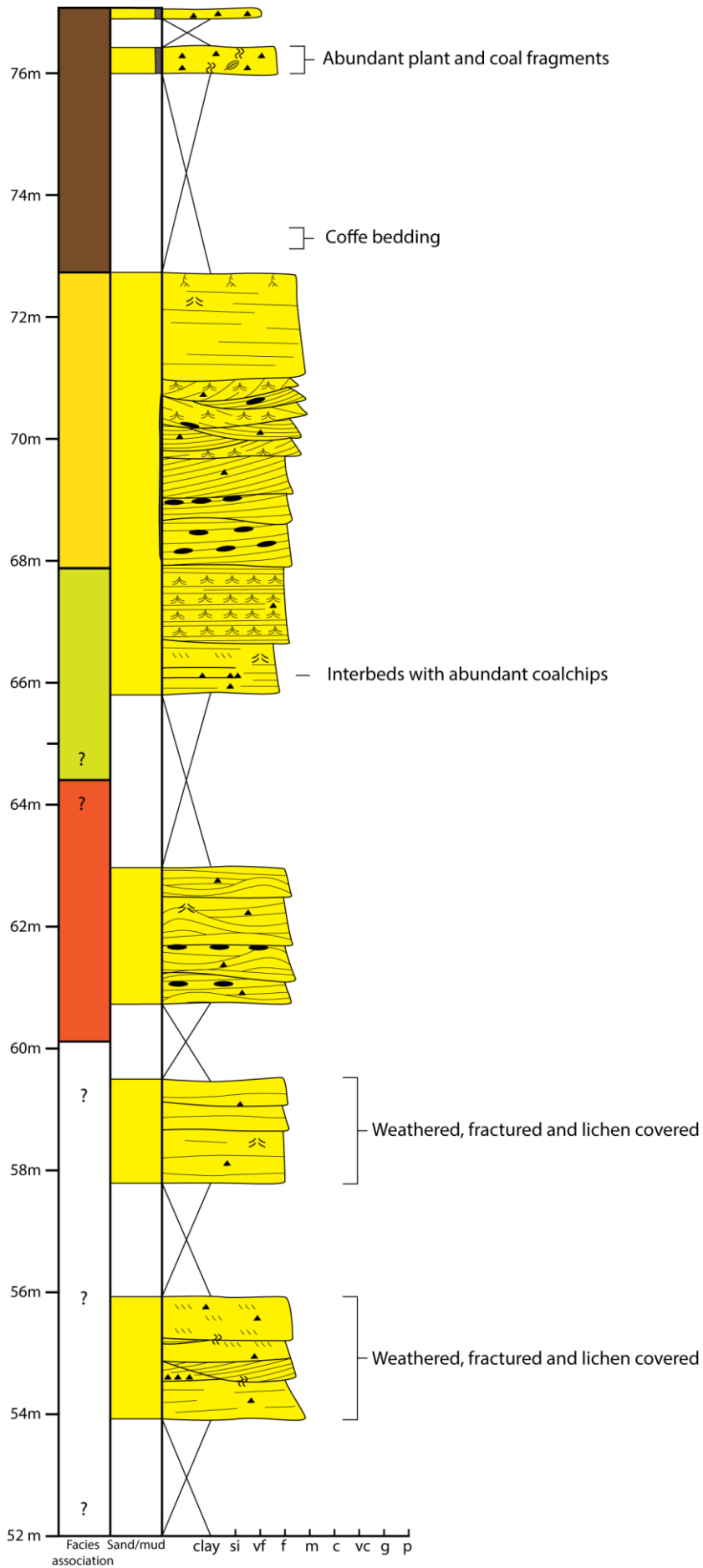
Log E



Log F



Log F



Appendix 2: Paleocurrent Data

Log:	FA1		FA2		FA3- Lower		FA3 – Upper	
	Current:	Crest:	Current:	Crest:	Current:	Crest:	Current:	Crest:
A	129	114/294		90/270				
	52/242	148/328		110/290				
	150/330	140/320		136/314				
	131/311	50/230		120/300				
		45/225		150/330				
		20/200		125/305				
				70/250				
				50/230				
				20/200				
				85/265				
				89/269				
				70/230				
				55/235				
				170/350				
				76/256				
			111/291					
B	324	80/260		24/204	73		20	
	104/284	112/292		28/208	115		90	
	138/318	110/290		58/238	84		112	
	120/300	62/242		52/232	56		94	
	130/310			60/240	108		116	
				65/245	48		342	
				42/222	348		65	
				58/238	66		158	
				60/240	48		60	
					20		293	
					90		61	
				60		60		
						65		
						59		
C								
D				34/214				
				16/196				
				150/330				
				172/352				
E							132	
							172	
							138	
							140	
							160	
							140	
							174	
							166	
							116	
							172	
F								